

Supporting Information

Catalytic reductive deoxygenation of esters to ethers driven by a hydrosilane activation through non-covalent interactions with a fluorinated borate salt

Vincent Rysak,^a Ruchi Dixit,^b Xavier Trivelli,^c Nicolas Merle,^a Francine Agbossou-Niedercorn,^a Kumar Vanka^{*b} and Christophe Michon^{*a,d}

a. Univ. Lille, CNRS, Centrale Lille, Univ. Artois, UMR 8181 - UCCS - Unité de Catalyse et Chimie du Solide, F-59000 Lille, France.

b. Physical and Material Chemistry Division, CSIR-National Chemical Laboratory, Dr. Homi Bhabha Road, Pune 411008, Maharashtra, India.

E-mail: k.vanka@ncl.res.in

c. Univ. Lille, CNRS, INRA, Centrale Lille, Univ. Artois, FR 2638 – IMEC –Institut Michel-Eugène Chevreul, Lille, F-59000, France.

d. New address: Université de Strasbourg, Université de Haute-Alsace, Ecole Européenne de Chimie, Polymères et Matériaux, CNRS, LIMA, UMR 7042, 25 rue Becquerel, 67087 Strasbourg, France.

E-mail: cmichon@unistra.fr

I) General methods and instrumentation.	2
II) Additional experimental data.	3
III) Additional computational data	10
IV) General procedures.	23
V) Characterization of compounds.	24
VI) References.	28
VII) ^1H , ^{13}C NMR spectra of isolated compounds.	30
VIII) Computational details	46

I) General methods and instrumentation.

All solvents were dried using standard methods and stored over molecular sieves (4 Å). All salts were weighted in a glovebox filled of Argon below 5 ppm of H₂O and O₂. All reactions were carried out under a dry nitrogen atmosphere and were repeated at least twice.

Analytical thin layer chromatography (TLC) was performed on Merck pre-coated 0.20 mm silica gel Alugram Sil 60 G/UV₂₅₄ plates.

Flash chromatography was carried out with Macherey silica gel (Kielselgel 60).

Gas chromatography analyses were done on GC Shimadzu 2010+ with FID detectors using Supelco SPB-5 column (30 m, 0.25 mm, 0.25 µm) and with nitrogen as gas carrier with tetradecane as internal standard.

GC-MS analyses were performed on a Shimadzu QP2010+ using Supelco column SLBTM-5ms (30 m, 0.25 mm, 0.25 µm).

Routine ¹H (300 MHz) and ¹³C (75 or 125 MHz) NMR spectra were acquired on Bruker Avance spectrometers. Chemical shifts (δ) are reported downfield of Me₄Si in ppm and coupling constants are expressed in Hz. 1,3,5-trimethoxybenzene and 1,2,4,5-tetrachlorobenzene were used as internal standards when needed.

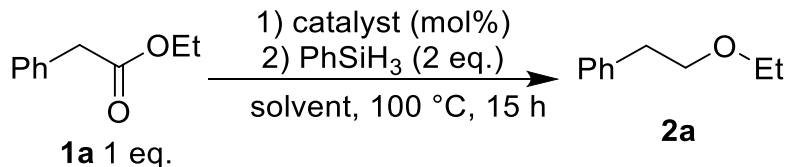
HRMS-ESI analyses were performed on a ThermoFisher Scientific Exactive spectrometer with a resolution of 100.000 at PSM-GRITA-Pharm. Dept.-University Lille Nord de-France.

BARF salts were purchased from Strem or prepared as reported^{S1} and subsequently dried under high vacuum (10⁻⁷mbar, 14h, 50°C). All BARF salts were stored and weighted in a glovebox.

Ester substrates were purchased and used as received or prepared following our general procedure.

II) Additional experimental data: screenings

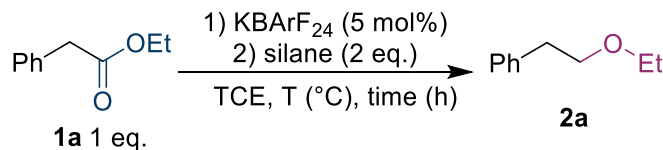
Table S1. Screening of other catalysts and reaction conditions.



Entry	Catalyst (mol%)	Solvent	Time (h)	Yield 2a (%) ^[a]
1	Ph ₃ CB(C ₆ F ₅) ₄ (5) ^[c]	TCE ^[b]	15	0
2	Ph ₃ CB(C ₆ F ₅) ₄ (5) ^[c]	1,4-dioxane	15	0
3	Ph ₃ CB(C ₆ F ₅) ₄ (5) ^[c]	Anisole	15	0
4	Ph ₃ CB(C ₆ F ₅) ₄ (5) ^[c]	(nBu) ₂ O	15	0
5	Ph ₃ CB(C ₆ F ₅) ₄ (5) ^[c]	CPME ^[d]	15	19
6	Ph ₃ CB(C ₆ F ₅) ₄ (5) ^[c]	decane	15	0
7	Ph ₃ CB(C ₆ F ₅) ₄ (5) ^[c] + KH (5)	TCE	15	0
8	Ph ₃ CB(C ₆ F ₅) ₄ (5) ^[c] + KH (5)	Toluene	15	0
9	KOH	TCE	15	0
10	KOH	Toluene	15	0
11	KH	TCE	15	0
12	KH	Toluene	15	0
13	KCl	TCE	15	0
14	KF	TCE	15	0
15	KF	Toluene	15	0
16	KPF ₆	TCE	15	0

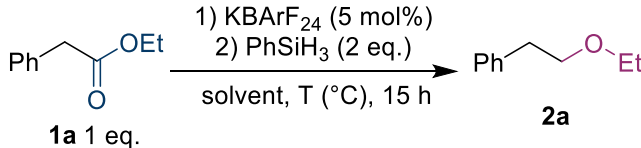
[a] Determined by GC. [b] TCE: 1,1',2,2'-tetrachloroethane. [c] trityl tetra(pentafluorophenyl)borate.

[d] CPME: cyclopentylmethylether.

Table S2. Screening of hydrosilanes.

Entry	Silane (eq.)	Time (h)	Yield ^a (%)
1	PhSiH ₃ (2)	15	100
2	PhSiH ₃ (1)	15	31
3	PhSiH ₃ (2)	6	95
4	Ph ₂ SiH ₂ (2)	6	85
5	HexylSiH ₃ (2)	6	86
6	PhMe ₂ SiH (2)	6	44
7	TMDS (2)	6	24
8	Et ₃ SiH (2)	24	32
9	(EtO) ₃ SiH (2)	24	0
10	Ph ₃ SiH (2)	6	0

[a] Determined by GC. [b] TCE: 1,1',2,2'-tetrachloroethane.

Table S3. Screening of solvents.

Entry	Solvent	T (°C)	Yield (%) ^[a]
1	TCE ^[b]	100	100
2	TCE ^[b]	50	-
3	Dichloromethane	40	-
4	Toluene	100	-
5	Anisole	100	-
6	Tetrahydrofuran	65	-
7	Cyclopentylmethylether	100	-
8	Dioxane	100	-
9	Acetonitrile	100	-

[a] Determined by GC. [b] TCE: 1,1',2,2'-tetrachloroethane.

NMR study

NMR experiments were performed on the following spectrometers:

- AvanceIII HD 600 equiped with a 5 mm cryo-probe HDCNF (CP-QCI) at 298 K and 343 K.

- AvanceIII 300 equiped with a 5 mm probe broad-band direct (BBO) at 298 K and 373 K.

The following experiments were performed : 1D-¹H, 1D-¹H{¹⁹F}, 1D-¹H-TOCSY selective ($T_m=200$ ms), 1D-¹H-NOESY selective ($T_m=500$ ms)

2D-¹H-*T1*(*inversion recovery*), 2D-¹H-DOSY,

1D-¹¹B{¹H}, 1D-¹¹B{¹H} (*inverse-gated*, DEPTH and Hahn echoes), 2D-¹H-¹¹B-HSQC(10 Hz),

1D-¹⁹F{¹H}, 2D-¹⁹F-*T1*(*inversion recovery*), 2D-¹⁹F-DOSY,

1D-¹³C{¹H/¹⁹F}, 1D-¹H-¹³C-DEPT135(167 Hz), 1D-¹⁹F-¹³C-DEPT45(250 Hz), 2D-¹H-¹³C-HSQC(167 Hz),

2D-¹H-¹³C-{¹⁹F}-HMBC(10 Hz), 2D-¹⁹F-¹³C-HSQC(250 Hz), 2D-¹⁹F-¹³C-HMQC(250 Hz), 2D-¹⁹F-¹³C-HMBC(10 Hz),

2D-¹H-²⁹Si-HSQC(200 Hz), 2D-¹H-²⁹Si-HSQC-DEPT(200 Hz).

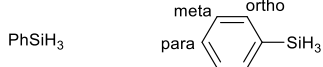
Three samples were studied:

- **sample A**: NaBArF₂₄ (1.12 mmol) in TCE-d² (0.6 mL, dry)

- **sample B**: NaBArF₂₄ (1.12 mmol) + PhSiH₃ (1 eq., 1.12 mmol) in TCE-d² (0.6 mL, dry)

- **sample C**: NaBArF₂₄ (1.12 mmol) + PhSiH₃ (10 eq., 11.2 mmol) in TCE-d² (0.6 mL, dry)

Table S4. ¹H and ¹³C NMR data of samples **B** and **C** in TCE-d² at 343 K focusing on PhSiH₃.



		H_nSi CS (¹ H) / CS (¹³ C)	Ipsos C ² J (H _{Si} -C _i) CS (¹³ C)	Ortho CH CS (¹ H) / CS (¹³ C)	Meta CH CS (¹ H) / CS (¹³ C)	Para CH CS (¹ H) / CS (¹³ C)
Sample B	Major species 1	4.16 / nd	- 128.2	7.55 / 135.8	7.31 / 127.9	7.36 / 129.7
	Minor species 2	5.19 / nd	- 130.1	7.64 / 133.8	7.40 / ca.128.2	7.46 / ca.131.0
	Major species 1	4.15 / -58.9	4.4 128.1	7.55 / 135.7	7.32 / 127.9	7.37 / 129.7
Sample C	Minor species 2	5.18 / -17.1	8.8 130.0	7.64 / 134.2	7.42 / 128.3	7.45 / 131.1

According the ¹H and ¹³C NMR data of samples **B** and **C** (Table S4), we observed 2 silane species in solution, a major **1** (PhSiH₃) and a minor **2**, which were not in exchange. Trace amounts of other species were observed but not reported. Investigations by ²⁹Si NMR experiments failed in characterizing the species.

Table S5. ^1H , ^{13}C and ^{19}F NMR data of samples **A**, **B** and **C** (averaged values) in TCE-d² at 343 K focusing on NaBArF₂₄.

The figure shows the chemical structure of NaBArF₂₄ (left), which consists of a central boron atom bonded to four phenyl groups (Ph) and four trifluoromethyl groups (CF₃). The phenyl groups are labeled 'meta', 'ortho', and 'para' relative to the boron atom. The trifluoromethyl groups are labeled 'ipso'. A sodium cation (Na⁺) and a fluoride anion (F⁻) are shown as counterions. To the right, two possible intermediates are shown within a dashed box:

- I:** Shows a Ph-Si-H group interacting with a boron atom through a C-F bond. The silicon atom is bonded to a phenyl group (Ph) and two fluorine atoms (F). The boron atom is bonded to a phenyl group (Ph) and three trifluoromethyl groups (CF₃). A dashed line indicates the interaction between the silicon-hydrogen bond and the boron-trifluoromethyl bond.
- II:** Shows a Ph-Si-H group interacting with a boron atom through a Si-H bond. The silicon atom is bonded to a phenyl group (Ph) and two fluorine atoms (F). The boron atom is bonded to a phenyl group (Ph) and three trifluoromethyl groups (CF₃). A dashed line indicates the interaction between the silicon-hydrogen bond and the boron-trifluoromethyl bond.

Species

	Ipso C CS (^{13}C)	Ortho CH CS (^1H) / CS (^{13}C)	Meta C CS (^{13}C) / $^2J(\text{C}-\text{F})$	Meta CF ₃ CS (^{19}F) / CS (^{13}C) / $^1J(\text{C}-\text{F})$	Para CH CS (^1H) / CS (^{13}C)	Presence in sample (relative abundance Ref. 1.000)
1 possible adduct	141.8	7.95 137.5	131.8 33.6	-62.7 122.9 273.8	8.16 126.4	B (0.65) and C (0.72)
2		7.55 150.0	131.0 33.0	-62.5 123.5 273.5	7.77 120.7	B (0.40)
3 NaBArF ₂₄	161.5	7.67 134.6	128.7 31.4	-62.0 124.5 273.2	7.49 117.3	A (1.00) and B (1.00) and C (1.00)
4	-	7.79 128.6	131.4 33.4	-62.6 123.2 272.8	7.84 122.3	A (0.11) and B (0.20) and C (0.12)
5	-	8.12 133.8	131.5 33.4	-62.62 23.1 273.3	8.02 125.2	A (0.12)

According to the ^1H , ^{13}C and ^{19}F NMR data of samples **A**, **B** and **C** (Table S5), we observed 5 species in solution. Among the most abundant, **3** was the starting NaBArF₂₄ and **1** may appear as a possible adduct between NaBArF₂₄ and PhSiH₃ (intermediates **I** and/or **II** vide supra Table S5). It was worth to note an exchange was observed between species **1** and **2**. Other species were minor compounds: **4** and **5** being impurities present with the NaBArF₂₄ reagent and **2** being a transient intermediate only observed in sample **B**. By comparing species **3** (NaBArF₂₄) and **1**, the latter showed the averaged para aromatic carbons and related protons comprised between the CF₃ groups had deshielded chemical shifts respectively of about 10 ppm and 0.65 ppm (Table S5). While averaged ipso aromatic carbons bound to the boron atom were shielded of about 20 ppm, the related meta and ortho aromatic carbons as well as ortho protons had higher chemical shifts. Though these NMR features may suggest an adduct between NaBArF₂₄ and PhSiH₃ with possible interactions between the silane $\sigma(\text{Si}-\text{H})$ and the borate $\sigma(\text{C}_{\text{para}}-\text{H})$ and $p(\text{C}_{\text{para}})$ orbitals (intermediates **I** and/or **II** vide supra Table S5), further interpretations proved to be difficult.

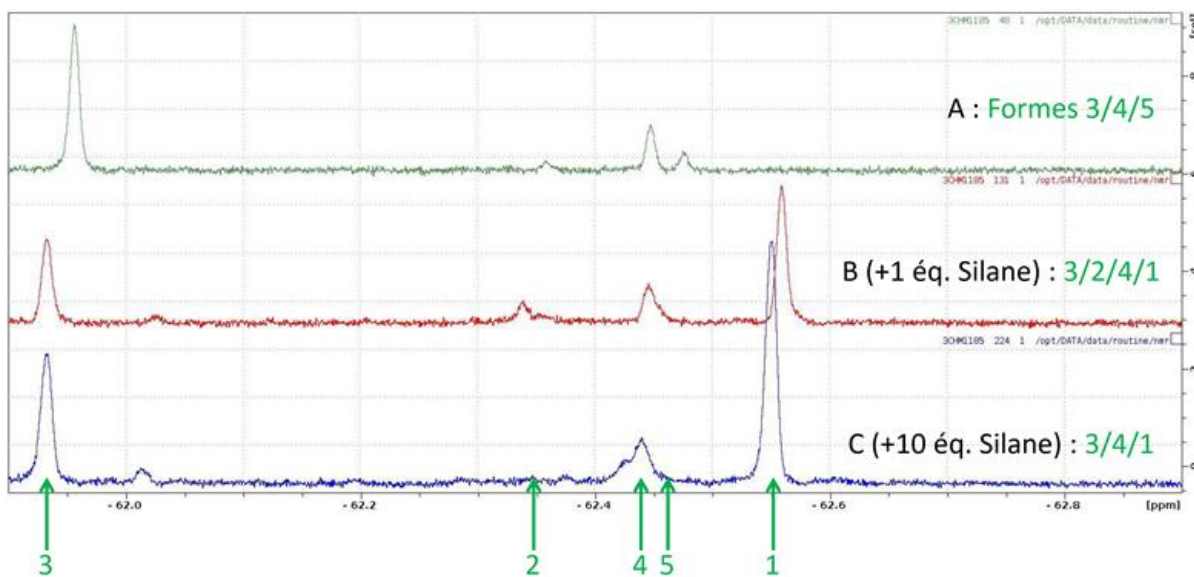


Figure S1. $^{19}\text{F}\{\text{NON-}^1\text{H}\}$ NMR spectrum of samples **A**, **B** and **C** at 298 K.
Species **3** is NaBArF_{24} . Species **1** is a possible adduct between NaBArF_{24} and PhSiH_3 . Minor species **4** and **5** are impurities in the starting NaBArF_{24} . Species **2** appeared as an intermediate only present in sample **B**.

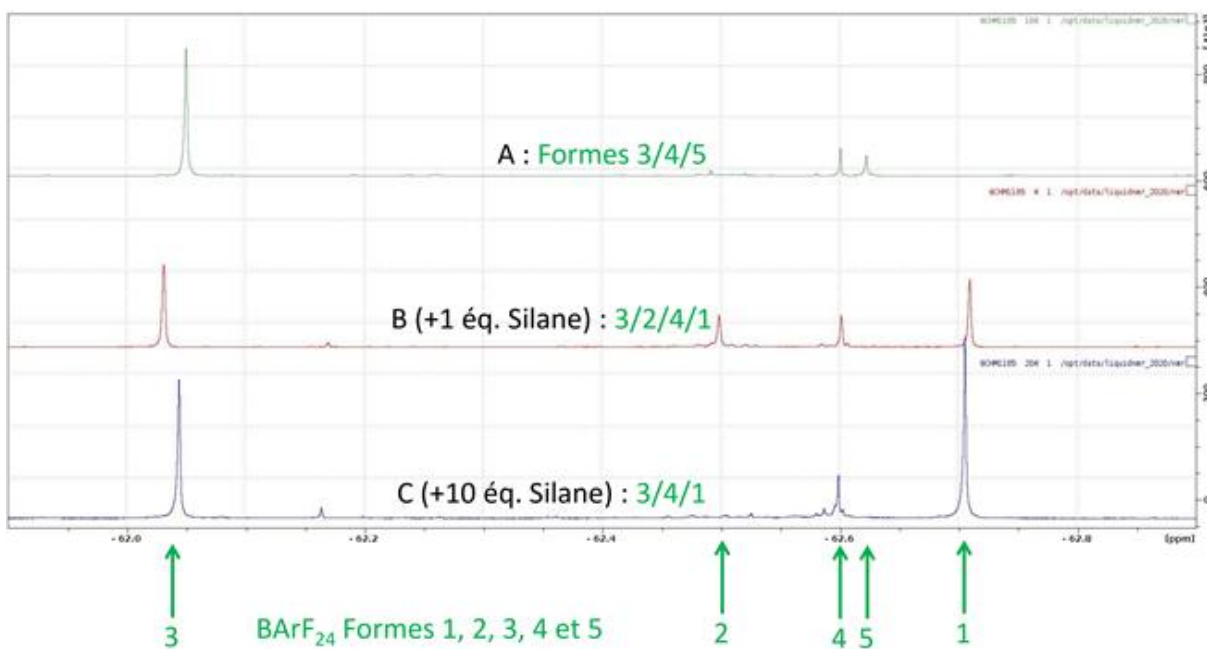


Figure S2. $^{19}\text{F}\{^1\text{H}\}$ NMR spectrum of samples **A**, **B** and **C** at 343K.
Species **3** is NaBArF_{24} . Species **1** is a possible adduct between NaBArF_{24} and PhSiH_3 . Minor species **4** and **5** are impurities in the starting NaBArF_{24} . Species **2** appeared as an intermediate only present in sample **B**.

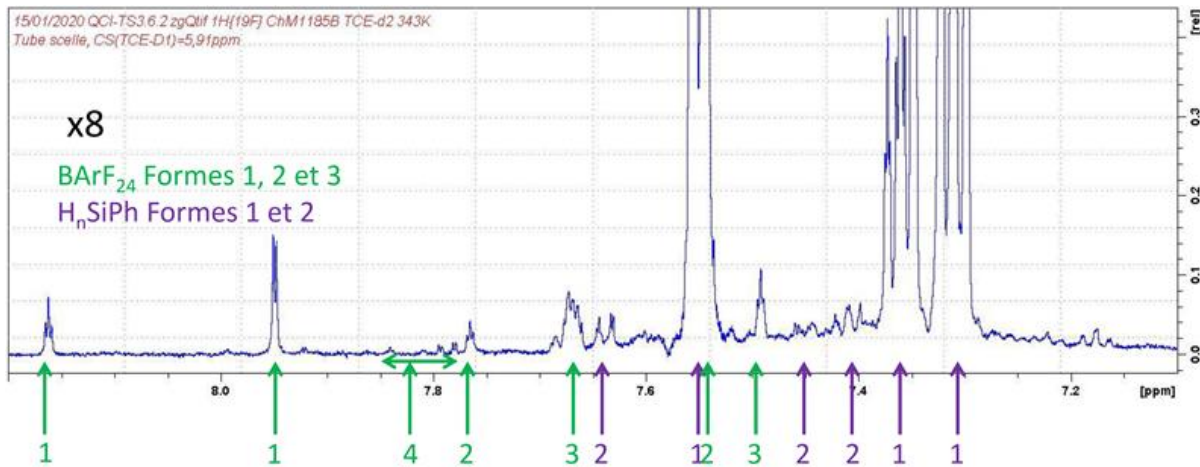


Figure S3: $^1\text{H}\{^9\text{F}\}$ NMR spectrum (aromatic H) of sample **B** at 343K.
Species **3** is NaBArF₂₄. Species **1** is a possible adduct between NaBArF₂₄ and PhSiH₃. Minor species **4** and **5** are impurities in the starting NaBArF₂₄. Species **2** appeared as an intermediate only present in sample **B**.

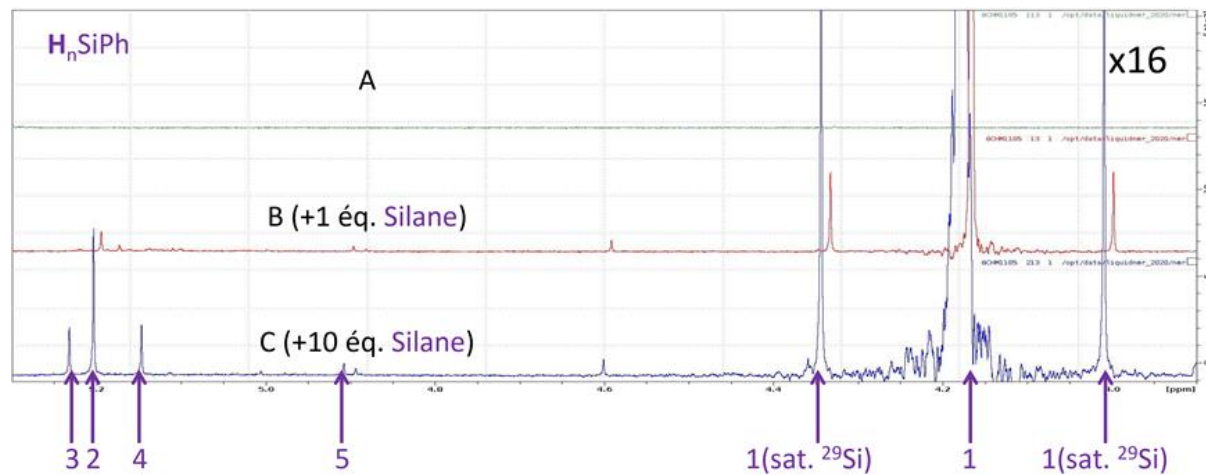


Figure S4: $^1\text{H}\{^9\text{F}\}$ NMR spectrum (aliphatic H) of samples **A**, **B** and **C** at 343K.
Species **3** is NaBArF₂₄. Species **1** is a possible adduct between NaBArF₂₄ and PhSiH₃. Minor species **4** and **5** are impurities in the starting NaBArF₂₄. Species **2** appeared as an intermediate only present in sample **B**.

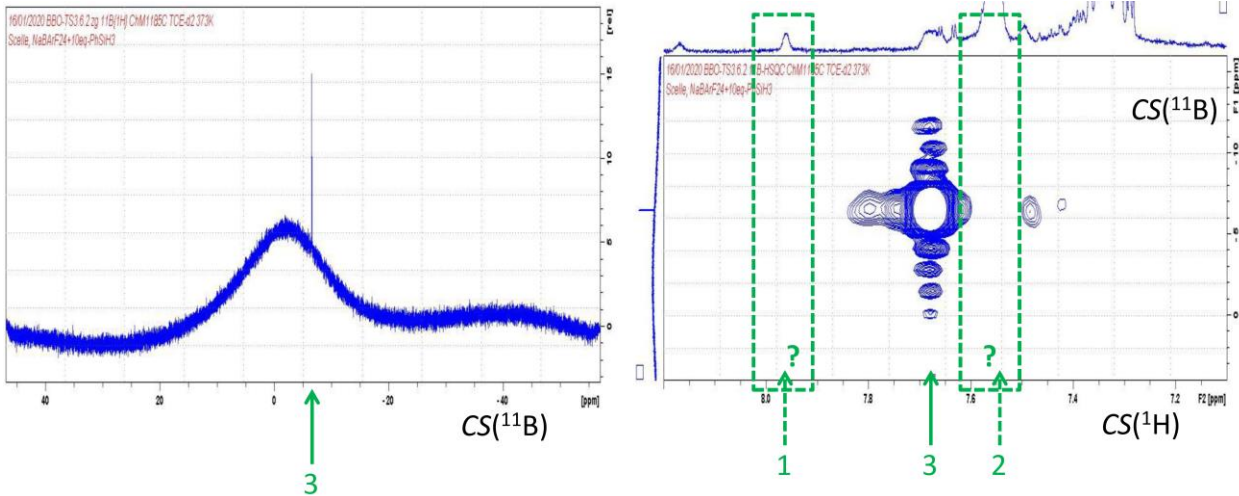


Figure S5. $^{11}\text{B}\{\text{H}\}$ NMR spectrum of sample G (left). Same versus a 1D- ^1H spectrum non decoupled of ^{19}F (right).

It was worth to note the boron of species **3** was the single observed in spite the existence of species **1** and **2** in similar abundance. The boron signal of species **3** is fine and proves the boron atom is in a tetrahedral environment. This might suggest the boron atoms of species **1** and **2** don't have a strict tetrahedral geometry and would imply unidentified broader signals which can be hardly resolved from the broad signals issued from the NMR tube (pyrex) and the probe glassware. The couplings of the ortho ^1H from species **1** (doublet at 7.95 ppm) and **2** (hidden under the silane) are clearly different from the one of species **3** (broad multiplet at 7.67 ppm).

III) Additional computational data:

All the calculations in this study have been performed with density functional theory (DFT), with the aid of the Turbomole 7.1 suite of programs,^{S2} using the PBE functional^{S3}. The TZVP^{S4} basis set has been employed. The resolution of identity (RI),^{S5} along with the multipole accelerated resolution of identity (marij)^{S6} approximations have been employed for an accurate and efficient treatment of the electronic Coulomb term in the DFT calculations. Solvent corrections were incorporated with optimization calculations using the COSMO model^{S7}, with 1,1,2,2-tetrachloroethane ($\epsilon = 8.2$) as the solvent. For the solvent free systems, the calculations were done without solvent correction. In addition, the intrinsic reaction coordinate (IRC)^{S8} calculations were done with all the transition states in order to further confirm that they were the correct transition state, yielding the correct reactant and product structures. The values reported are ΔG values, with zero-point energy corrections, internal energy and entropic contributions included through frequency calculations on the optimized minima, with the temperature set to 298.15 K. The translational entropy term in the calculated structures was corrected through a free volume correction introduced by Mammen *et al.*^{S9} This volume correction is to account for the unreasonable enhancement in translational entropy that is generally observed in computational softwares. Harmonic frequency calculations were performed for all stationary points to confirm them as local minima or transition state structures. Then, in order to find the efficiency of the catalytic cycle in our mechanism, we have calculated the relative efficiency with the AUTOF^{S10,S11} program by employing the “Energetic Span Model” (ESM), on all the free energy profiles discussed in the manuscript. The turn over frequency (TOF) calculations take into account the principal rate-determining transition state, potentially rate-influencing transition states and intermediates during the catalysis process. The TOF were calculated by the following equation:

$$\text{TOF} = \frac{K_B T}{h} e^{-\delta E / RT}$$

$\delta E = TTDTS - TTDI$ If TDTs appears after TDI

$\delta E = TTDTS - TTDI - \Delta Gr$ If TDTs appears before TDI

This model has been employed to calculate the TOFs for the free energy profiles obtained for the mechanisms in solvent phase discussed in the manuscript. This model can also be employed for stoichiometric reactions, where the TOF would correspond to the efficiency of the reaction.

The nature of the interaction in intermediate species was investigated with the natural bond orbital (NBO) analysis procedures as implemented in the Gaussian 09 program. The analysis was performed at the PBEPBE/TZVP optimized geometry using the PBEPBE density functional together with the all electron TZVP basis set.

In order to gain insight into the interaction of the catalyst with the substrate moiety, the intermolecular charge transfer in the complex has been analysed with the natural bond orbital (NBO) analysis. The energetic estimate of donor (i) – acceptor (j) orbital interactions can be obtained by the second order perturbation theory analysis of the Fock matrix in the NBO basis.

The donor–acceptor interaction energy $E(2)$ is given by

$$E(2) = \Delta E(i,j) = q(i,j)F(i,j)^2 / \{\varepsilon(i) - \varepsilon(j)\}$$

Where $q(i)$ is the donor orbital occupancy, $\varepsilon(i)$ and $\varepsilon(j)$ are the diagonal elements (orbital energies), and $F(i,j)$ is the off-diagonal NBO Fock matrix element. In the present investigation, the important interactions between the K^+ ion of the catalyst and the oxygen atoms of the substrate have been analyzed.

NCI analysis.

The NCI plot^{S12} iso-surfaces have recently been used to characterize noncovalent interactions. They correspond to both favourable and unfavourable interactions, as differentiated by the sign of the second-density Hessian eigenvalue and defined by the isosurface color. The color scheme is a red yellow-green-blue scale with red for ρ_{cut}^+ (repulsive) and blue for ρ_{cut}^- (attractive).^{S13} The Turbomole 7.1 suite of programs, using the PBE / TZVP level of theory, has been used to generate the NCI plot.

For **Intermediate_2**, we have computed the NCI plot which is represented in Figure S6 and Figure S7. Several small and green isosurfaces that characterize weak non-covalent interactions throughout the catalyst and the reactant in **Intermediate_2** can be observed. The green isosurfaces, which are of the interest, have been circled with red and further marked with white arrows. Hence, these isosurfaces clearly indicate an attractive interaction between the K^+ of the catalyst and the two oxygens of the ester reactant, as shown in Figure S6. Similarly, the weak interactions between the C-F and Si-H bonds have been shown by green isosurfaces circled in red in Figure S7.

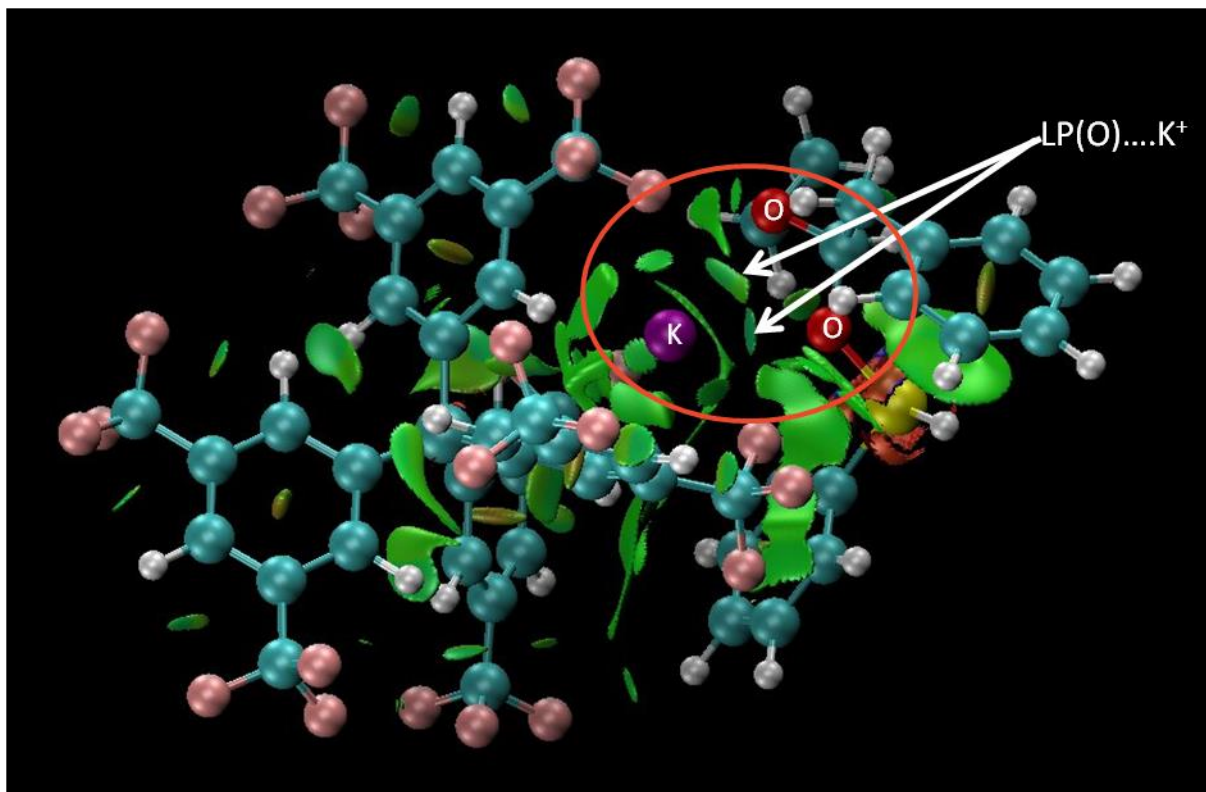


Figure S6. Visualized non-covalent interactions in **Intermediate_2** between the K^+ of the catalyst and both the oxygens of the ester reactant.

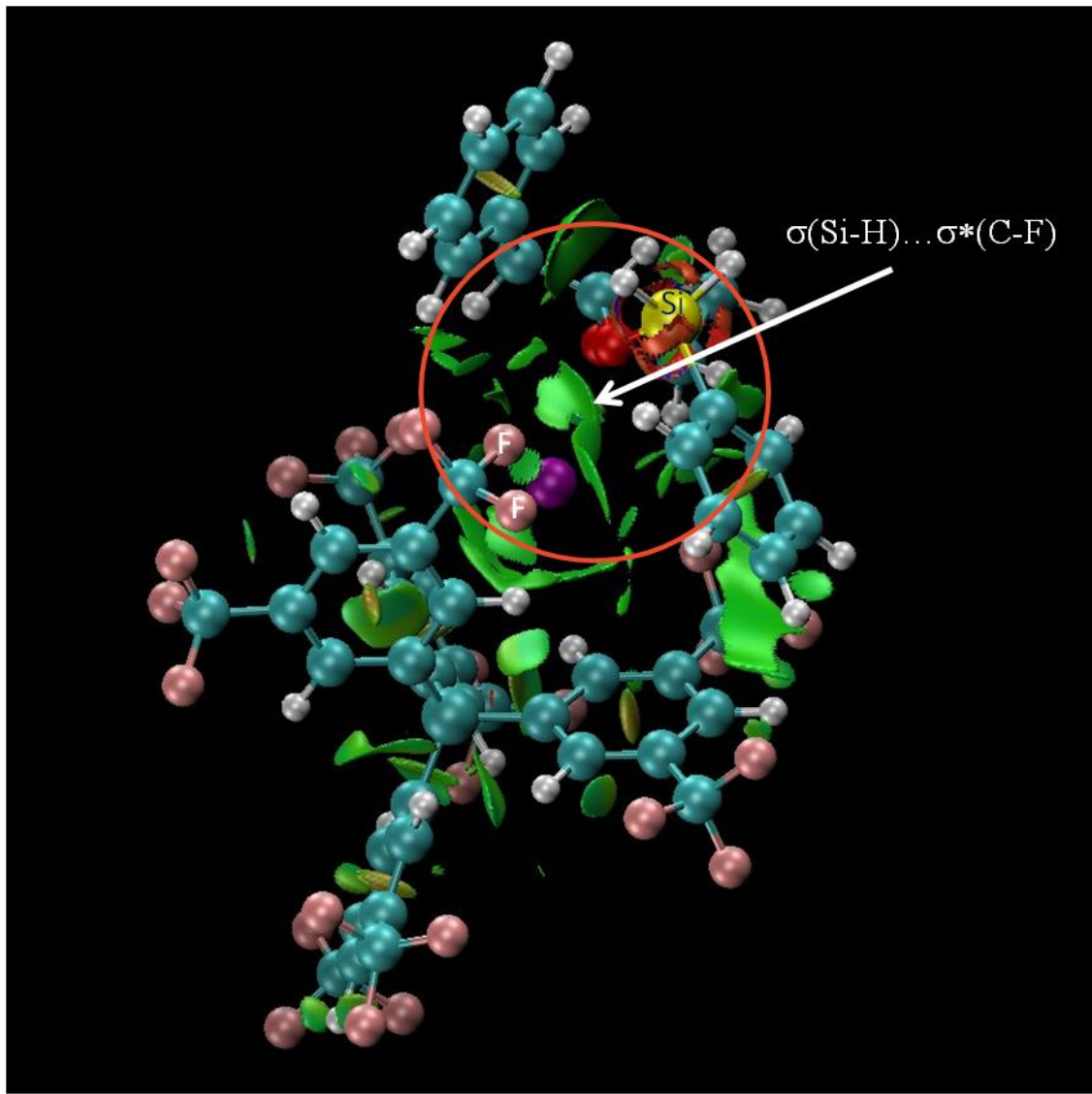


Figure S7. Visualized non-covalent interactions in **Intermediate_2** between the C-F and the Si-H bonds.

NBO analysis

NBO analysis has been employed in order to understand the role of the cation (K^+) in the catalysis (see Figure S8, Table S6 and the SI for details). We have focused on the 2nd order perturbation energy extracted from the NBO analysis to figure out about the possible non-covalent interaction between two separate moieties. In the present study, an interaction of interest is between the K^+ ion of the $K\text{BArF}_{24}$ catalyst and the oxygen atom of the ester reactant.^{S14} From the interaction energy values (28.5 kcal/mol and 38.7 kcal/mol shown in Table S6, entries 1 and 2) and the NBO images (shown in Figure S8), it is clear that there is a moderate to high overlap between K^+ and oxygen of the ester reactant. Furthermore, we have also looked at the orbital interaction between the Si center of the silane reagent with the fluorine atoms of the $K\text{BArF}_{24}$ catalyst.^{S15} We have seen one weaker interaction (19.0 kcal/mol shown in Table S6, entries 3 and 4) and one comparatively stronger interaction (58.2 kcal/mol) between the Si-H bond of the silane reagent and the C-F bond of the $K\text{BArF}_{24}$ catalyst (shown in Figure S9).

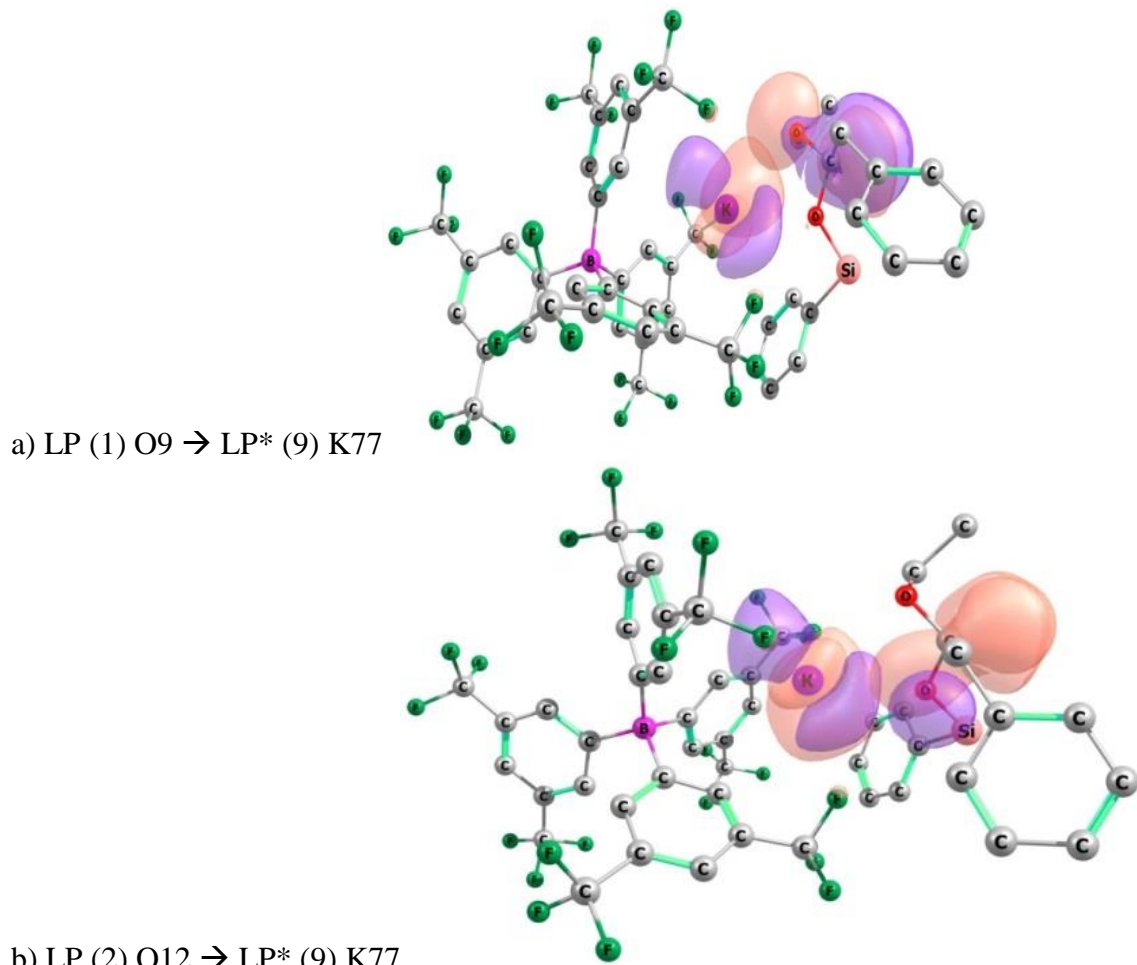
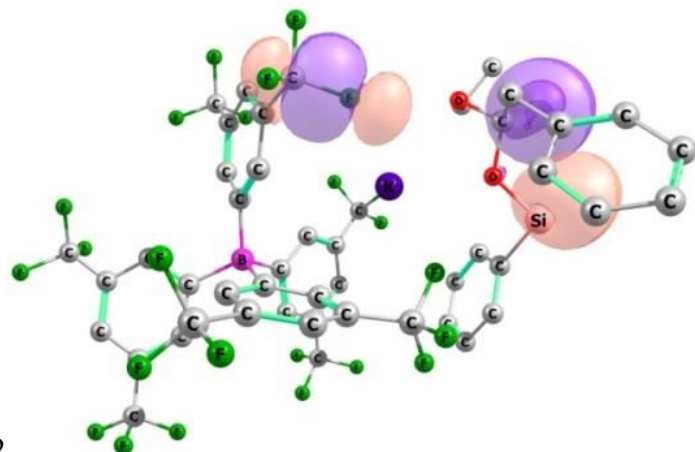


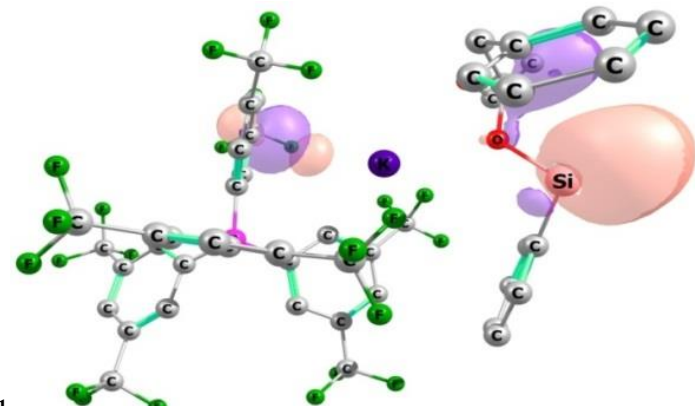
Figure S8. Second order perturbation theory analysis of the Fock matrix in NBO basis showing the important interactions between the K^+ ion of the catalyst and the oxygen atom of the reactant species: a) LP (1) O9 → LP* (9) K77, b) LP (2) O12 → LP* (9) K77.

Table S6. Interaction energy values from the NBO analysis for: the interaction between the K⁺ ion of the catalyst and the oxygen atom of the reactant species (entries 1 and 2) and the interaction between the Si center of the substrate with the fluorine of the catalyst (entries 3 and 4).

Entry	Donor(i)	Occupancy	Acceptor(j)	Occupancy	E2
1	LP (1) O9	1.95	LP* (9) K77	0.005	28.5
2	LP (2) O12	1.89	LP* (9) K77	0.005	38.7
3	BD (1) Si13-H78	1.98	BD* (1) C58-F62	1.97	58.2
4	BD (1) Si13-H78	1.98	BD* (1) C58-F61	1.95	19.0



a) BD (1) Si13 - H78 → BD* (1) C58 - F62



b) BD (1) Si13 - H78 → BD* (1) C58 - F61

Figure S9. Second order perturbation theory analysis of the Fock matrix in NBO basis showing the important interaction between Si center of the substrate with the fluoride of the catalyst: a) BD (1) Si13 - H78 → BD* (1) C58 - F62 and b) BD (1) Si13 - H78 → BD* (1) C58 - F61.

Reaction mechanism in presence of KBArF₂₄ catalyst.

In order to understand the mechanism of this reductive deoxygenation reaction, we have performed full quantum chemical calculations using density functional theory (DFT) at the PBE/TZVP level of theory. In the first step of the reaction, PhSiH₃ forms a metastable complex with the KBArF₂₄ catalyst (Figure S10). The potassium cation of the catalyst shows a cation–pi interaction with the phenyl group attached to Si and the resulting complex is additionally stabilized by the weak interactions between the Si center of the reagent and the fluoride atoms of the BArF₂₄ anion (see the NBO analysis Figure S8 and Table S6). The reaction free energy (ΔG) for this complex formation is 1.1 kcal/mol. In the second step of the reaction, both oxygens of the ester reactant show moderate to weak interactions with the potassium cation,^{S14} whereas weak interactions between C-F and Si-H bonds^{S15} have also been found (Figure S10 and see the NBO analysis Figure S9 and Table S6).

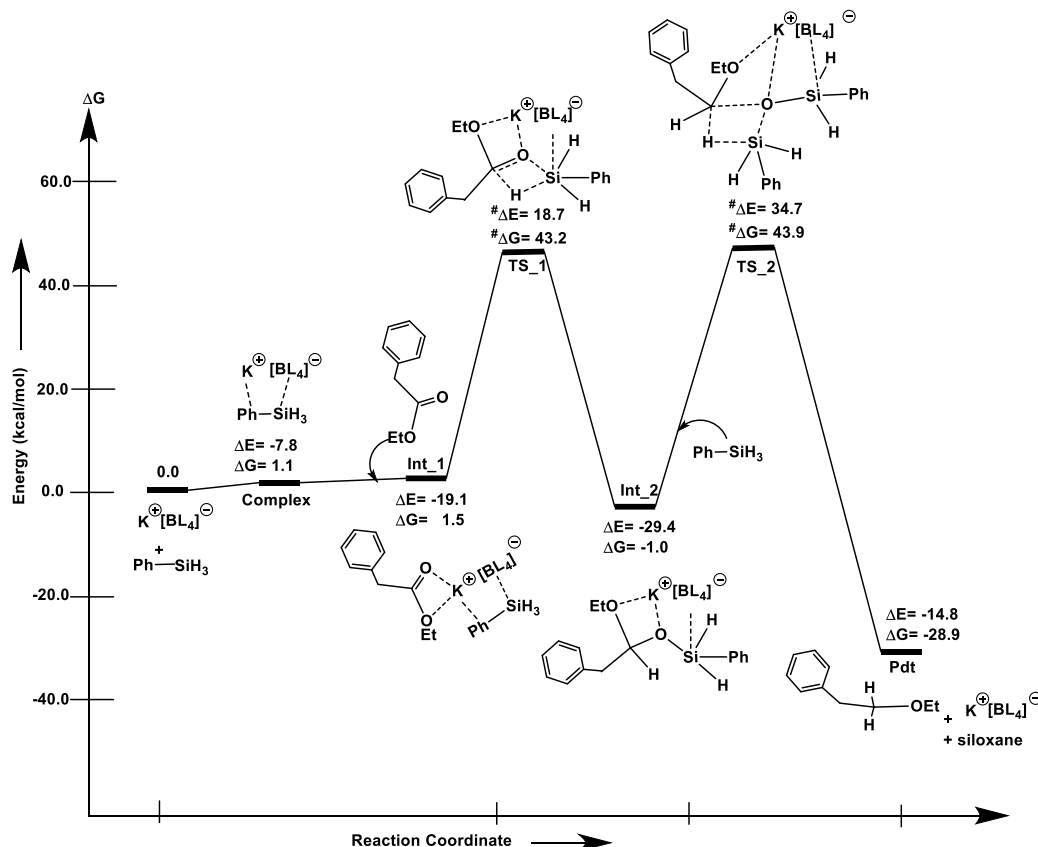


Figure S10. The reaction profile for the desired reductive deoxygenation of esters to ethers through hydrosilylation in the presence of catalyst. The values (in kcal/mol) have been calculated at the PBE/TZVP level of theory at 298 K. At 373K, barriers were higher: TS_1 = 54.1 kcal/mol (373 K) and TS_2 = 49.3 kcal/mol (373 K) [gas phase values]. In the liquid phase, the barriers calculated at 373 K were also higher: TS_1 = 54.1 kcal/mol (373 K) and TS_2 = 49.3 kcal/mol (373 K).

These non-covalent interactions are further supported by results from visualization with the NCI plot (see Figures S6 and S7). All these interactions lead to the formation of intermediate Int_1 with

a reaction free energy (ΔG) of 1.5 kcal/mol. Additional calculations with n hexylSiH₃, another possible hydrosilane, indicated the intermediate Int_1 was thermodynamically less stable by 6.0 kcal/mol which is acceptable under the given reaction conditions. By comparison to the regular silane activation modes operating through oxidative addition, cooperation metal-ligand, double activation metal-substrate or heterolytic polar electrophilic activation,^{S16} our catalytic reaction relies on a silane activation through noncovalent interactions. Though it may appear similar to the already reported examples using frustrated Lewis pairs as catalysts,^{S17,S18} it apparently proceeds in a different way. It is worth to note that an intermediate involving a cation – pi interaction between the potassium and the phenyl group attached to the ester reagent is not favourable (see the mechanism S1 and Figures S10, S12). Moreover, a pentavalent silicon intermediate resulting from the coordination of one oxygen atom of the ester to the silicon centre of phenylsilane is not stable and therefore not considered further (see the mechanism S2 and Figures S10, S12).

In the next step, intermediate Int_2 formation takes place *via* a four-membered transition state TS_1 implying the ester reagent and a first molecule of phenylsilane and shows the most favourable calculated activation free energy barrier at 43.2 kcal/mol^{S19} (Figures S10 and S12, Scheme S1). It is worth noting that the ΔG corresponding to the energy barriers have been calculated at room temperature and the obtained values may appear high even after volume corrections for the translational entropy term. This is due to the overestimation of the entropy loss during the reaction in the calculations. The real values of the energy barriers are, therefore, likely to be lower.

Further calculations of the barriers at 373 K led to higher values by comparison to the barriers calculated at 298 K: 48.1 kcal/mol for TS_1 (instead of 43.2) and 46.3 kcal/mol for TS_2 (instead of 43.9) [gas phase]. Moreover, while considering possible interactions of solvent with the reagents and catalyst, the barriers calculated at 373 K were also higher: 54.1 kcal/mol for TS_1 (instead of 43.2) and 49.3 kcal/mol for TS_2 (instead of 43.9) [liquid phase].

Transition state TS_1 implies the hydride from the silane reagent is transferred to the carbonyl carbon of the ester reactant reducing the C=O double bond into a single bond with formation of the Si-O bond. For this step, the reaction free energy (ΔG) is highly favourable, by 2.5 kcal/mol, leading to the formation of intermediate Int_2. It is also relevant that a transition-state based on a single cation–pi interaction of the potassium with the phenyl group of the silane leads to a highly unfavourable energy barrier (see the mechanism S3 and Scheme S1).

In the last step of the reaction mechanism, the second phenylsilane reagent molecule is also added, and makes another four membered transition state TS_2 implying the partially reduced ester reagent as acetal and a second molecule of phenylsilane from intermediate Int_2 with an activation free energy barrier of 43.9 kcal/mol (Figure S10). In this transition state, the hydride of the phenyl silane is transferred to the carbon of the ester group to break simultaneously the C-O bond and form the reduced ether product along with the siloxane co-product and the regenerated catalyst. It is worth to note the C-O-Si bond is preferentially cleaved as respect to the C-O-Et bond. The thermodynamics study suggests that the formation of the ethylether product is more stable by 5.8 kcal/mol in comparison to the silylated ether, and the energy barrier for the formation of the ethylether product is also lower by 8.9 kcal/mol (Figures S10, S12). Hence, the reaction free energy (ΔG) for the product formation step is of 28.9 kcal/mol. Considering the favourable value of the turnover frequency (TOF) (8.30×10^5 times of the efficiency than the non-catalyst case, Table S4), obtained from the calculations with the Energetic Span Model (ESM) which allows to consider the whole mechanism kinetics as well as thermodynamics,^{S20} we can conclude the reductive deoxygenation reaction may be feasible under the experimental reaction conditions.

In order to understand the solvent effect, the calculations done with TCE have also been performed with toluene (Figure S11). This solvent does not allow the reaction to proceed experimentally and is also not favourable according our calculations. In addition, turn over frequency (TOF) have been calculated using the Energetic Span Model (ESM) which allows to consider the whole mechanism kinetics as well as thermodynamics.^{S20} The relative efficiency values with and without catalyst (respectively $5.9 \times 10^{-21} \text{ s}^{-1}$ and $7.1 \times 10^{-27} \text{ s}^{-1}$) indicate that the mechanism with catalyst is approximately 8.30×10^5 times more efficient than the corresponding mechanism without catalyst in the solvent phase. We also observe the reaction in TCE solvent is favoured being 3.7×10^6 times more efficient than in toluene (table S7).

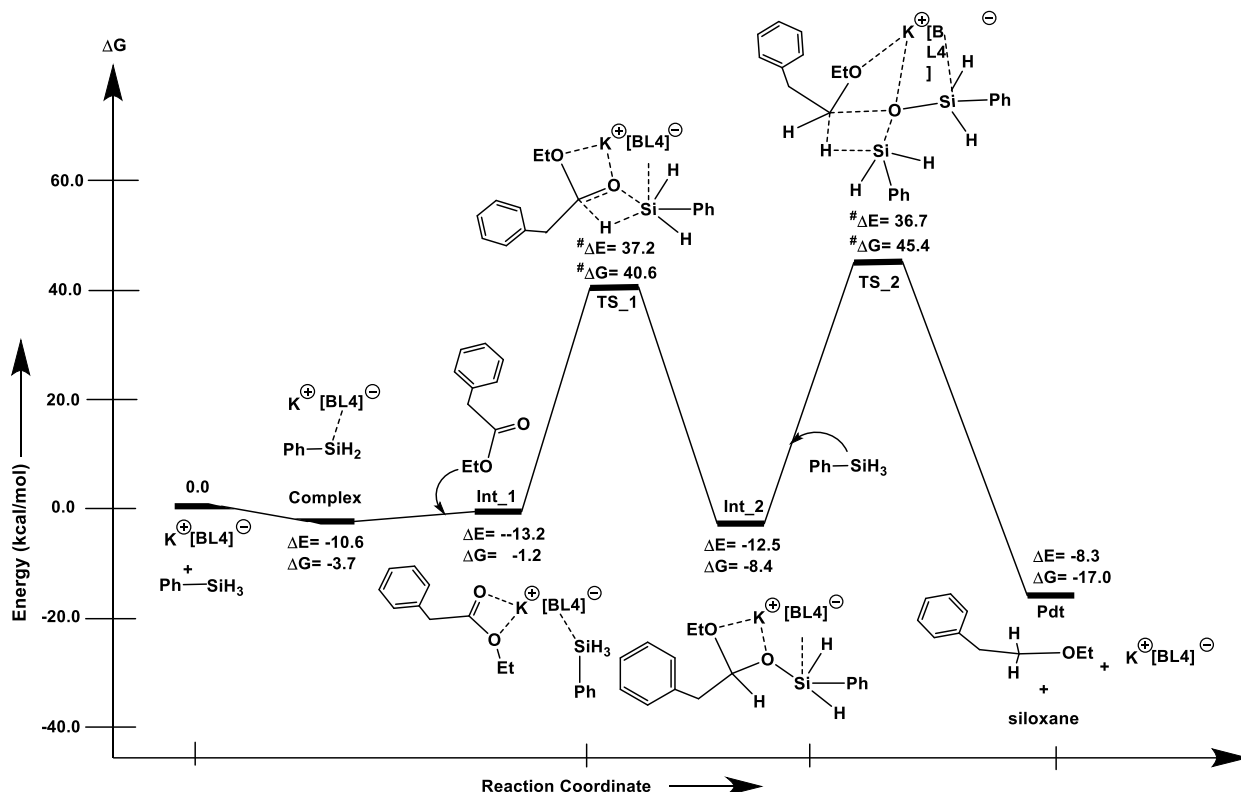


Figure S11. The reaction profile for the desired reductive deoxygenation of esters to ethers through hydrosilylation in the presence of catalyst in toluene solvent. The values (in kcal/mol) have been calculated at the PBE/TZVP level of theory (gas phase).

Table S7. The values for the relative efficiency obtained for both the mechanisms in the solvent phase.

Mechanism	Relative Efficiency
With the catalyst in TCE solvent	$5.9 \times 10^{-21} \text{ s}^{-1}$
With the catalyst in Toluene solvent	$2.2 \times 10^{-27} \text{ s}^{-1}$
Without the catalyst in TCE solvent	$7.1 \times 10^{-27} \text{ s}^{-1}$

The relative efficiency values indicate that the mechanism with catalyst is approximately 8.3×10^5 times more efficient than the corresponding mechanism without catalyst in the TCE solvent, and is also 2.7×10^6 times more efficient than in toluene solvent.

Reaction mechanism in absence of catalyst.

In order to probe our theoretical study, we have also investigated the mechanism without the catalyst (see Figure S12). In the first step, the reactants (ester and PhSiH_3) form intermediate_1 via a four-membered transition state TS_1 with an activation free energy barrier of 53.1 kcal/mol. The activation energy barriers of transition state TS_1 for the two cases: “with-catalyst” and “without-catalyst”, are 43.2 kcal/mol and 53.1 kcal/mol respectively. This suggests that the case without catalyst, where the barrier is ~ 10.0 kcal/mol higher than the catalytic pathway, is unfavourable and unlikely to take place under the experimental reaction conditions. As control experiments confirm this result (see table 1, entry 10), we have concluded the reductive deoxygenation reaction proceeds exclusively in the presence of the catalyst.

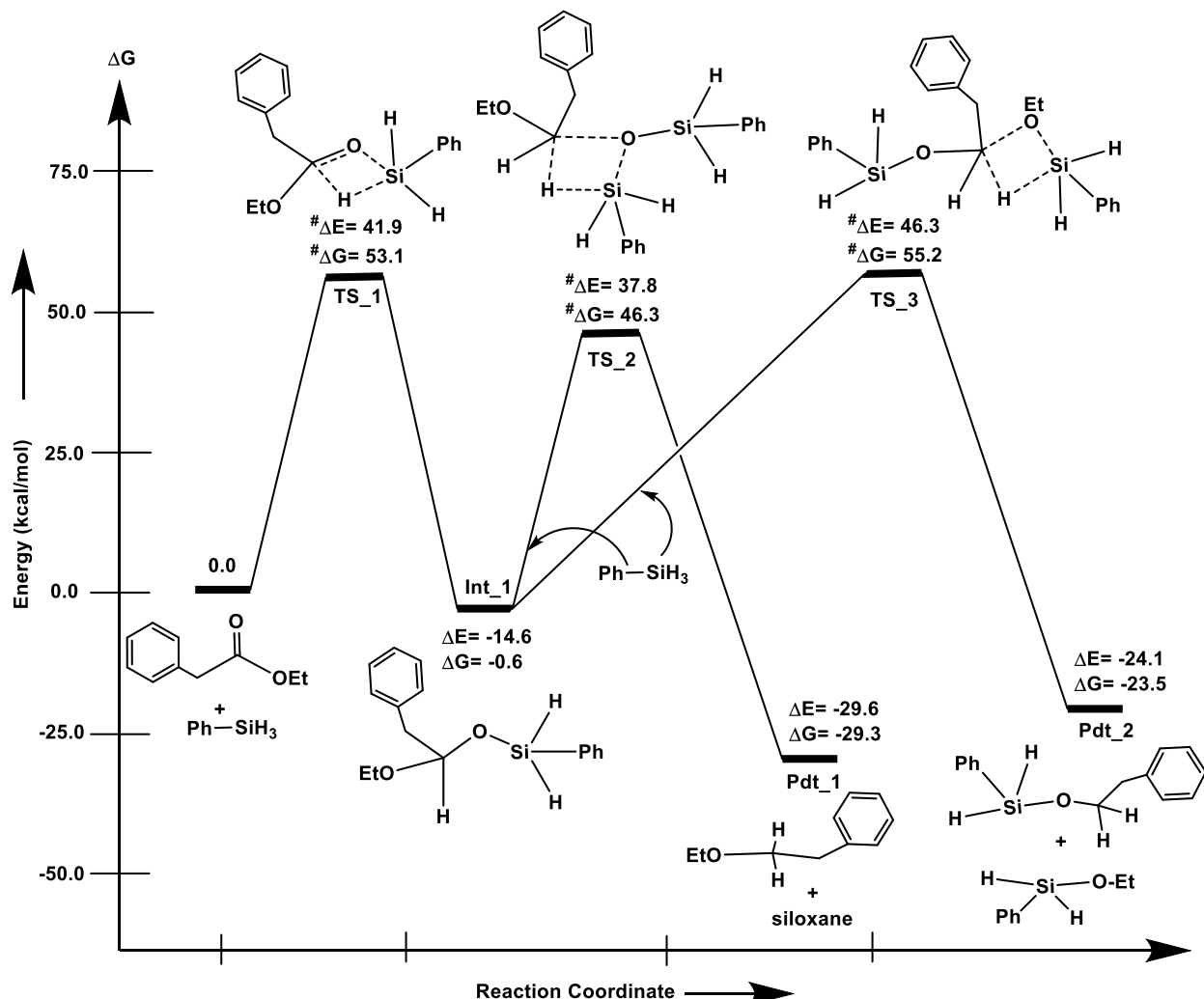


Figure S12. The two possible reaction profiles for the reductive deoxygenation of esters to ethers (ethyl- or silyl-ether) through hydrosilylation in the absence of catalyst. The values (in kcal/mol) have been calculated at the PBE/TZVP level of theory (gas phase).

The second reduction step has two possibilities. The first, also proposed in the mechanism Figure S10, implies the cleavage of the C-O-Si bond. The second results in the cleavage of the C-O-Et bond. The study of the thermodynamics suggests that the product, **Pdt_1**, formation is more

favourable by 5.9 kcal/mol over **Pdt_2** formation, and that the barrier is 8.9 kcal/mol lower as well. This indicates that the cleavage of the C-O-Si bond would be the preferred one.

Discarded reaction mechanism S1. (see Figure S12)

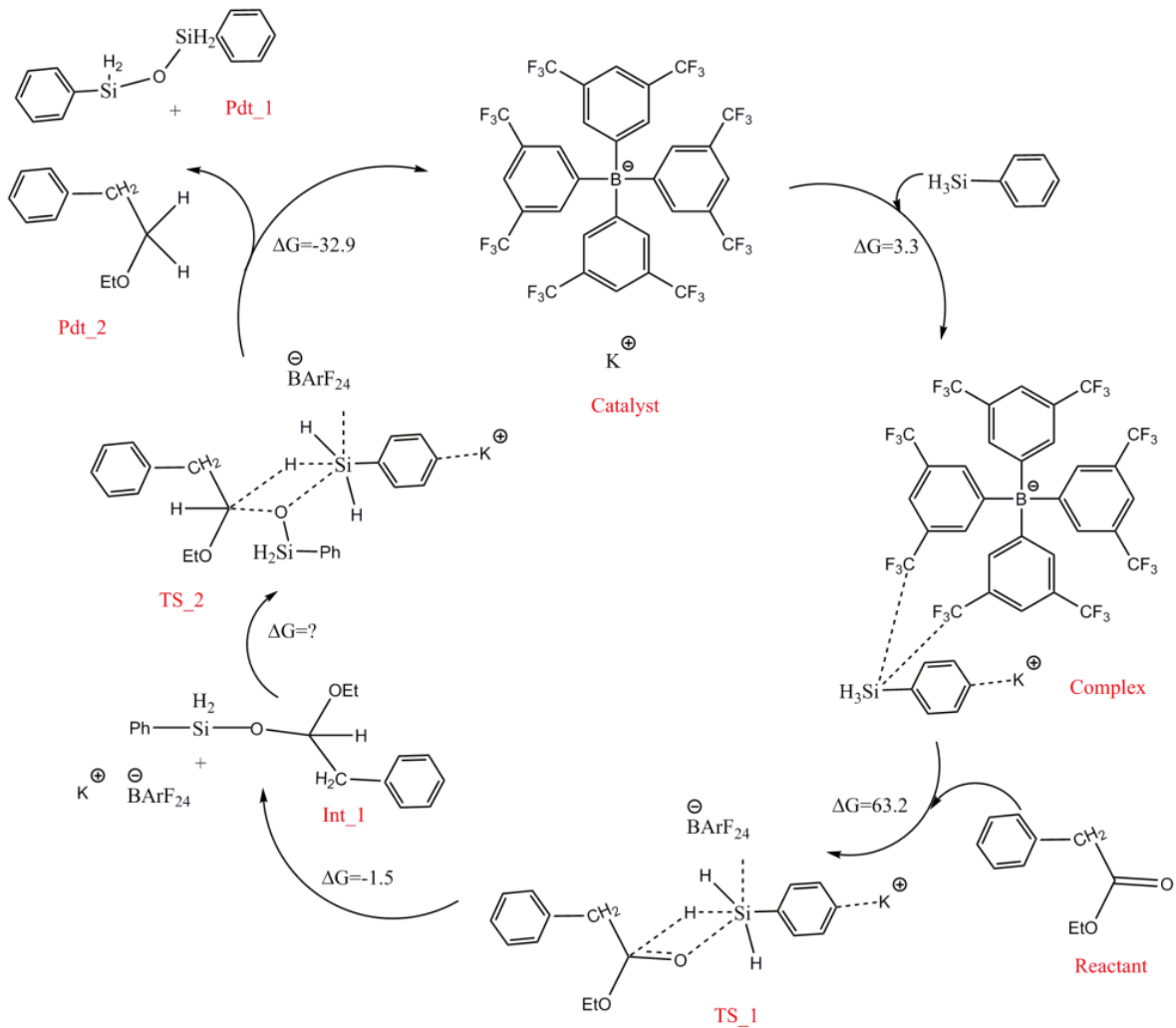
In the first step, the phenyl group attached to reactant ester shows the cation – pi interaction with the catalyst. This is not feasible as the reaction free energy (ΔG) of this step is 11.7 kcal/mol. In the next step, the Si of PhSiH₃ shows weak interaction with the fluorine of the complex. The reaction free energy (ΔG) of this step is unfavourable by 16.6 kcal/mol. Hence this mechanism has been discarded.

Discarded reaction mechanism S2. (see Figure S12)

In this mechanism, the catalyst and PhSiH₃ form a complex as proposed in Mechanism 1. In the second step, the oxygen atom of the ester substrate and the Si of PhSiH₃ reagent bind together to form a pentavalent Si. However, it has been observed that the Si has no coordination with the oxygen atom of the ester, which means such a pentavalent Si is not stable. Hence, this mechanism has also been discarded.

Discarded reaction mechanism S3. (see Scheme S1)

In the first step, PhSiH₃ forms a metastable complex with the catalyst. The potassium cation of the catalyst shows cation – pi interaction with the phenyl group attached to Si and the complex is more stabilized by the weak interaction between the Si and the F of the catalyst. The reaction free energy (ΔG) for this complex formation is 3.3 kcal/mol (calculated without volume correction). In the second step, the ester approaches towards the complex and goes through a four-membered transition state (ts_1) where the hydride is transferred from the Si center to the carbonyl carbon of the ester and the C=O double bond converts into a single bond, along with the formation of the Si–O bond, which leads to Int_1. If the reaction free energy (ΔG) of this step is favourable by 1.5 kcal/mol, the activation energy barrier ($\Delta G^\#$) is 63.2 kcal/mol, which is highly unfavourable. Indeed, the activation energy barrier for formation of int_1 calculated in the absence of catalyst was found to be 54.8 kcal/mol. Therefore, such energy value implies that this reaction should go through a different pathway.



Scheme S1. Discarded reaction mechanism S3. The values (in kcal/mol) have been calculated at the PBE/TZVP level of theory without volume correction (gas phase).

IV) General procedures

General procedure for the synthesis of esters:

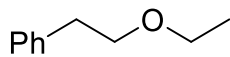
The selected carboxylic acid (1 eq.) is dissolved in absolute ethanol (100 mL) with concentrated H₂SO₄ (5 mol%) and the resulting solution is refluxed for 15 hours under stirring. After cooling and evaporation of the solvent under vacuum, the resulting residue is dissolved in dichloromethane and washed 3 times with a 1M aqueous solution of NaOH. The organic phase is then dried over MgSO₄ and evaporated under vacuum to afford the expected ester in quantitative yield.

General procedure for the catalysed reductive deoxygenations of esters:

In a glovebox, KBArF₂₄ (2 mol%) is transferred in a Schlenk tube. Then, under a nitrogen flow, anhydrous tetrachloroethane (2 mL), the selected ester (0.15 mmol, 1 eq.) and phenylsilane (0.3 mmol, 2 eq.) are respectively added through syringes and the resulting solution is heated at 100°C under stirring for 15 hours. Afterwards, the resulting solution is subsequently evaporated under vacuum and the residue is dissolved in dichloromethane and washed with brine. The organic phase is then dried over MgSO₄ and evaporated under vacuum to afford the crude product which was directly purified by flash chromatography on silica gel or by preparative TLC.

V) Characterization of compounds.

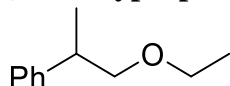
(2-ethoxyethyl)benzene 2a/2c/2s CAS [1817-90-9]^{S21}



Isolated as a colorless oil after flash chromatography on silica gel using a (7/3) petroleum spirit and diethyl ether mixture ($R_f = 0.6$), 47% yield.

¹H NMR (CDCl₃): δ 7.27 (m, 5H_{Ar}), 3.66 (t, $J = 7.3$, 2H), 3.52 (t, $J = 7.0$, 2H), 2.92 (t, $J = 7.3$, 2H), 1.23 (t, $J = 7.0$, 3H). **¹³C{¹H} NMR (CDCl₃):** δ 139.1 (C), 129.0 (2CH), 128.4 (2CH), 126.3 (CH), 71.7 (CH₂), 66.4 (CH₂), 36.5 (CH₂), 15.3 (CH₃).

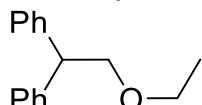
(1-ethoxypropan-2-yl)benzene 2b CAS [417705-20-5]^{S22}



Isolated as a colorless oil after flash chromatography on silica gel using a (8/2) petroleum spirit and diethyl ether mixture ($R_f = 0.7$), 93% yield.

¹H NMR (CDCl₃): δ 7.18 (m, 5H_{Ar}), 3.41 (m, 4H), 2.94 (m, 1H), 1.22 (d, $J = 7.0$, 3H), 1.10 (t, $J = 7.0$, 3H). **¹³C{¹H} NMR (CDCl₃):** δ 144.7 (C), 128.5 (2CH), 127.5 (2CH), 126.4 (CH), 76.7 (CH₂), 66.4 (CH₂), 40.2 (CH), 18.6 (CH₃), 15.3 (CH₃).

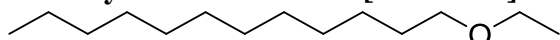
(2-ethoxyethane-1,1-diyl)dibenzene 2d CAS [86171-63-3]^{S23}



Isolated as a colorless oil after flash chromatography on silica gel using a (7/3) petroleum spirit and diethyl ether mixture ($R_f = 0.5$), 63% yield.

¹H NMR (CDCl₃): δ 7.16 (m, 10H_{Ar}), 4.20 (t, $J = 7.3$, 1H), 3.87 (d, $J = 7.3$, 2H), 3.42 (q, $J = 7.0$, 2H), 1.07 (t, $J = 7.0$, 3H). **¹³C{¹H} NMR (CDCl₃):** δ 142.6 (2C), 128.5 (4CH), 125.5 (4CH), 126.5 (2CH), 73.91 (CH₂), 66.6 (CH₂), 51.2 (CH), 15.2 (CH₃).

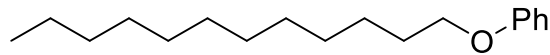
1-ethoxydodecane 2f CAS [7289-37-4]^{S24}



Isolated as a colorless oil after flash chromatography on silica gel using pure petroleum spirit ($R_f = 0.3$), 88% yield.

¹H NMR (CDCl₃): δ 3.45 (q, $J = 7.0$, 2H), 3.38 (t, $J = 7.0$, 2H), 1.57 (m, 2H), 1.24 (brs, 18H), 1.18 (t, $J = 7.0$, 3H), 0.86 (t, $J = 7.0$, 3H). **¹³C{¹H} NMR (CDCl₃):** δ 70.8 (CH₂), 66.0 (CH₂), 31.9 (CH₂), 29.8 (CH₂), 29.6 (2CH₂), 29.5 (2CH₂), 29.3 (2CH₂), 26.2 (CH₂), 22.7 (CH₂), 15.2 (CH₃), 14.1(CH₃).

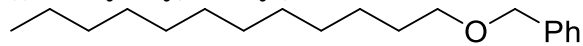
dodecyloxybenzene 2g CAS [35021-68-2]^{S25}



Isolated as a colorless oil after flash chromatography on silica gel using (9/1) petroleum spirit and diethyl ether mixture ($R_f = 0.3$), 83% yield.

¹H NMR (CDCl₃): δ 7.19 (m, 2H_{Ar}), 6.83 (m, 3H_{Ar}), 3.88 (t, $J = 6.6$, 2H), 1.71 (q, $J = 6.5$, 2H), 1.36 (brs, 2H), 1.24 (brs, 16H), 0.81 (t, $J = 7.0$, 3H). **¹³C{¹H} NMR (CDCl₃)**: δ 159.3 (C), 129.5 (2CH_{Ar}), 120.6 (CH_{Ar}) 114.7 (2CH_{Ar}), 68.1 (CH₂), 32.1 (CH₂), 29.8 (CH₂), 29.8 (CH₂), 29.8 (CH₂), 29.7 (CH₂), 29.6 (CH₂), 29.5 (CH₂), 26.2 (CH₂), 22.8 (CH₂), 14.3 (CH₃).

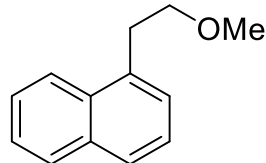
((dodecyloxy)methyl)benzene 2h CAS [39695-18-6]^{S26}



Isolated as a colorless oil after flash chromatography on silica gel using (8/2) petroleum spirit and diethyl ether mixture ($R_f = 0.3$), 76% yield.

¹H NMR (CDCl₃): δ 7.32 (m, 5H_{Ar}), 4.70 (s, 2H), 3.64 (t, $J = 6.6$, 2H), 1.57 (m, 4H), 1.27 (brs, 16H), 0.88 (t, $J = 6.7$, 3H). **¹³C{¹H} NMR (CDCl₃)**: δ 141.0 (C), 128.7 (2CH_{Ar}), 127.8 (CH_{Ar}) 127.1 (2CH_{Ar}), 65.5 (CH₂), 63.3 (CH₂), 33.3 (CH₂), 32.1 (CH₂), 29.8 (CH₂), 29.8 (CH₂), 29.8 (CH₂), 29.7 (CH₂), 29.6 (CH₂), 29.5 (CH₂), 25.9 (CH₂), 22.8 (CH₂), 14.2 (CH₃).

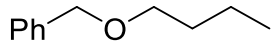
1-(2-methoxyethyl)naphthalene 2i CAS [91909-27-2]^{S27}



Isolated as a white solid after flash chromatography on silica gel using a (9/1) petroleum spirit and diethyl ether mixture ($R_f = 0.4$), 94% yield.

¹H NMR (CDCl₃): δ 8.10 (d, $J = 8.5$, 1H_{Ar}), 7.87 (dd, $J = 7.6$ -1.8, 1H_{Ar}), 7.75 (d, $J = 8.2$, 1H_{Ar}), 7.51 (m, 2H_{Ar}), 7.40 (m, 2H_{Ar}), 3.76 (t, $J = 7.4$, 2H), 0.88 (t, $J = 7.4$, 2H and s, 3H). **¹³C{¹H} NMR (CDCl₃)**: δ 134.8 (C), 133.9 (C), 132.1 (C), 128.8 (CH), 127.1 (CH), 126.8 (CH), 125.9 (CH), 125.6 (CH), 125.5 (CH), 123.7 (CH), 73.1 (CH₂), 58.7 (CH₃), 32.3 (CH₂).

(butoxymethyl)benzene 2j/2u CAS [588-67-0]^{S28}

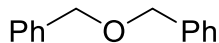


Isolated as a colorless oil after flash chromatography on silica gel using a (5/5) petroleum spirit and diethyl ether mixture ($R_f = 0.7$), 73% yield.

$^1\text{H NMR}$ (CDCl_3): δ 7.25 (m, 4H_{Ar}), 7.17 (m, 1H), 4.41 (bs, 2H), 3.39 (t, $J = 6.5$, 2H), 1.52 (m, 2H), 1.33 (m, 2H), 0.84 (t, $J = 7.3$, 3H).

$^{13}\text{C}\{\text{H}\} \text{NMR}$ (CDCl_3): δ 138.9 (C), 128.4 (CH_{Ar}), 128.7 (2CH_{Ar}), 127.5 (CH_{Ar}), 73.0 (CH₂), 70.3 (CH₂), 32.0 (CH₂), 19.5 (CH₂), 14.0 (CH₃).

(oxybis(methylene))dibenzene 2k CAS [103-50-4]^{S29}

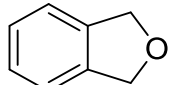


Isolated as a colorless oil after flash chromatography on silica gel using a (70/30) petroleum ether and triethylamine mixture ($R_f = 0.5$), 78% yield.

$^1\text{H NMR}$ (CDCl_3): δ 7.33 (m, 10H_{Ar}), 4.57 (bs, 2CH₂).

$^{13}\text{C}\{\text{H}\} \text{NMR}$ (CDCl_3): δ 138.3 (2C), 128.4 (4CH_{Ar}), 127.8 (4CH_{Ar}), 127.6 (2CH_{Ar}), 72.1 (2CH₂).

1,3-dihydroisobenzofuran 2n CAS [496-14-0]^{S30}

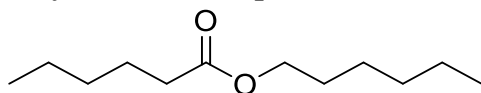


Isolated as a white solid after flash chromatography on silica gel using a (8/2) petroleum spirit and diethyl ether mixture ($R_f = 0.3$), 51% yield.

$^1\text{H NMR}$ (CDCl_3): δ 7.30 (m, 4H_{Ar}), 5.17 (s, 4H).

$^{13}\text{C}\{\text{H}\} \text{NMR}$ (CDCl_3): δ 139.2 (2C), 127.2 (2CH_{Ar}), 121.0 (2CH_{Ar}), 73.5 (2CH₂).

hexyl hexanoate 2q₁ CAS [6378-65-0]^{S31}

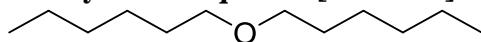


Isolated as a colorless oil after flash chromatography on silica gel using (8/2) petroleum spirit and diethyl ether mixture ($R_f = 0.6$), 48% yield.

$^1\text{H NMR}$ (CDCl_3): δ 3.99 (t, $J = 6.7$, 2H), 2.22 (t, $J = 7.5$, 2H), 1.55 (m, 4H), 1.24 (brs, 10H), 0.82 (brs, 6H).

$^{13}\text{C}\{\text{H}\} \text{NMR}$ (CDCl_3): δ 174.0 (C), 64.4 (CH₂), 34.4 (CH₂), 31.4 (CH₂), 31.3 (CH₂), 28.6 (CH₂), 25.6 (CH₂), 24.7 (CH₂), 22.5 (CH₂), 22.3 (CH₂), 14.0 (CH₃), 13.9 (CH₃).

Dihexyl ether 2q₂ CAS [112-58-3]^{S32}

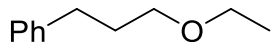


Isolated as a colorless oil after flash chromatography on silica gel using (8/2) petroleum spirit and diethyl ether mixture ($R_f = 0.8$), 51% yield.

$^1\text{H NMR}$ (CDCl_3): δ 3.32 (t, $J = 6.7$, 4H), 1.49 (m, 4H), 1.27 (brs, 12H), 0.83 (brs, 6H).

$^{13}\text{C}\{\text{H}\} \text{NMR}$ (CDCl_3): δ 71.1 (2CH₂), 31.9 (2CH₂), 29.9 (2CH₂), 26.0 (2CH₂), 22.8 (2CH₂), 14.2 (2CH₃).

(3-ethoxypropyl)benzene 2t/2v CAS [5848-56-6]^{S21}

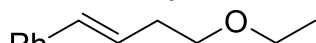


Isolated as a colorless oil after flash chromatography on silica gel using a (99/1) petroleum ether and triethylamine mixture ($R_f = 0.4$), 89% yield.

^1H NMR (CDCl₃): δ 7.27 (m, 2H_{Ar}), 7.19 (m, 3H_{Ar}), 3.46 (q, $J = 7.0$, 2H), 3.44 (t, $J = 6.5$, 2H), 2.71 (t, $J = 7.7$, 2H), 1.91 (m, 2H), 1.22 (t, $J = 7.1$, 3H).

$^{13}\text{C}\{^1\text{H}\}$ NMR (CDCl₃): δ 142.2 (C), 128.6 (2CH_{Ar}), 128.4 (2CH_{Ar}), 125.9 (CH_{Ar}), 69.9 (CH₂), 66.2 (CH₂), 32.5 (CH₂), 31.5 (CH₂), 15.4 (CH₃).

(E)-(4-ethoxybut-1-en-1-yl)benzene 2w CAS [114068-10-9]^{S33}

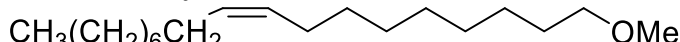


Isolated as a colorless oil after flash chromatography on silica gel using a (7/3) petroleum spirit and diethyl ether mixture ($R_f = 0.6$), 71% yield.

^1H NMR (CDCl₃): δ 7.29 (m, 5H_{Ar}), 6.46 (d, $J = 15.9$, 1H), 6.25 (dt, $J = 15.9, J = 6.9$, 1H), 3.53 (m, 4H), 2.50 (qd, $J = 6.9, J = 1.4$, 2H), 1.22 (t, $J = 7$, 3H).

$^{13}\text{C}\{^1\text{H}\}$ NMR (CDCl₃): δ 137.7 (C), 131.6 (CH), 128.6 (2CH_{Ar}), 127.2 (CH), 127.1 (CH), 126.2 (2CH_{Ar}), 70.3 (CH₂), 66.4 (CH₂), 33.7 (CH₂), 15.35(CH₃).

(Z)-1-methoxyoctadec-9-ene 2x CAS [57205-42-2]^{S33}

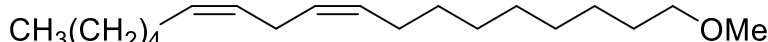


Isolated as a colorless oil after flash chromatography on silica gel using a (7/3) dichloromethane and diethyl ether mixture ($R_f = 0.6$), 88% yield.

^1H NMR (CDCl₃): δ 5.30 (m, 2H), 3.29 (t, $J = 6.7$, 2H), 3.25 (s, 3H), 1.88 (m, 4H), 1.48 (m, 2H), 1.22 (m, 22H), 0.81 (t, $J = 6.8$, 3H).

$^{13}\text{C}\{^1\text{H}\}$ NMR (CDCl₃): δ 130.5 (CH), 130.1 (CH), 73.1 (CH₂), 58.7 (OCH₃), 32.7 (CH₂), 32.1 (CH₂), 29.9 (CH₂), 29.8 (CH₂), 29.7 (CH₂), 29.7 (CH₂), 29.6 (CH₂), 29.5 (CH₂), 29.3 (CH₂), 29.3 (CH₂), 29.2 (CH₂), 27.4 (CH₂), 26.3 (CH₂), 22.8 (CH₂), 14.2 (CH₃).

(6Z,9Z)-18-methoxyoctadeca-6,9-diene 2y CAS [23405-45-0]^{S34}



Isolated as a colorless oil after flash chromatography on silica gel using a (7/3) dichloromethane and diethyl ether mixture ($R_f = 0.5$), 68% yield.

^1H NMR (CDCl₃): δ 5.36 (m, 4H), 3.36 (t, $J = 6.7$, 2H), 3.33 (s; 3H), 2.77 (t, $J = 6.0$, 2H) 2.06 (m, 4H), 1.55 (m, 2H), 1.34 (m, 16H), 0.89 (t, $J = 6.8$, 3H).

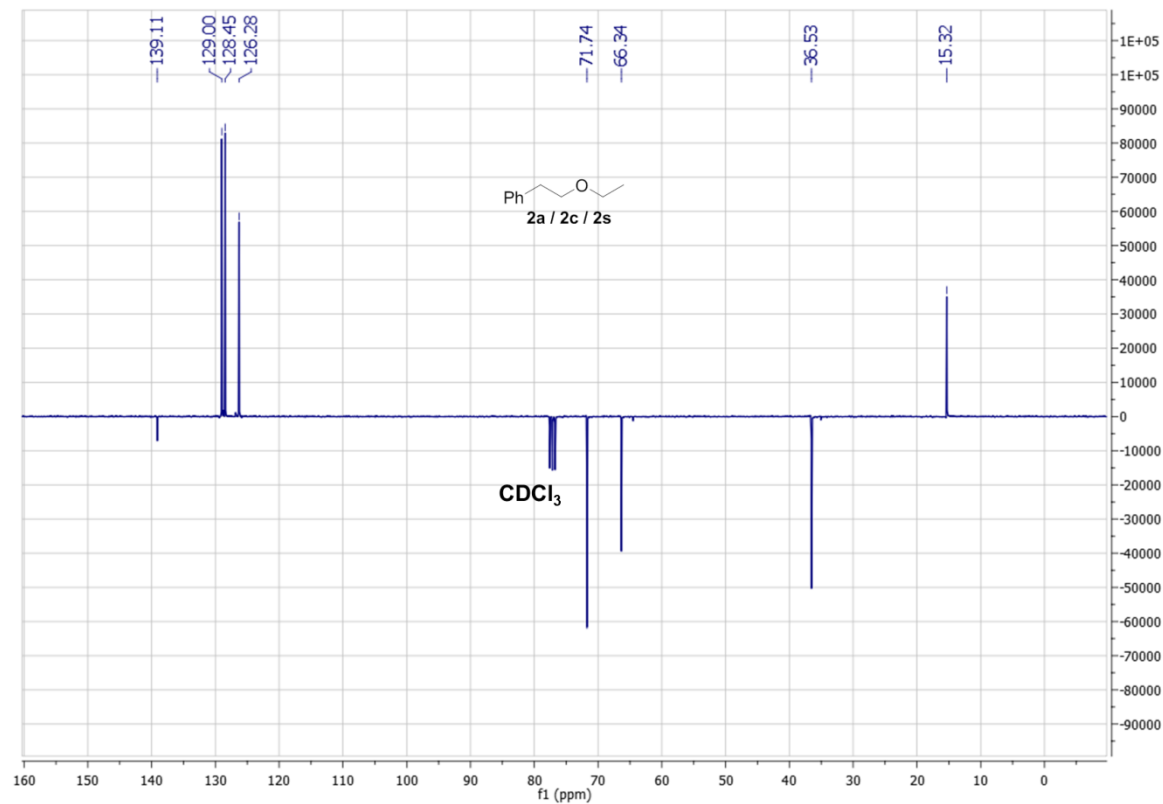
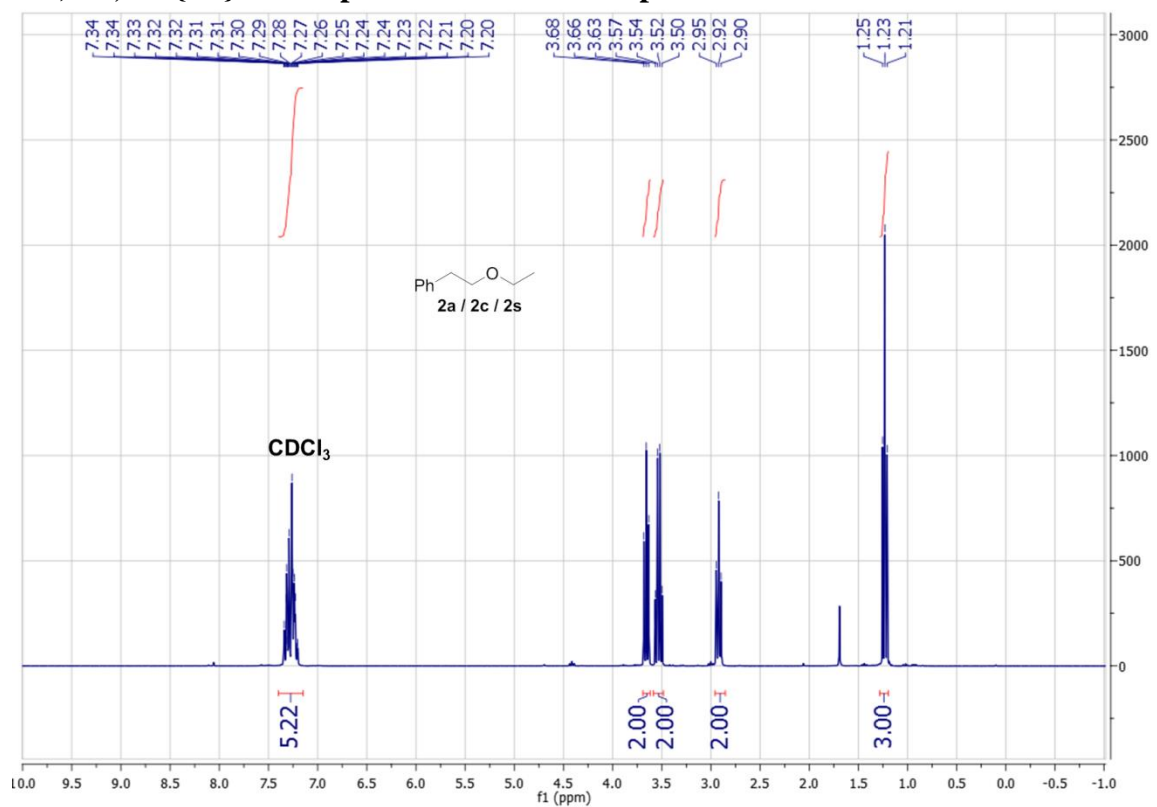
$^{13}\text{C}\{^1\text{H}\}$ NMR (CDCl₃): δ 130.4 (CH), 130.3 (CH), 128.2 (CH), 128.1 (CH), 73.1 (CH₂), 58.7 (OCH₃), 31.7 (CH₂), 29.8 (2CH₂), 29.6 (2CH₂), 29.5 (CH₂), 29.4 (CH₂), 27.4 (2CH₂), 26.3 (CH₂), 25.8 (CH₂), 22.7 (CH₂), 14.2 (CH₃).

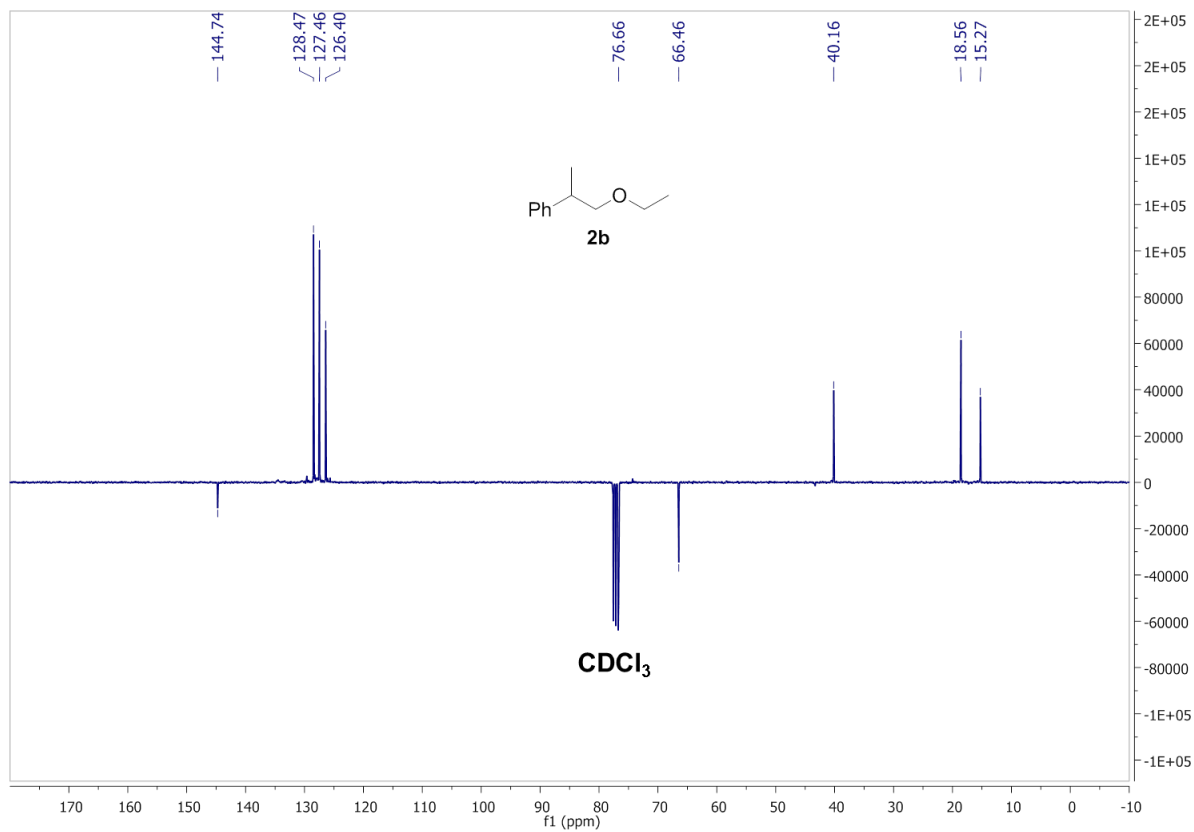
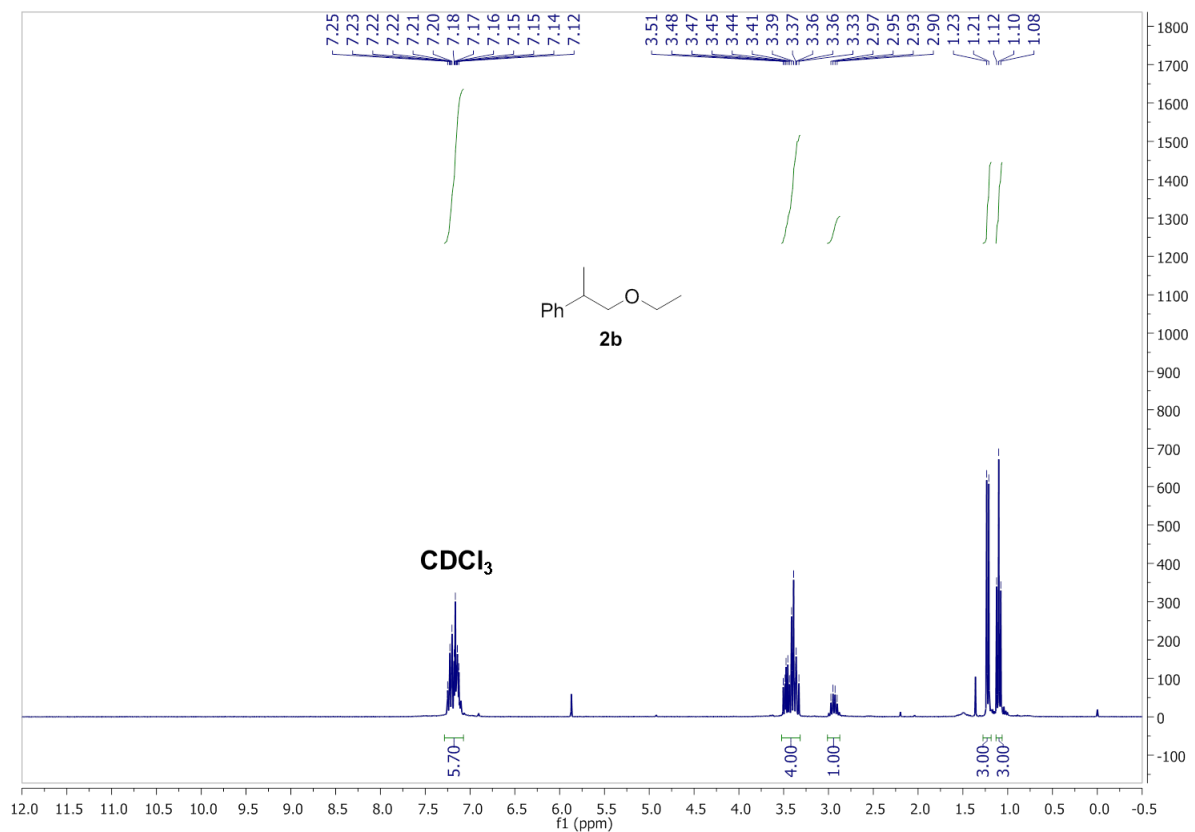
VI) References.

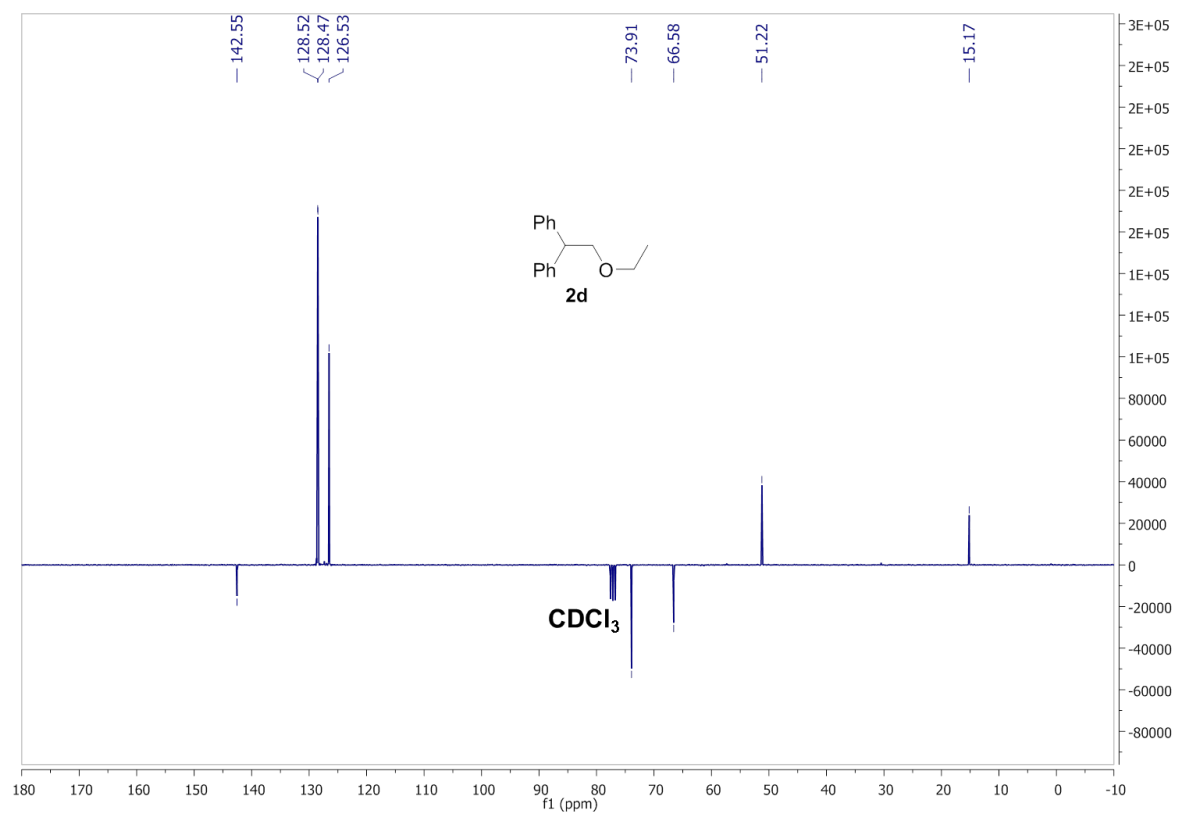
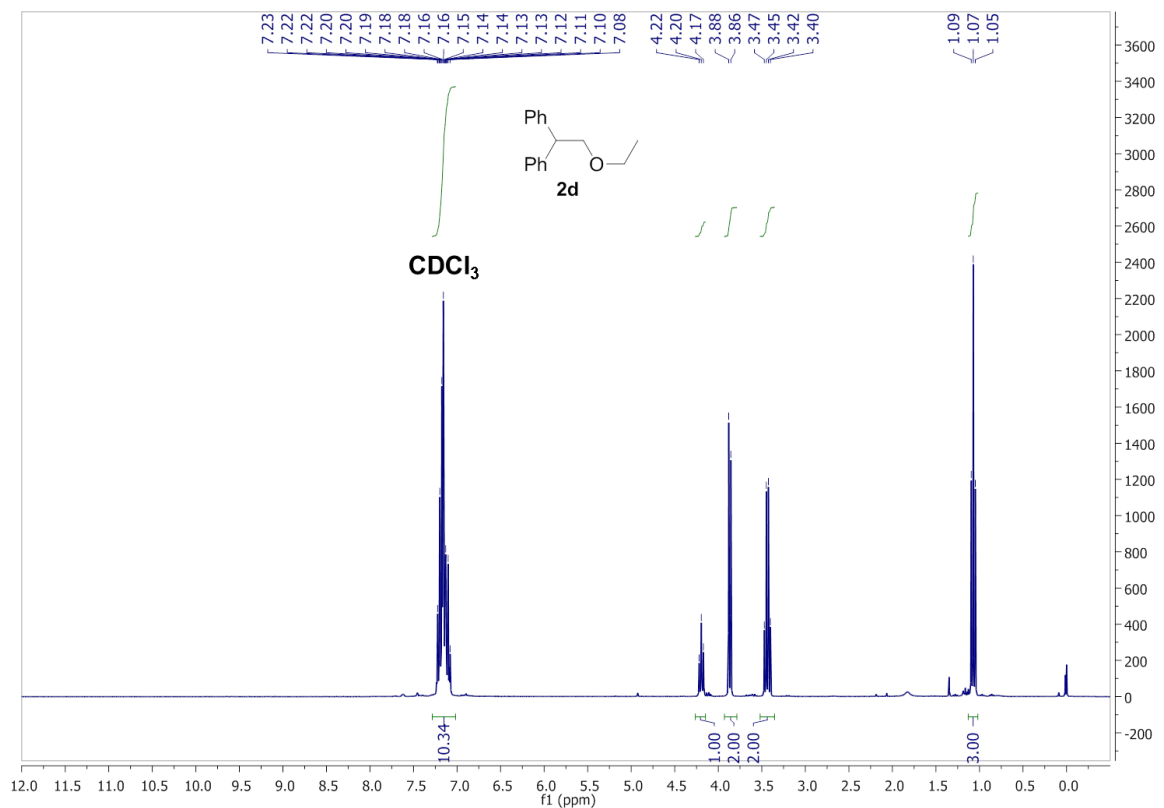
- S1) a) W. E. Buschmann, J. S. Miller, *Inorganic Syntheses*, 2002, **33**, 83; b) N. A. Yakelis, R. G. Bergman, *Organometallics*, 2005, **24**, 3579; c) M. Brookhart, B. Grant, A. F. Volpe, *Organometallics*, 1992, **11**, 3920.
- S2) TURBOMOLE V7.1 2016, a development of University of Karlsruhe and ForschungszentrumKarlsruhe GmbH, 1989-2007, TURBOMOLE GmbH, since 2007; available from <http://www.turbomole.com>.
- S3) J. P. Perdew, K. Burke, M. Ernzerhof, *Phys. Rev. Lett.*, 1996, **77**, 3865.
- S4) S. Ansgar, H. Christian, A. Reinhart, *J. Chem. Phys.*, 1994, **100**, 5829.
- S5) K. Eichkorn, O. Treutler, H. Öhm, M. Häser, R. Ahlrichs, *Chem. Phys. Lett.*, 1995, **240**, 283.
- S6) M. Sierka, A. Hogekamp, R. Ahlrichs, *J. Chem. Phys.*, 2003, **118**, 9136.
- S7) A. Klamt, G. Schüürmann, *J. Chem. Soc., Perkin Trans. 2*, 1993, 799.
- S8) K. Fukui, *Acc. Chem. Res.*, 1981, **14**, 363.
- S9) M. Mammen, E. I. Shakhnovich, J. M. Deutch, G. M. Whitesides, *J. Org. Chem.*, 1998, **63**, 3821.
- S10) S. Kozuch, J. M. L. Martin, *ACS Catal.*, 2011, **1**, 246.
- S11) A. Uhe, S. Kozuch, S. Shaik, *Comput. Chem.*, 2011, **32**, 978.
- S12) E. R. Johnson; S. Keinan; P. Mori-Sanchez; J. Contreras-García; A. J. Cohen; W. Yang. *J. Am. Chem. Soc.*, 2010, **132**, 6498.
- S13) J. Contreras-García, E. R. Johnson, S. Keinan, R. Chaudret, J.-P. Piquemal; D. N. Beratan; W. R. Yang. *J. Chem. Theory Comput.*, 2011, **7**, 625.
- S14) a) T. Popek, T. Lis, *Carbohydr. Res.*, 2002, **337**, 787; b) L. B. Jerzykiewicz, T. Lis, E. Zuziak, *Carbohydr. Res.*, 2005, **340**, 2422.
- S15) a) S.-Y. Kim, A. Saxena, G. Kwak, M. Fujiki, Y. Kawakami, *Chem. Commun.* **2004**, 538; b) A. Saxena, R. Rai, S.-Y. Kim, M. Fujiki, M. Naito, K. Okoshi, G. Kwak, *J. Polymer Sci.: Part A: Polymer Chem.*, 2006, **44**, 5060; c) T. Kawabe, M. Naito, M. Fujiki, *Polymer J.*, 2008, **40**, 317.
- S16) Oxidative addition: a) A. J. Chalk, J. F. Harrod, *J. Am. Chem. Soc.*, 1965, **87**, 16; b) I. Ojima, M. Nihonyanagi, T. Kogure, M. Komagai, S. Horiuchi, K. Nakatsugawa, Y. Nagai, *J. Organomet. Chem.*, 1975, **94**, 449; c) P. B. Glaser, T. Don Tilley, *J. Am. Chem. Soc.*, 2003, **125**, 13640; d) T. J. Steiman, C. Uyeda, *J. Am. Chem. Soc.*, 2015, **137**, 6104; double activation metal-substrate: e) J. Yang, P. S. White, M. Brookhart, *J. Am. Chem. Soc.*, 2008, **130**, 17509; f) T. T. Metsänen, P. Hrobárik, H. F. T. Klare, M. Kaupp, M. Oestreich, *J. Am. Chem. Soc.*, 2014, **136**, 6912; cooperation metal-ligand: e) K. A. Nolin, J. R. Krumper, M. D. Pluth, R. G. Bergman, F. D. Toste, *J. Am. Chem. Soc.*, 2007, **129**, 14684; f) M. A. Rankin, G. Schatte, R. McDonald, M. Stradiotto, *J. Am. Chem. Soc.*, 2007, **129**, 6390; g) M. A. Rankin, D. F. MacLean, R. McDonald, M. J. Ferguson, M. D. Lumsden, M. Stradiotto, *Organometallics*, 2009, **28**, 74; heterolytic polar electrophilic activation: g) M. Hamdaoui, C. Desrousseaux, H. Habbita, J.-P. Djukic, *Organometallics*, 2017, **36**, 4864; h) P. W. Smith, T. Don Tilley, *J. Am. Chem. Soc.*, 2018, **140**, 3880.
- S17) a) D. W. Stephan and G. Erker, *Angew. Chem. Int. Ed.*, 2015, **54**, 6400; b) M. Oestreich, J. Hermeke and J. Mohr, *Chem. Soc. Rev.*, 2015, **44**, 2202; c) D. W. Stephan, *Science*, 2016, **354**, 1236; d) Q. Shi, Z. Chen and J. Hu, *Current Org. Chem.*, 2018, **22**, 557; e) W. Meng, X. Feng and H. Du, *Acc. Chem. Res.*, 2018, **51**, 191; f) J. Lam, K. M. Szkop, E. Mosaferi and D. W. Stephan, *Chem. Soc. Rev.*, 2019, **48**, 3592.

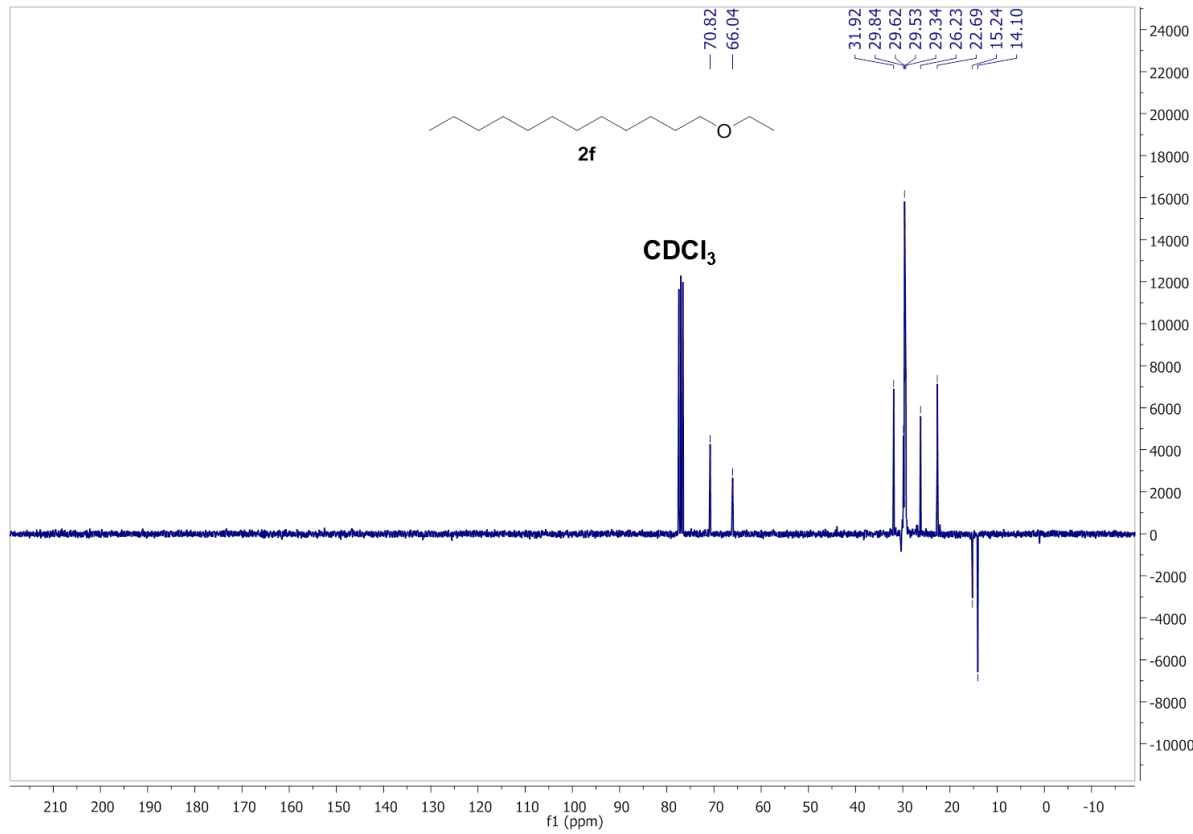
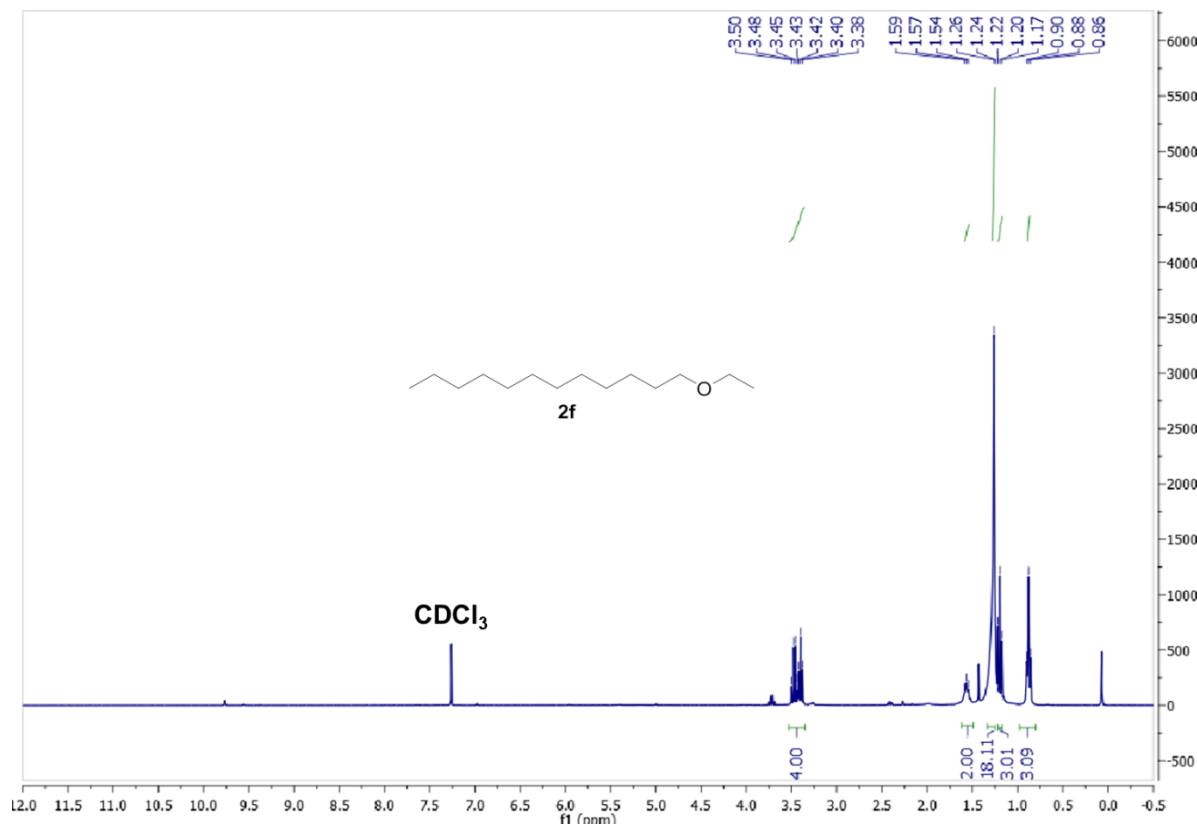
- S18) a) D. J. Parks, W. E. Piers, *J. Am. Chem. Soc.*, 1996, **118**, 9440; b) D. J. Parks, J. M. Blackwell, W. E. Piers, *J. Org. Chem.*, 2000, **65**, 3090; c) A. Berkefeld, W. E. Piers, M. Parvez, *J. Am. Chem. Soc.*, 2010, **132**, 10660; d) M. Mewald, R. Fröhlich, M. Oestreich, *Chem. Eur. J.*, 2011, **17**, 9406; e) A. J. V. Marwitz, L. G. Mercier, *Inorg. Chem.*, 2011, **50**, 12252; f) W. Nie, H. F. T. Klare, M. Oestreich, R. Fröhlich, G. Kehr, G. Erker, *Z. Naturforsch. B*, 2012, **67**, 987; g) D. Chen, V. Leich, F. Pan, J. Klankermayer, *Chem. Eur. J.*, 2012, **18**, 5184; h) L. Greb, P. Oña-Burgos, A. Kubas, F. C. Falk, F. Breher, K. Fink, J. Paradies, *Dalton Trans.*, 2012, **41**, 9056.
- S19) Examples of chemical reactions showing a barrier of ~ 43.0 kcal/mol or even higher for a reaction occurring at a temperature of 100°C: a) J. Florian, A. Warshel, *J. Phys. Chem. B*, 1998, **102**, 719; b) M. Yamakawa, H. Ito, R. Noyori, *J. Am. Chem. Soc.*, 2000, **122**, 1466; c) T. M. Nguyen, V. S. Nguyen, H. M. Matus, G. Gopakumar, D. A. Dixon, *J. Phys. Chem. A*, 2007, **111**, 679; d) T. B. Lee, M. L. McKee, *Inorg. Chem.*, 2009, **48**, 7564; e) L.-J. Song, T. Wang, X. Zhang, L. W. Chung, D. Y. Wu, *ACS Catal.*, 2017, **7**, 1361.
- S20) a) M. Mammen, E. I. Shakhnovich, J. M. Deutch, G. M. Whitesides, *J. Org. Chem.*, 1998, **63**, 3821; b) S. Kozuch, J. M. L. Martin, *ACS Catal.*, 2011, **1**, 246; c) A. Uhe, S. Kozuch, S. Shaik, *Comput. Chem.*, 2011, **32**, 978.
- S21) N. Sakai, T. Moriya, T. Konakahara, *J. Org. Chem.*, 2007, **72**, 5920.
- S22) a) D. R. Hou, J. Reibenspies, T. J. Colacot, K. Burgess, *Chem. Eur. J.*, 2001, **7**, 5391; b) P. H. Mazzocchi, D. Shook, L. Liu, *Heterocycles*, 1987, **26**, 1165.
- S23) a) M. Weiser, S. Hermann, A. Penner, H. A. Wagenknecht, *Beilstein J. Org. Chem.*, 2015, **11**, 568; b) R. Leardini, A. Tundo, G. Zanardi, G. F. Pedulli, *J. Chem. Soc., Perkin Trans. 2*, 1983, 285.
- S24) a) K. Matsubara, T. Iura, T. Maki, H. Nagashima, *J. Org. Chem.*, 2002, **67**, 4985; b) S. Uemura, S. Fukuzawa, *J. Chem. Soc., Perkin Trans. 1*, 1985, 471.
- S25) K. Swapna, S. N. Murthy, M. T. Jyothi, Y. V. D. Nageswar, *Org. Biomol. Chem.*, 2011, **9**, 5978.
- S26) a) N. Yasukawa, T. Kanie, M. Kuwata, Y. Monguchi, H. Sajiki, Y. Sawama, *Chem. Eur. J.*, 2017, **23**, 10974; b) A. Prades, R. Corberan, M. Poyatos, E. Peris, *Chem. Eur. J.*, 2008, **14**, 11474.
- S27) N. Hoffman, J.-P. Pete, *J. Org. Chem.*, 2002, **67**, 2315.
- S28) J. Alvarez-Builla, J. J. Vaquero, J. L. Garcia Navio, J. F. Cabello, C. Sunkel, M. Fau de Casa-Juana, F. Dorrego, L. Santos, *Tetrahedron*, 1990, **46**, 967.
- S29) G. A. Molander, B. Canturk, *Org. Lett.*, 2008, **10**, 2135.
- S30) M. Yasuda, M. Haga, A. Baba, *Organometallics*, 2009, **28**, 1998.
- S31) N. Yamamoto, Y. Obora, Y. Ishii, *J. Org. Chem.*, 2011, **76**, 2937.
- S32) T. Fujisaka, M. Nojima, S. Kusabayashi, *J. Org. Chem.*, 1985, **50**, 275.
- S33) S. Xu, J. S. Boschen, A. Biswas, T. Kobayashi, M. Pruski, T. L. Windus, A. D. Sadow, *Dalton Trans.*, 2015, **44**, 15897.
- S34) Y. Corre, V. Rysak, X. Trivelli, F. Agbossou-Niedercorn, C. Michon, *Eur. J. Org. Chem.*, 2017, **2017**, 4820.

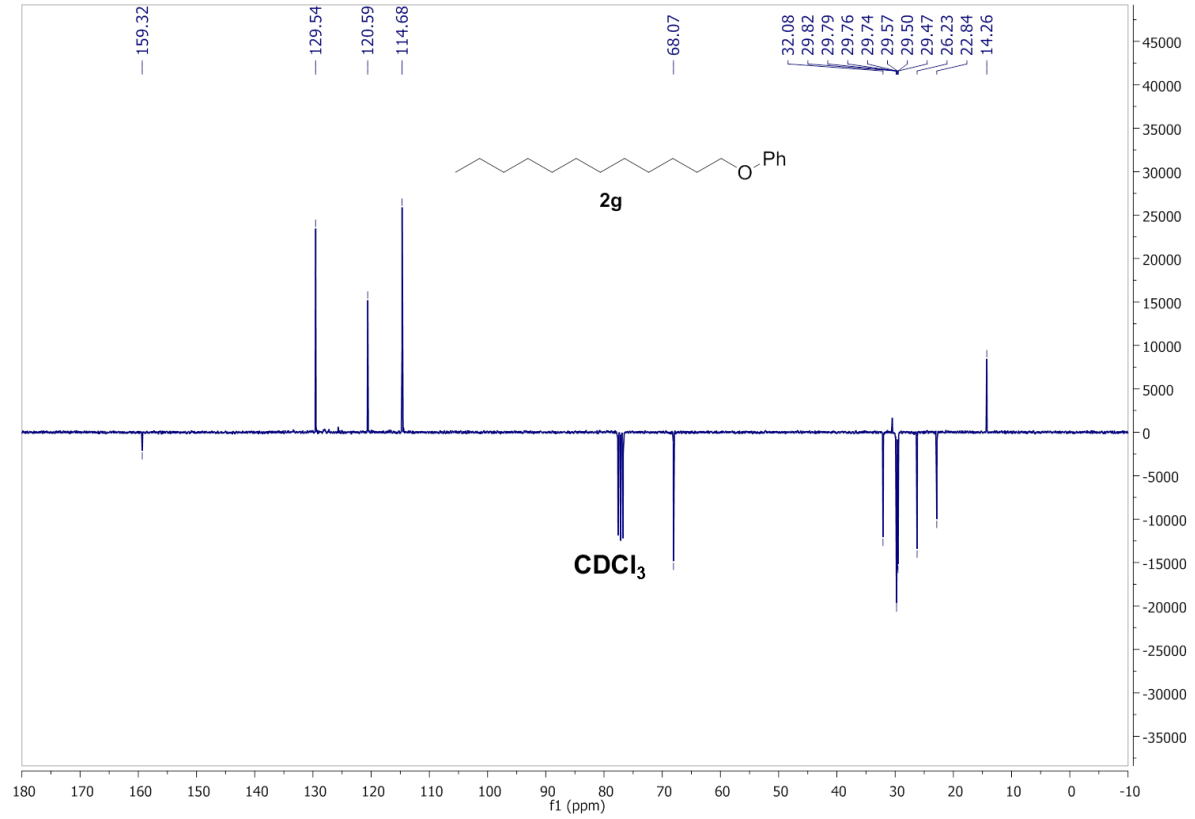
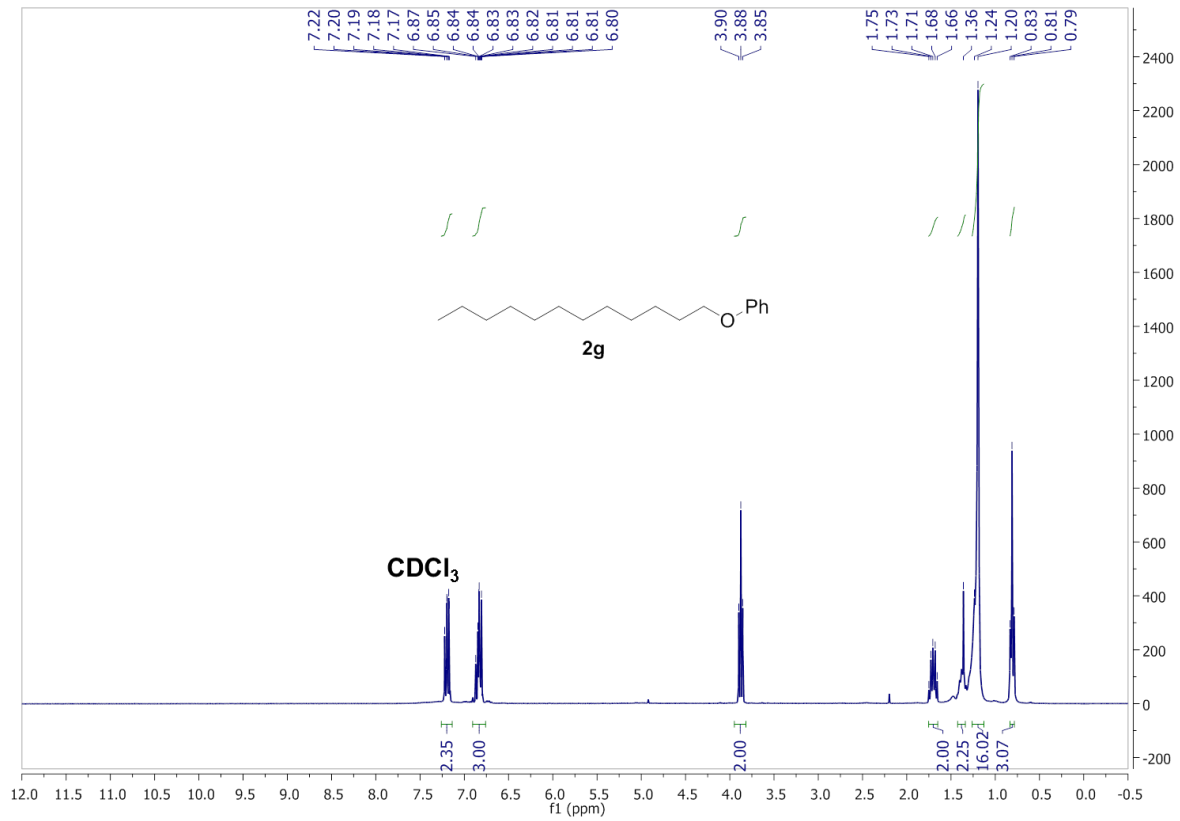
VII) ^1H , $^{13}\text{C}\{^1\text{H}\}$ NMR spectra of isolated compounds

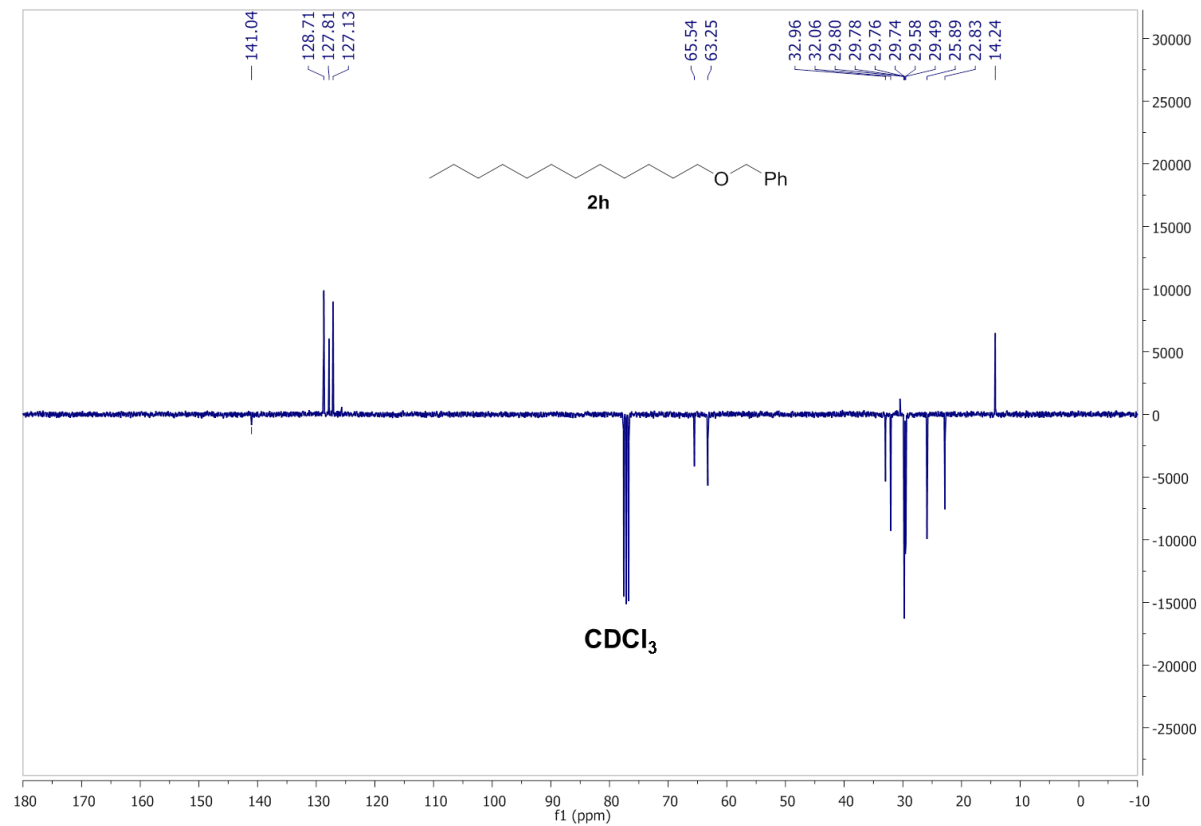
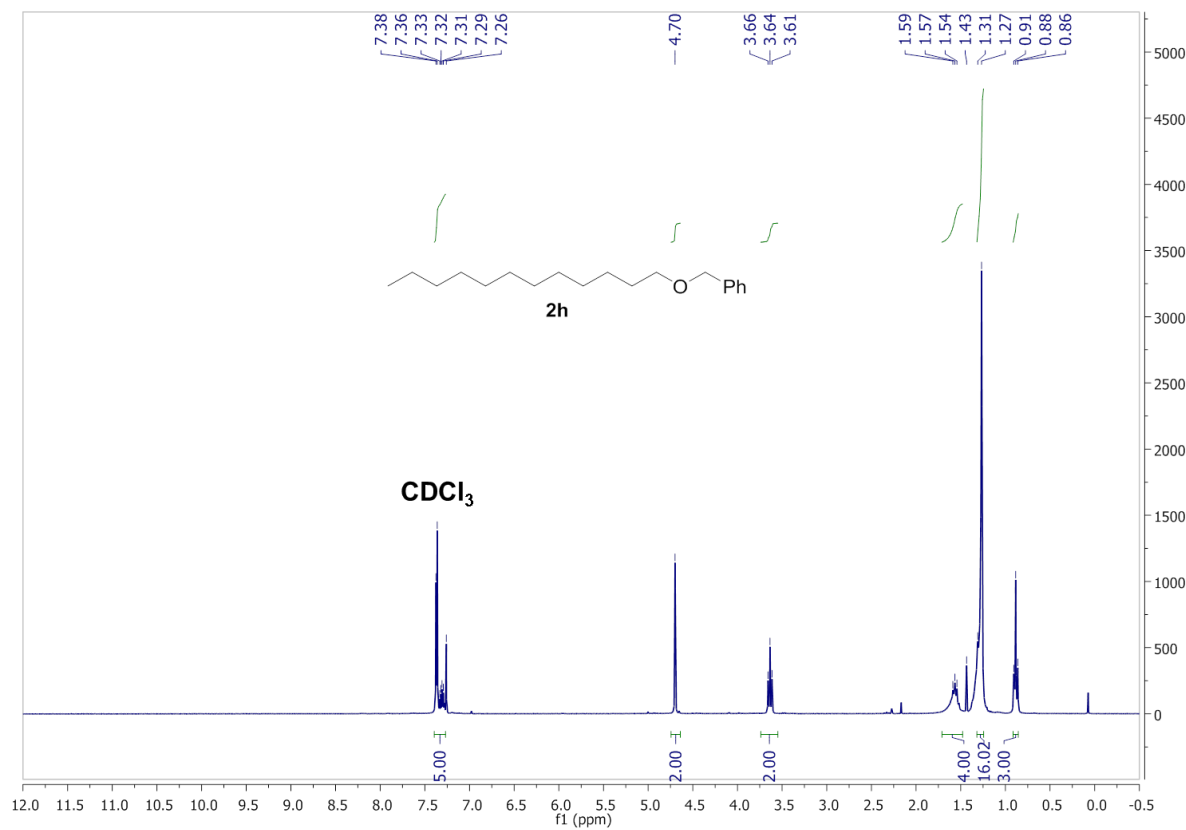


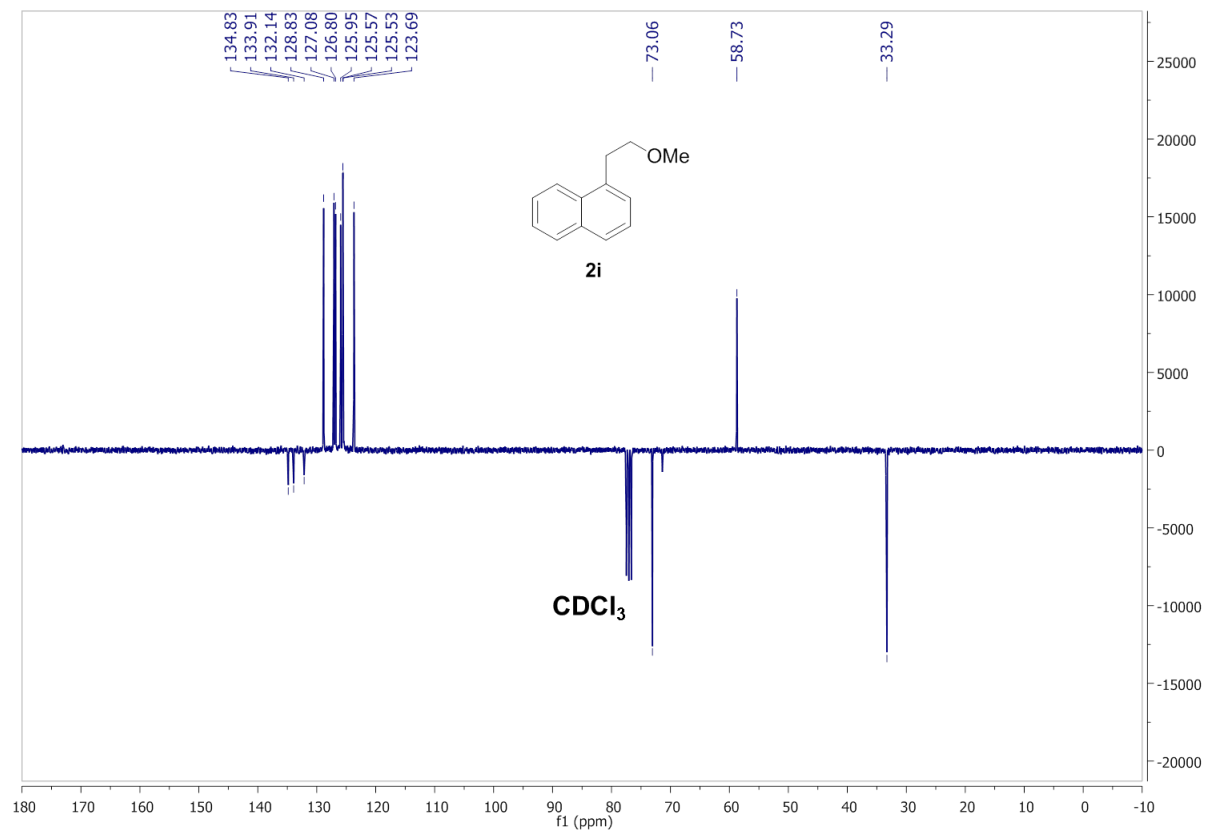
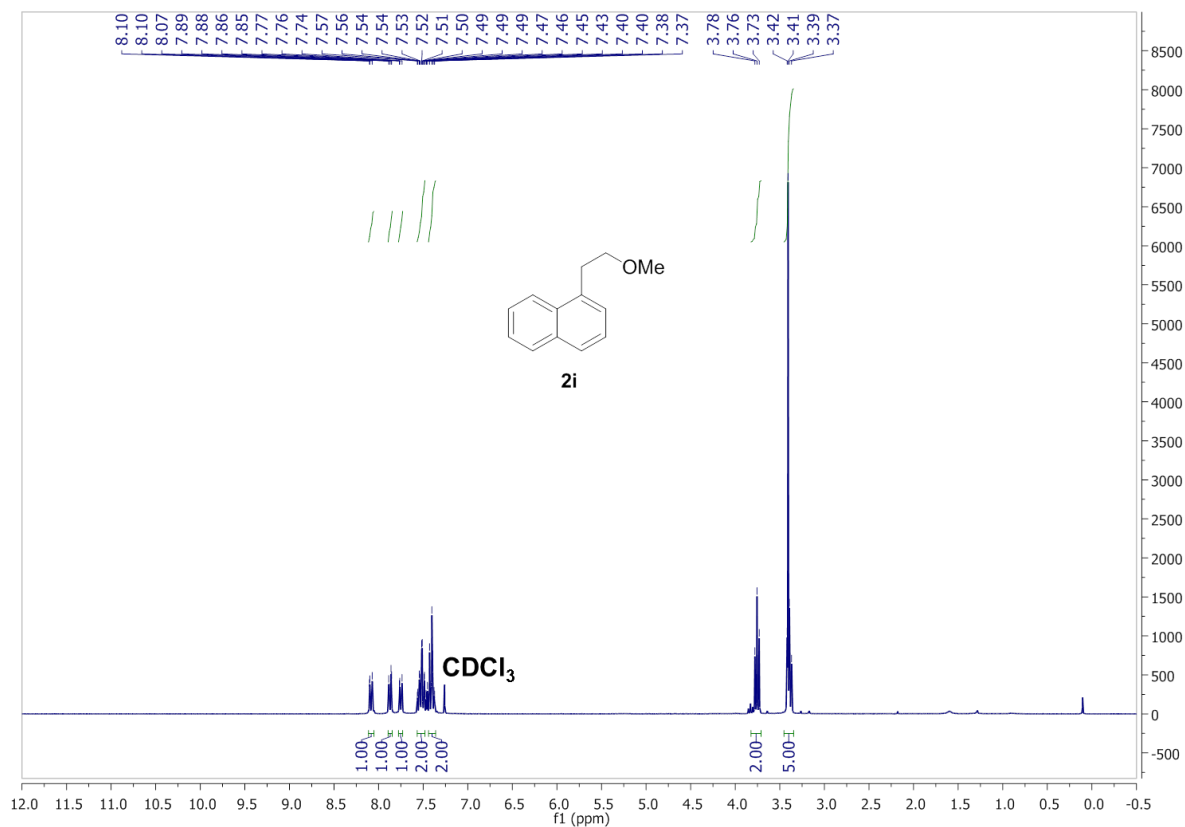


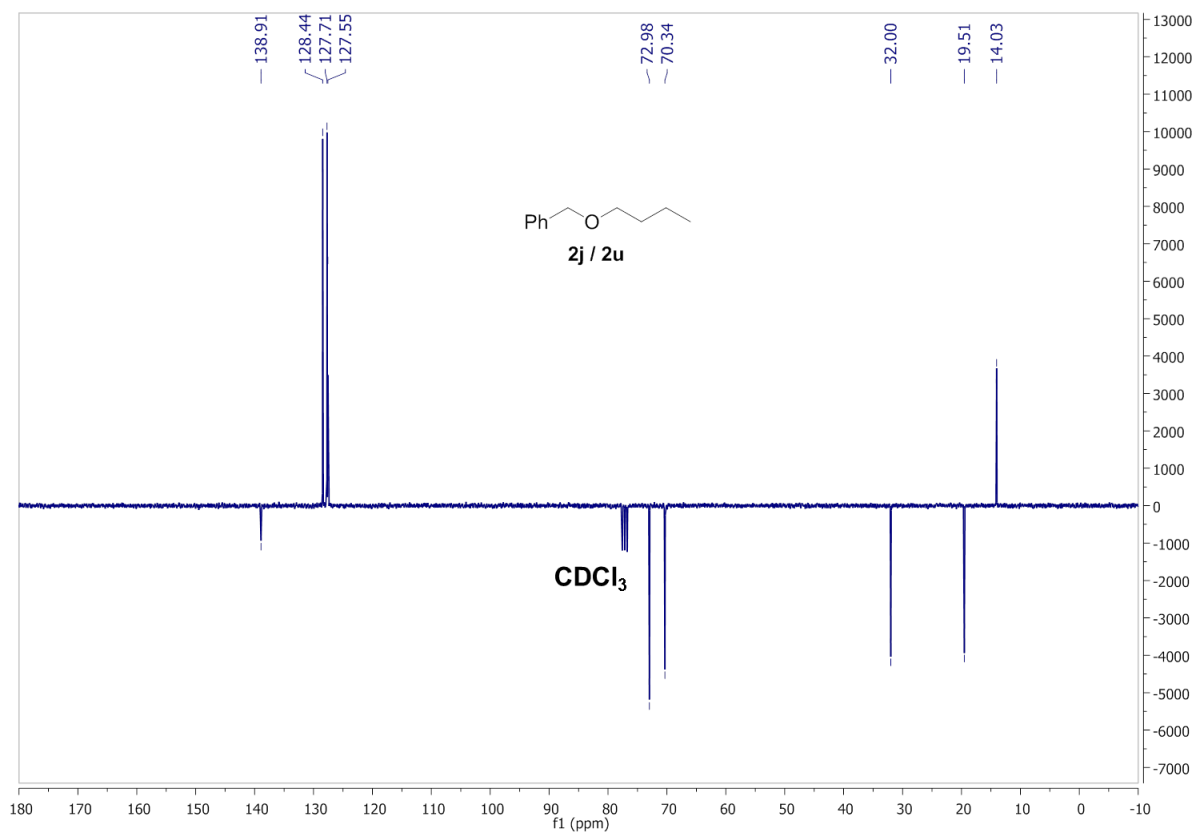
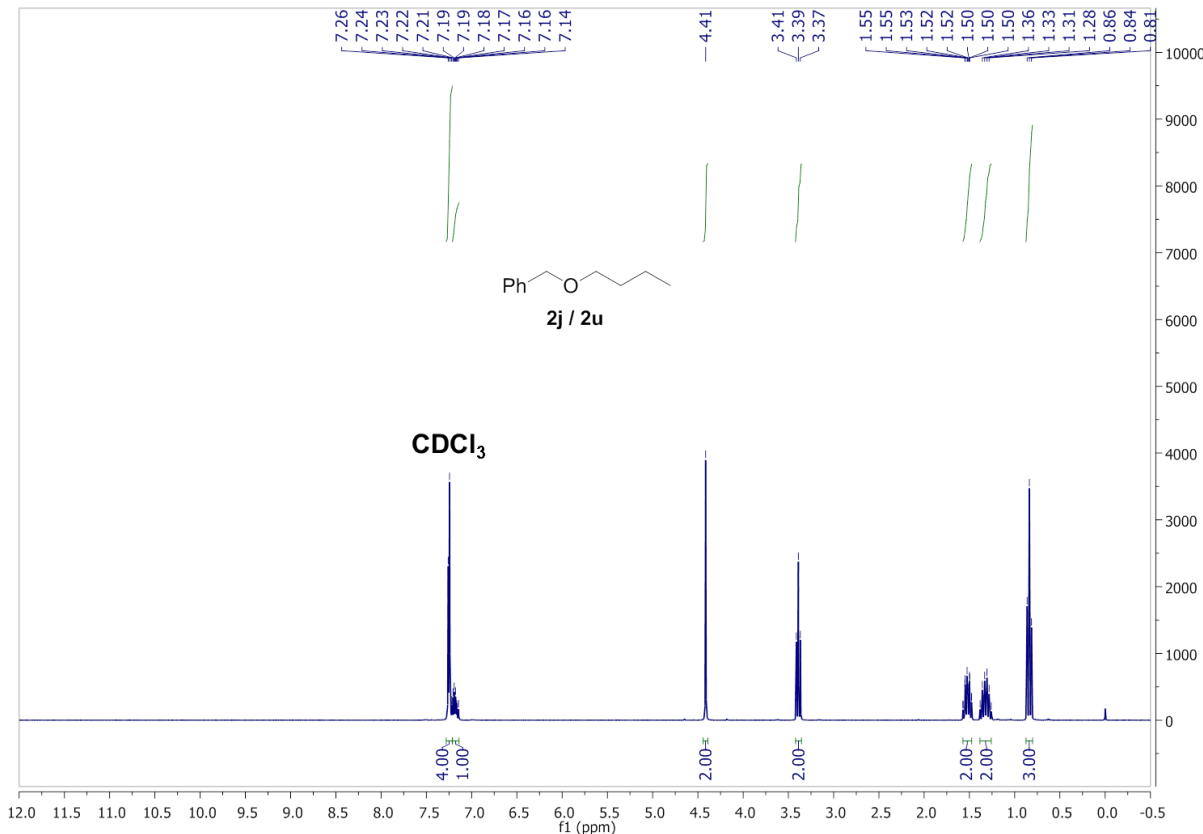


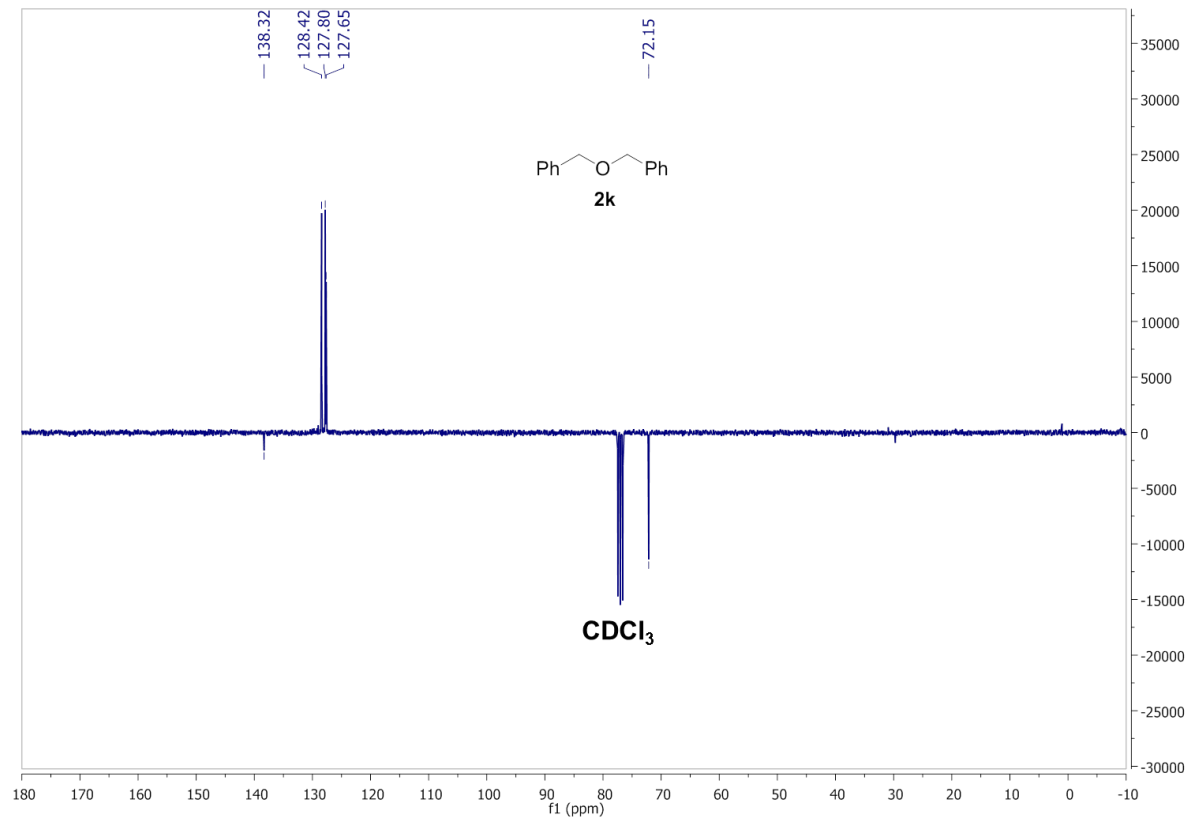
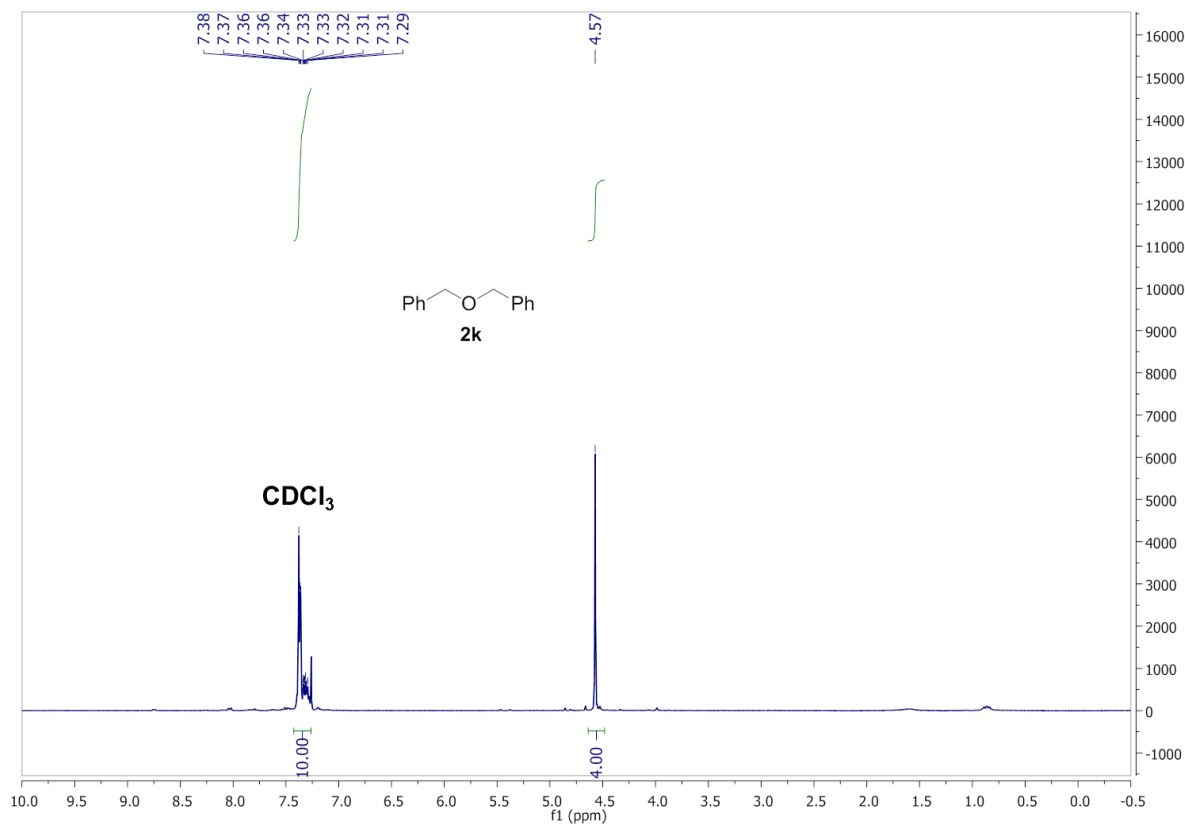


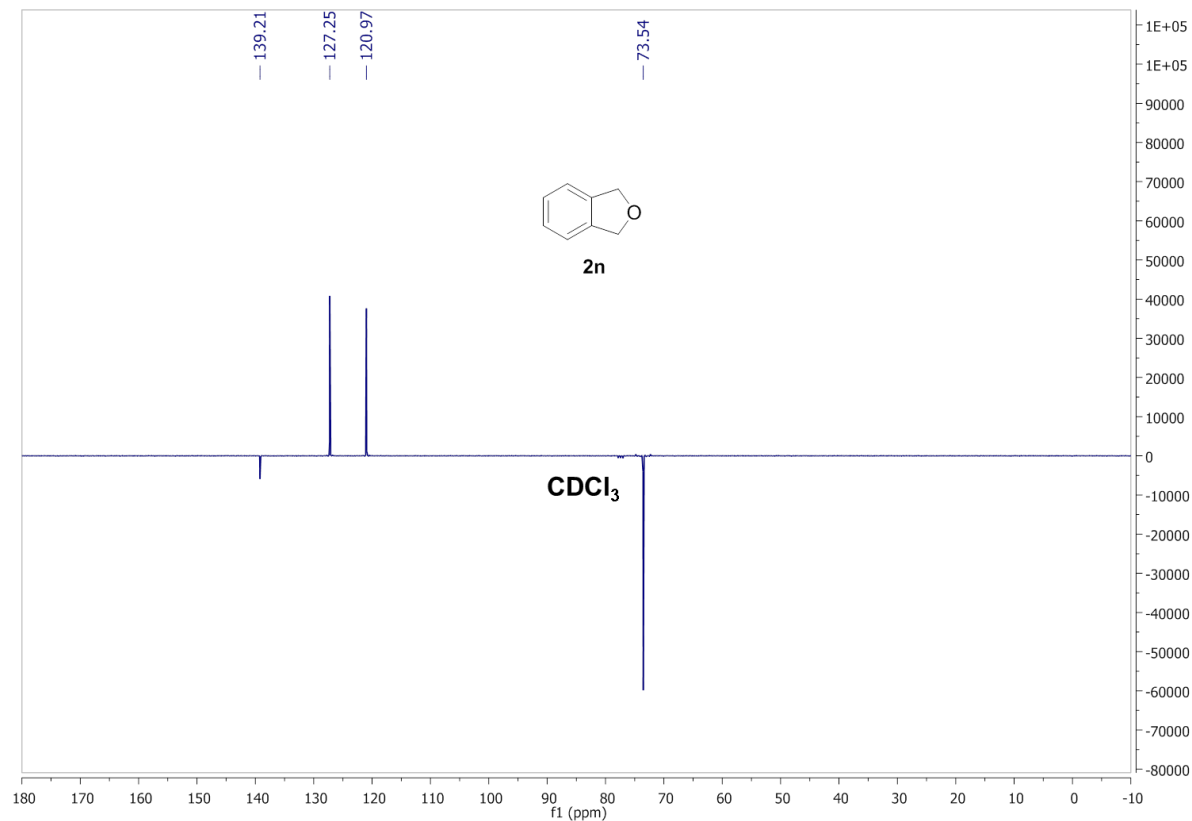
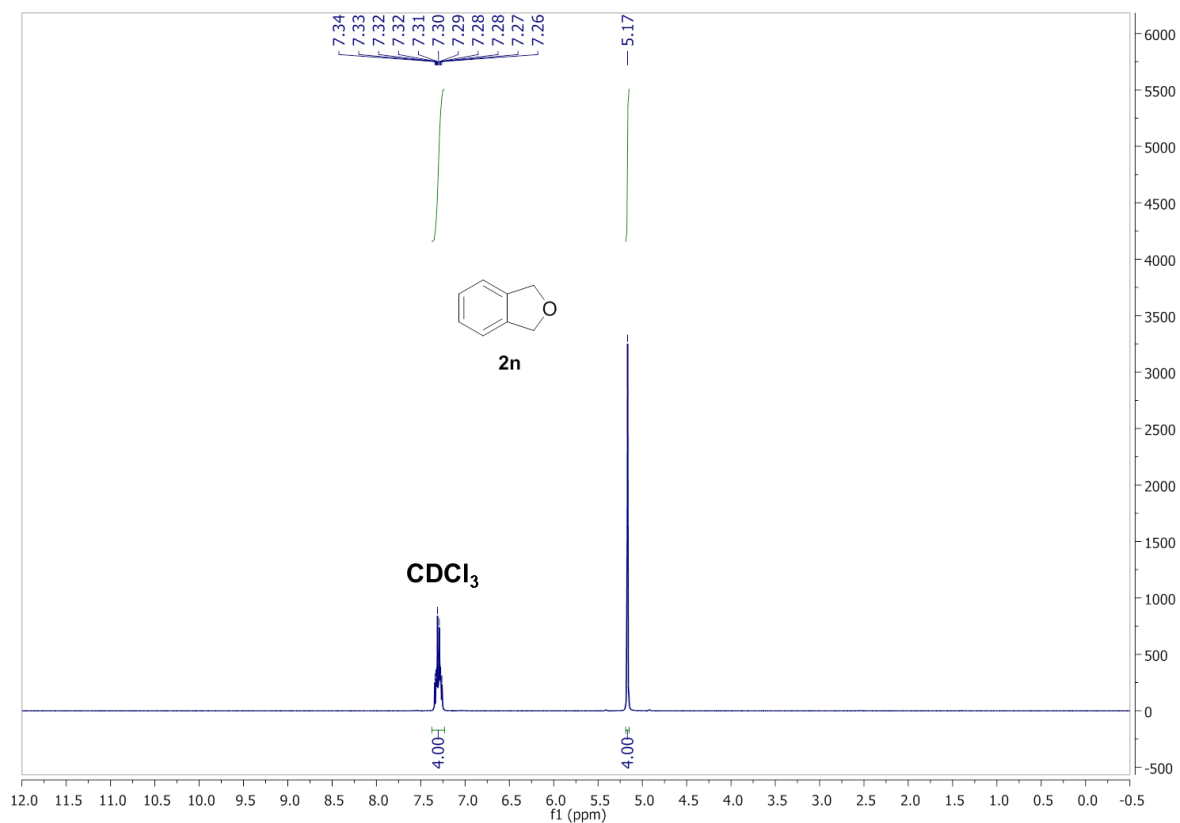


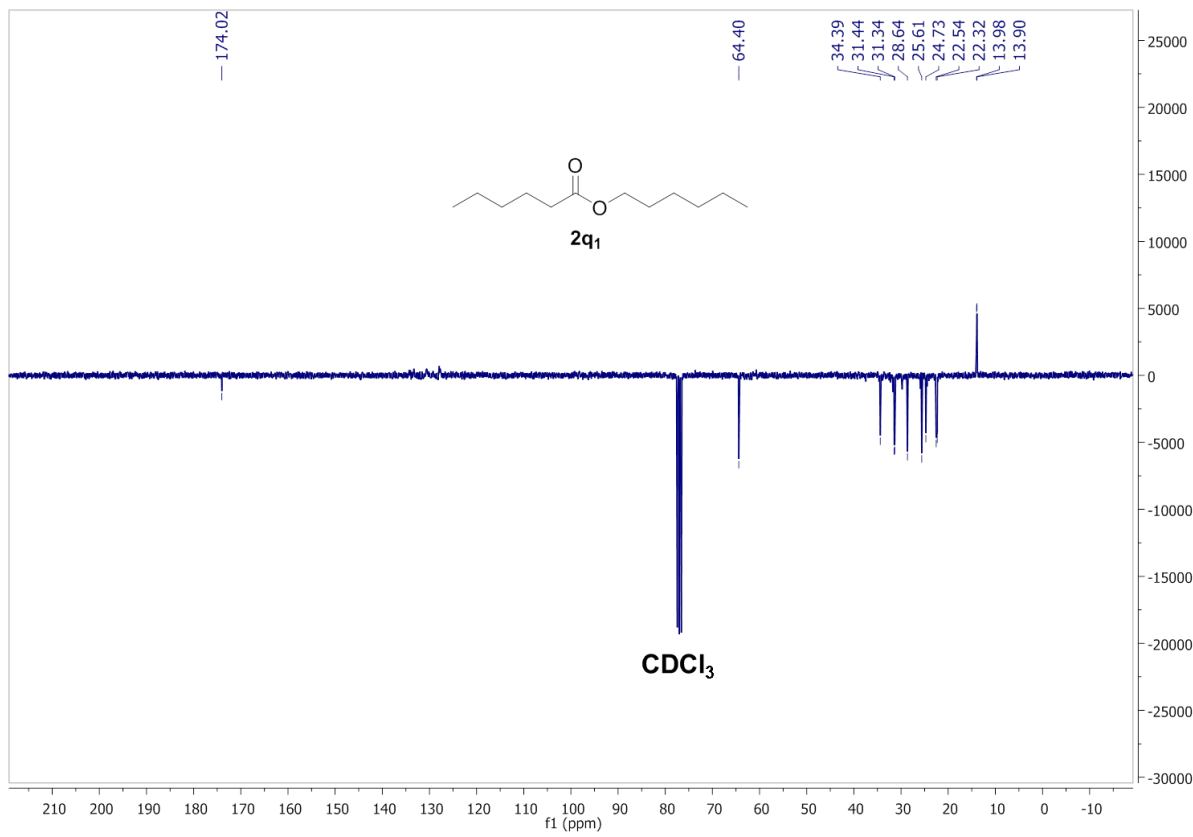
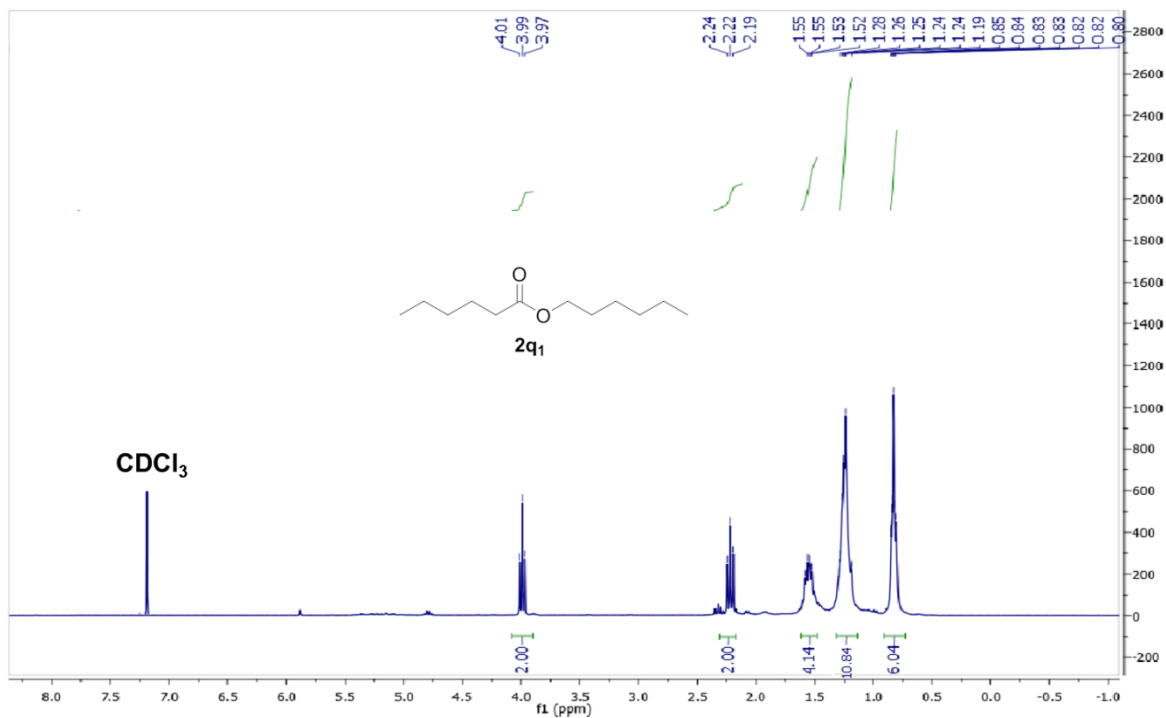


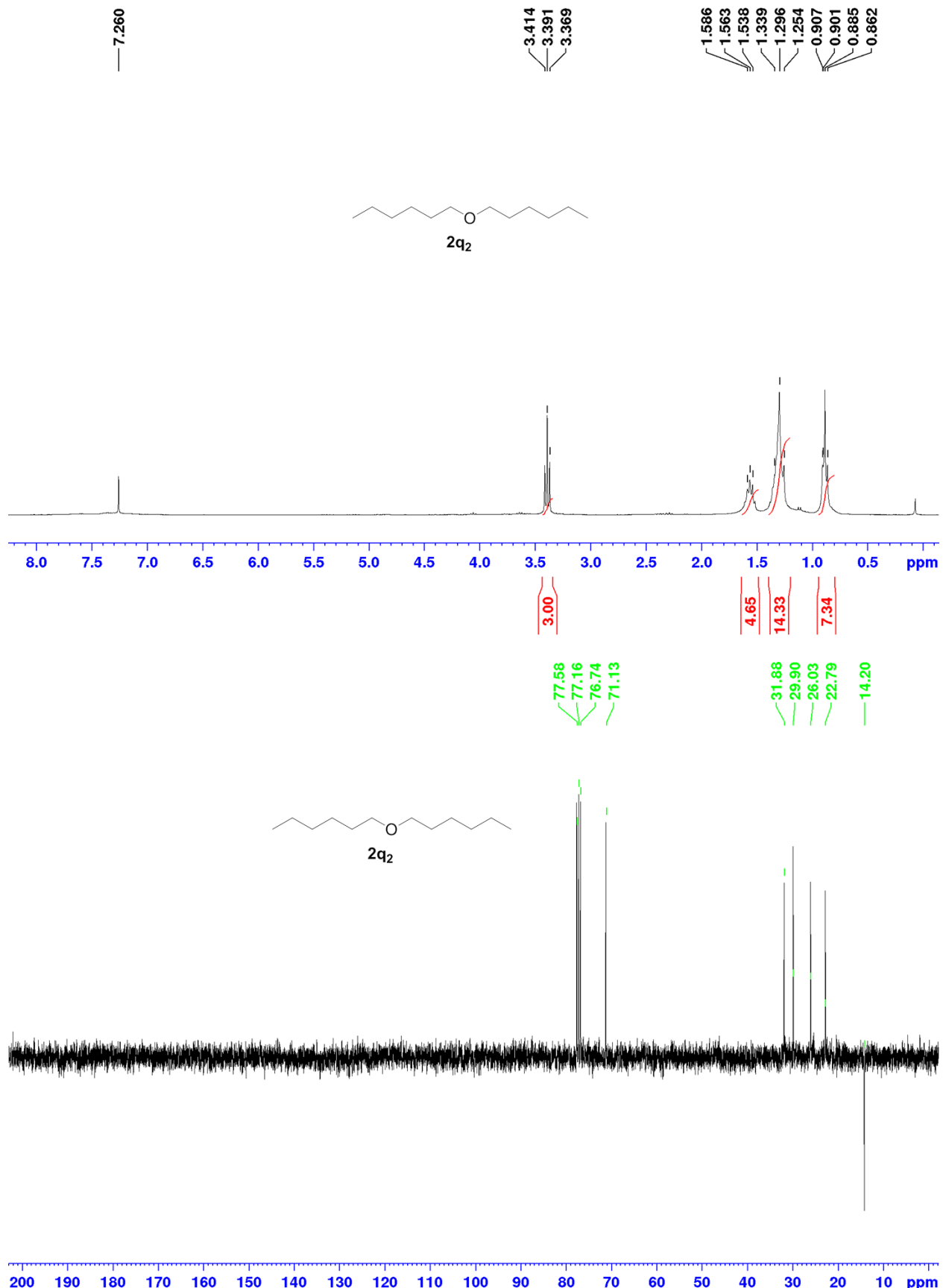


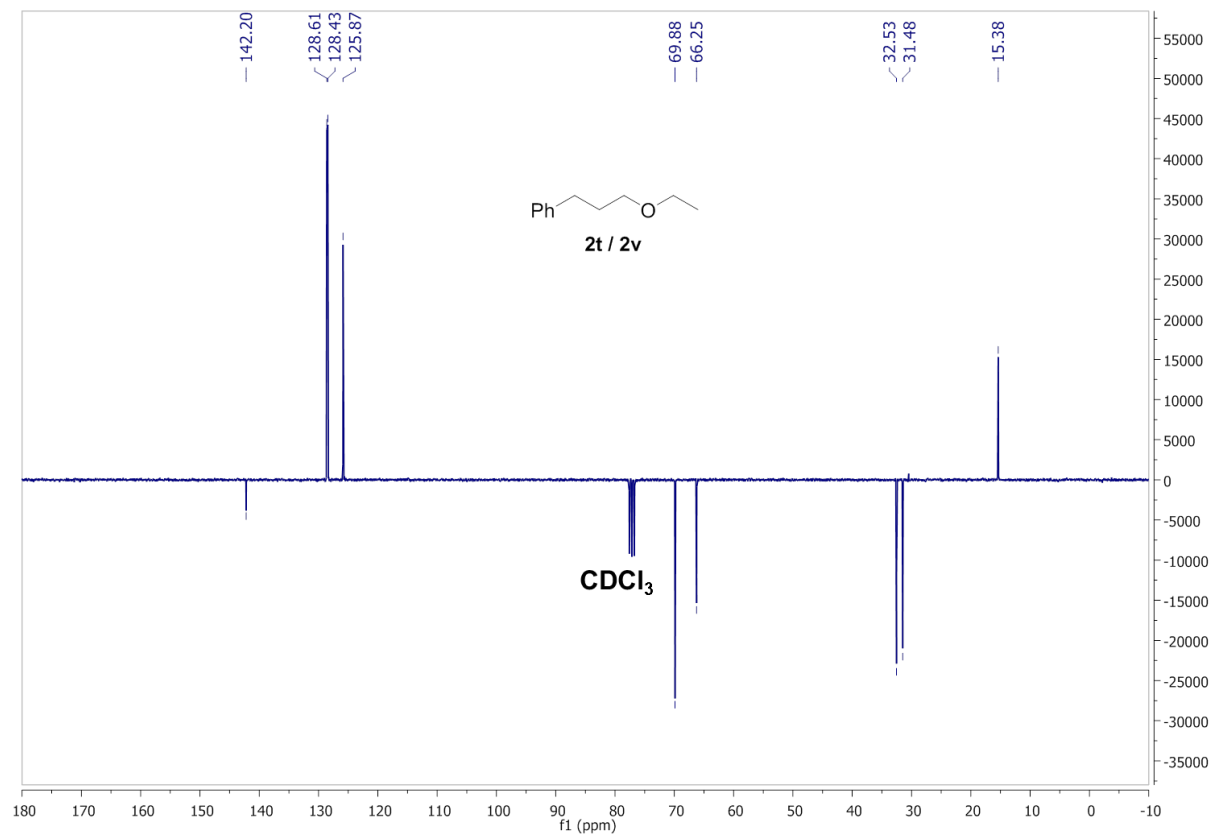
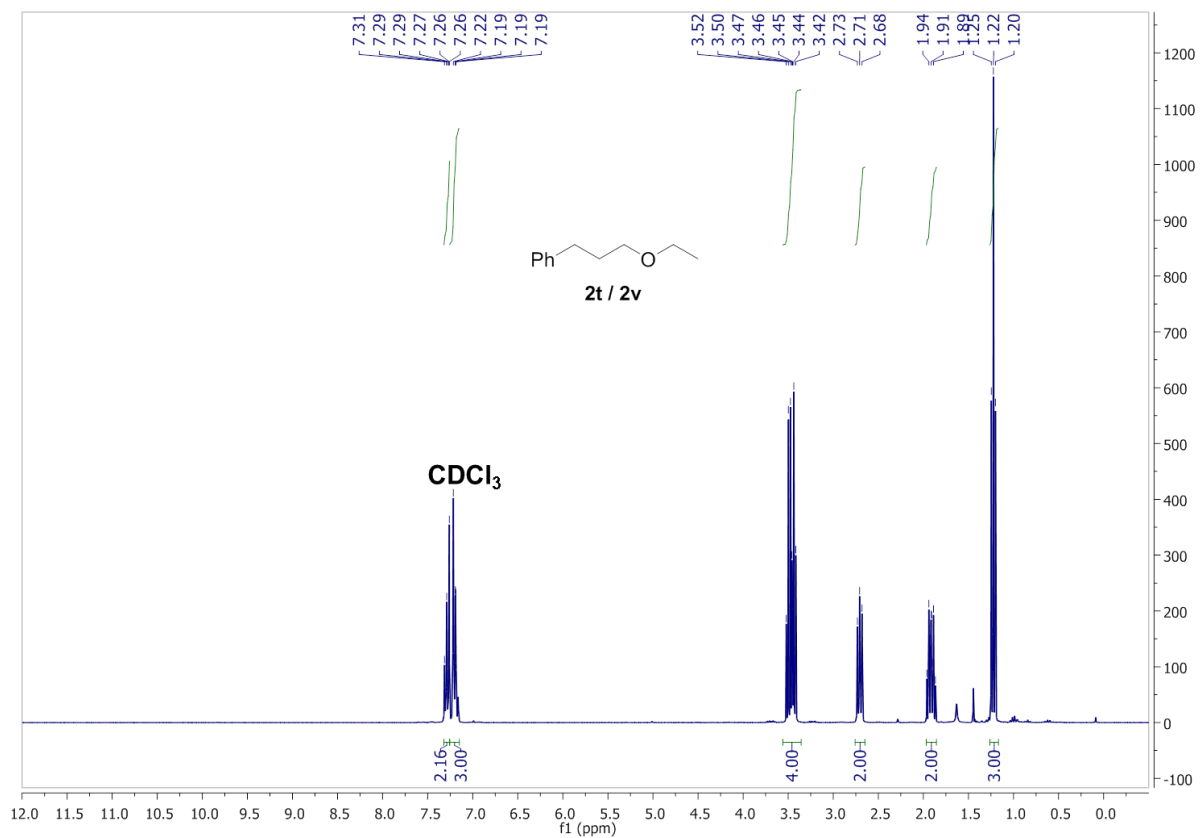


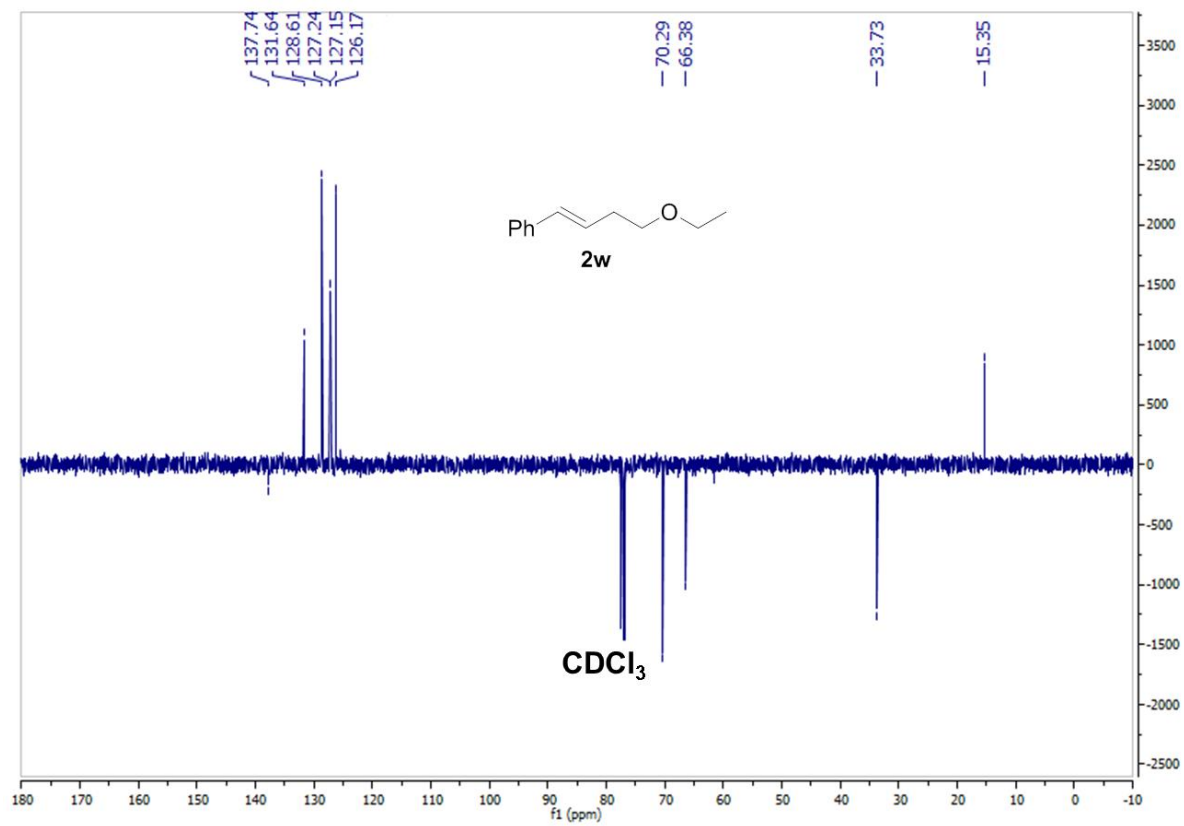
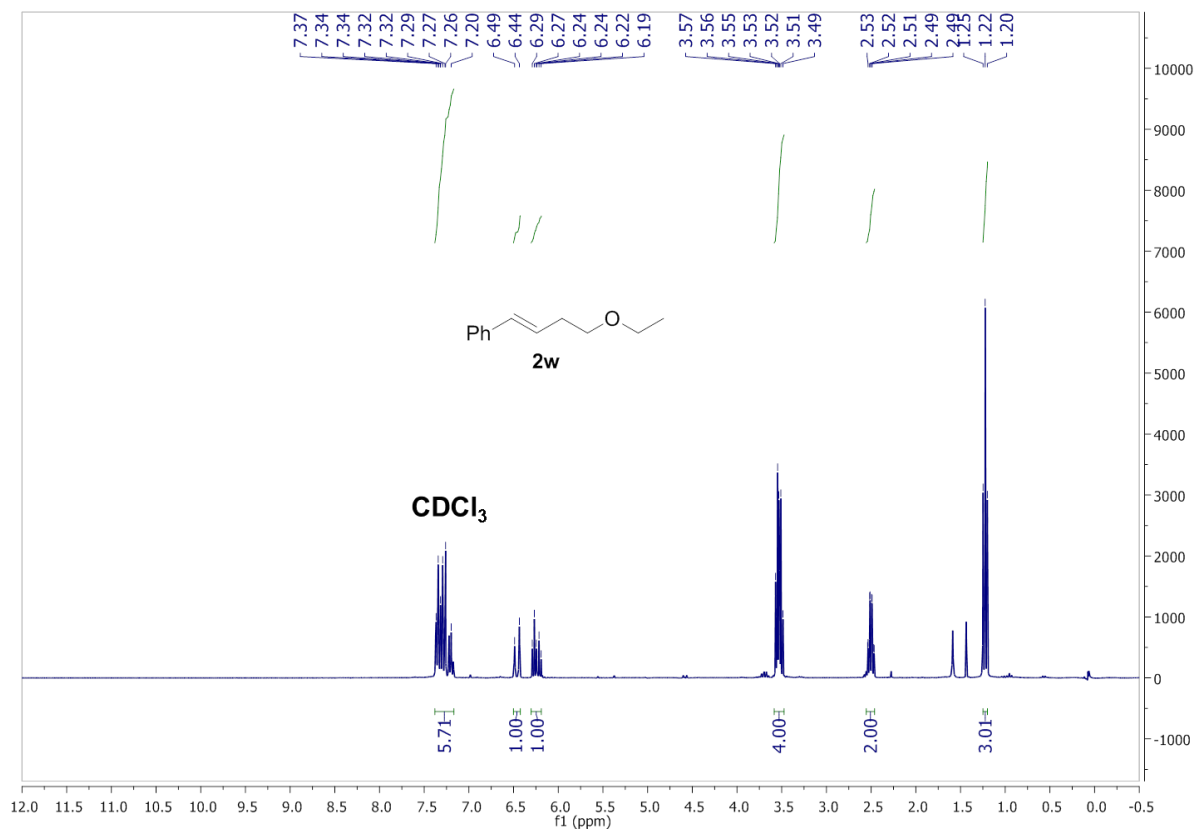


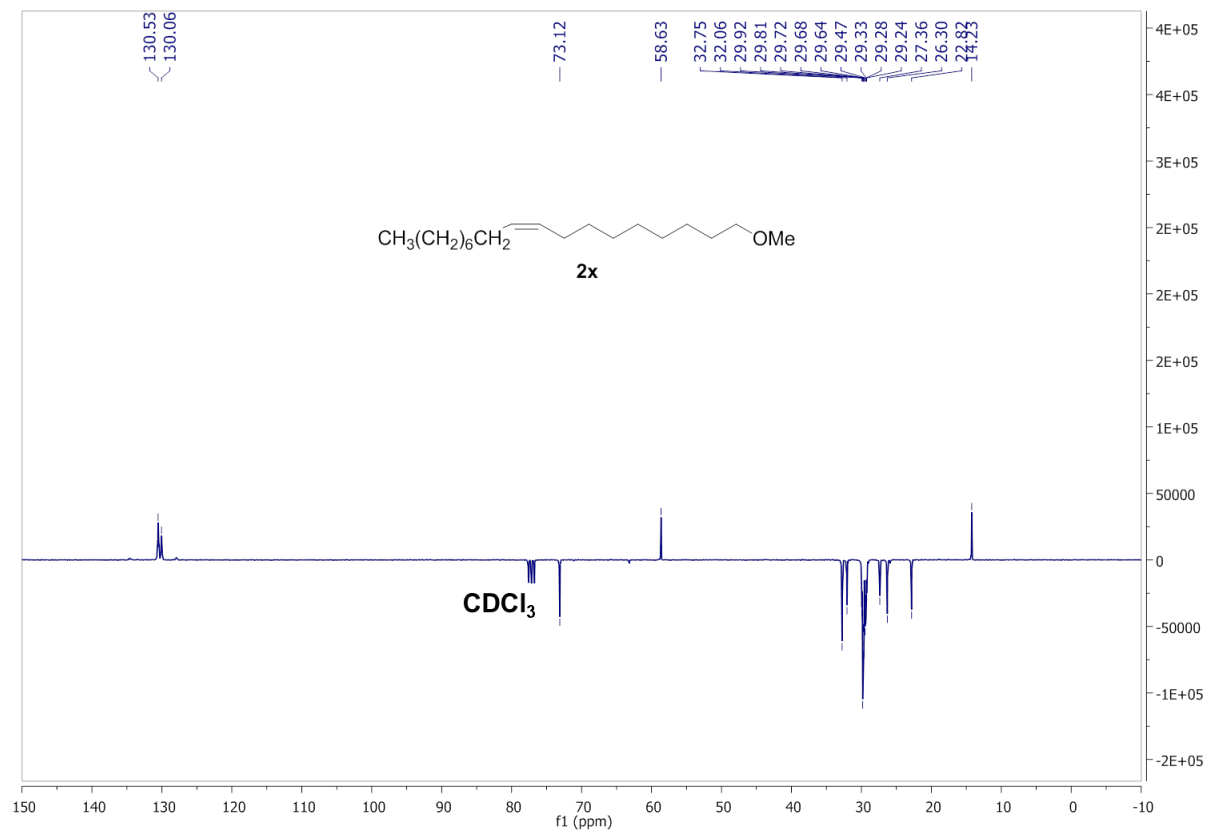
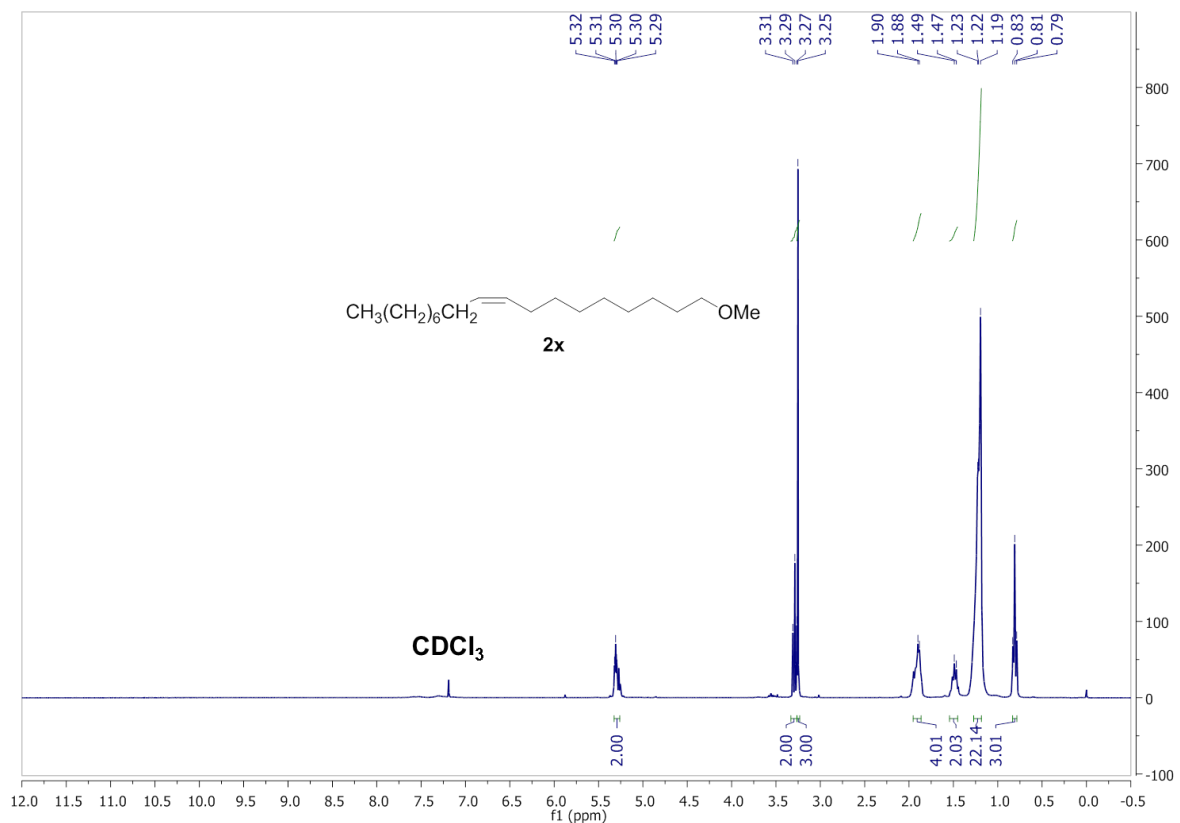


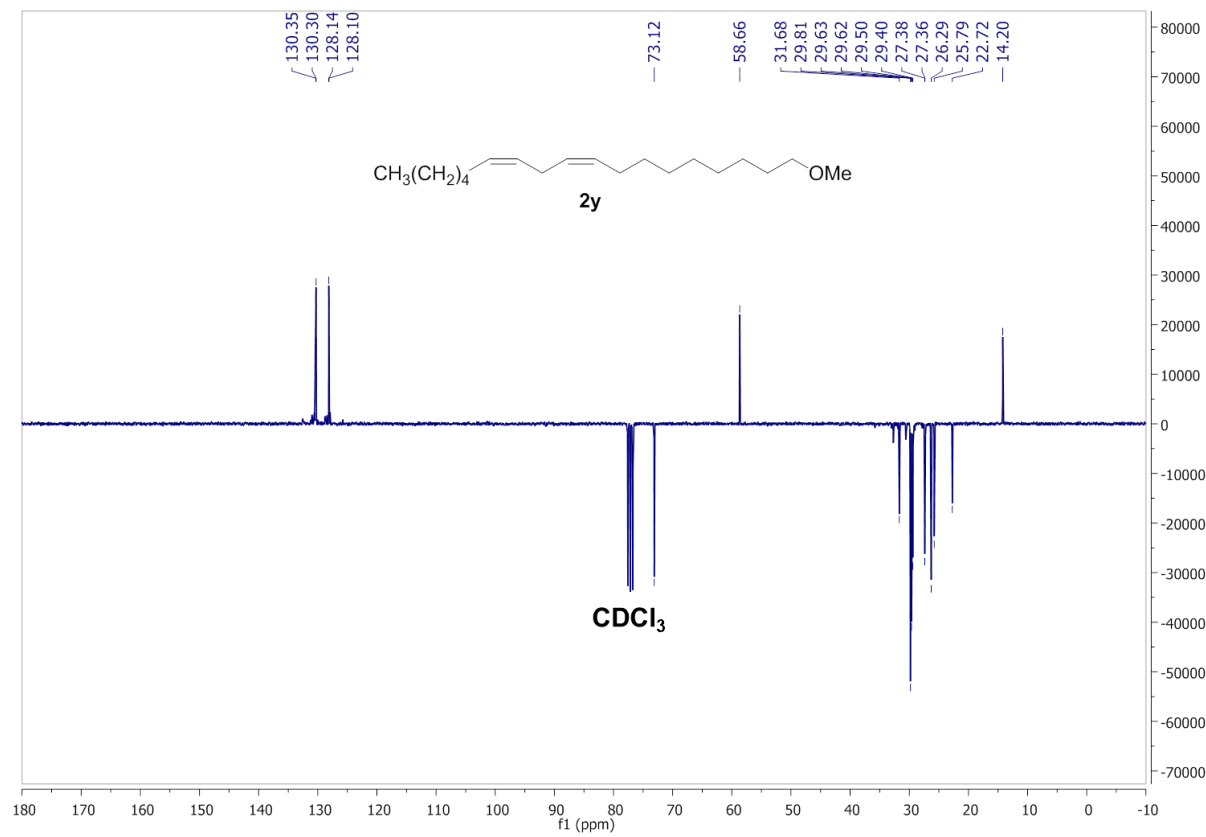
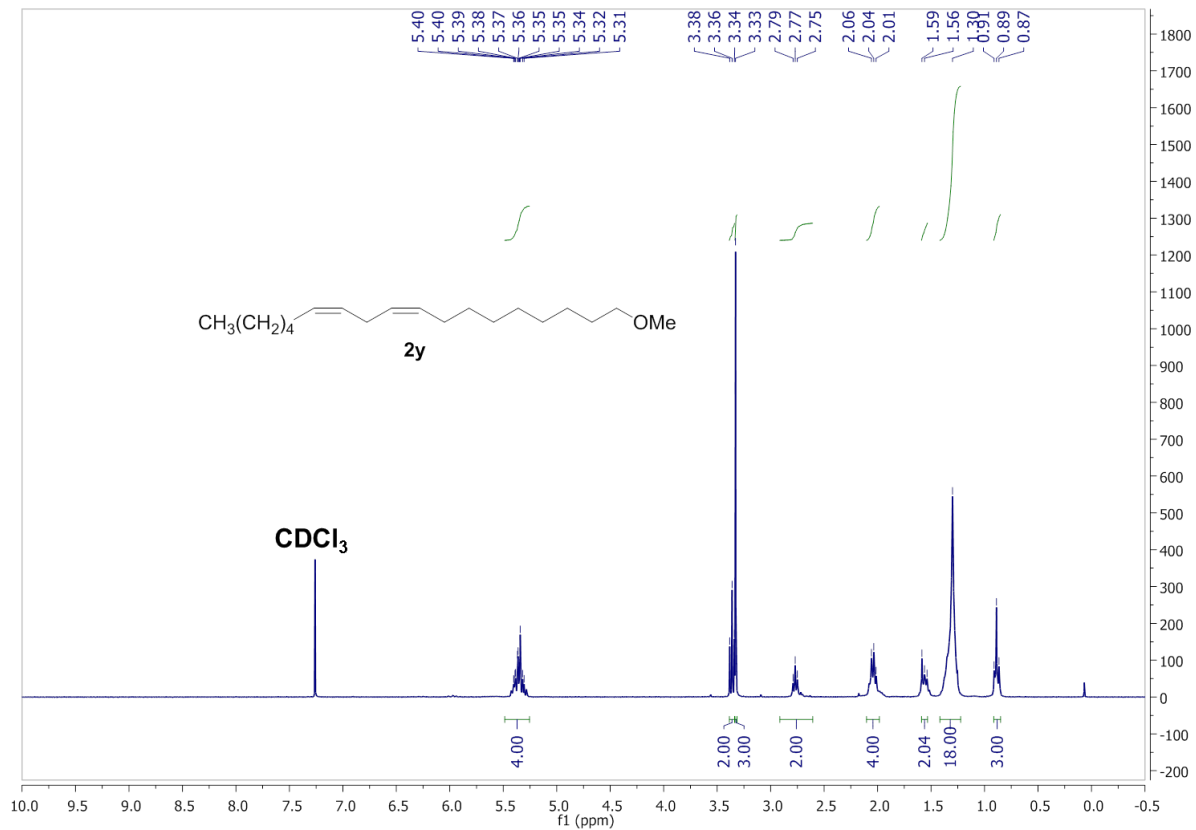












VIII) Computational details

PBE/TZVP optimized geometries for all the compounds and transition states

$\text{K}^+(\text{BL}_4)^-$

70			
C	12.9118270	12.6479130	20.9332000
C	12.1075030	12.3630900	22.0543770
C	11.1885180	11.3073260	22.0643320
C	11.0422290	10.4759180	20.9532890
C	11.8243790	10.7448760	19.8291330
C	12.7323220	11.8106200	19.8198530
C	12.0396550	15.5563250	21.5891580
C	13.3647360	15.1363530	21.8235640
C	14.0975320	15.9020340	22.7440360
C	13.5601410	17.0391930	23.3664830
C	12.2484380	17.4411900	23.1161600
C	11.4897950	16.6722510	22.2284880
B	14.0034820	13.8691010	20.9891090
C	15.3691400	13.3973780	21.7751470
C	16.5881310	14.0461270	21.5257180
C	17.7285510	13.8406080	22.3102780
C	17.7101150	12.9242190	23.3603480
C	16.5182440	12.2306770	23.6004160
C	15.3752330	12.4645560	22.8283100
C	16.4881320	11.1887690	24.6893390
F	17.2837000	11.5225460	25.7466780
C	18.9500950	14.6543280	21.9978680
F	18.6332910	16.0126760	21.9475170
C	10.0680430	17.0599520	21.9107810
F	9.6682190	12.2142320	23.6570350
F	9.2353760	15.9800440	21.9136270
C	14.4510710	17.8326350	24.2794070
F	15.4978860	18.4090190	23.5568220
C	10.3593600	11.0880020	23.3010180
F	11.1332220	10.7599490	24.3827630
C	11.7356960	9.8619690	18.6141720
F	12.8163440	9.0220390	18.5180390
C	14.4483410	14.3936380	19.4971820
C	15.2305440	13.5751060	18.6536000
C	15.6937750	14.0141750	17.4099980
C	15.4477050	15.3194710	16.9708380
C	14.6902710	16.1505060	17.7942990
C	14.1814130	15.6859180	19.0183330
C	16.5426670	13.0882940	16.5759640

F	16.0993800	11.8004090	16.6297000
C	14.4581130	17.5909890	17.4349360
F	15.0958440	18.4226900	18.3587590
F	10.6280190	9.0711290	18.6113880
F	11.7128180	10.5845590	17.4543880
F	9.4426090	10.0926790	23.1579890
F	13.8230040	18.8485540	24.9084820
F	15.0504060	17.0646410	25.2280900
F	9.5580690	17.9612460	22.7934540
F	9.9637880	17.6244750	20.6666820
F	19.9381610	14.5258930	22.9089210
F	19.4768240	14.3667920	20.7743770
F	15.2361190	10.9853020	25.1826020
F	16.9338130	9.9740970	24.2383410
F	14.9373260	17.9376750	16.2200650
F	13.1467410	17.9426610	17.4778310
F	16.5735320	13.4475240	15.2634610
F	17.8429160	13.0689360	17.0085890
H	13.2996700	11.9950340	18.9058850
H	10.3290720	9.6529570	20.9575600
H	15.1145090	15.5955020	23.0050740
H	11.8237950	18.3156600	23.6070550
H	18.5916540	12.7590630	23.9790950
H	14.4618820	11.9155330	23.0642630
H	13.5638350	16.3616180	19.6161200
H	15.8372930	15.6745910	16.0176850
H	16.6533520	14.7398520	20.6832930
H	15.5052280	12.5719370	18.9881710
H	11.4166270	14.9869290	20.8952530
H	12.1827210	12.9953900	22.9428070
K	16.5146840	17.8398810	20.8865270

PhSiH₃

15

C	0.1703290	-0.7926710	0.1686840
C	0.1705520	0.4033320	0.9114660
C	1.0400450	0.5039890	2.0150810
C	1.8853780	-0.5545370	2.3629420
C	1.8747340	-1.7355770	1.6118470
C	1.0154070	-1.8534370	0.5142270
Si	-0.9455700	1.8531090	0.4241690
H	-0.1779730	2.8854540	-0.3545930
H	-2.0741190	1.3539630	-0.4305970
H	1.0589370	1.4173520	2.6160310
H	2.5513500	-0.4587020	3.2232600
H	2.5326120	-2.5635060	1.8843610

H	1.0003880	-2.7746200	-0.0724490
H	-0.4982080	-0.9040360	-0.6889650
H	-1.4964390	2.5160810	1.6540620

$\text{K}^+ (\text{BL}_4)^-$ - PhSiH₃

85			
C	19.5817790	18.2370850	19.2500350
C	18.7749010	18.0953260	18.1013850
C	17.9346890	19.1686720	17.7406600
C	17.9007450	20.3454000	18.5023640
C	18.7082030	20.4670370	19.6408850
C	19.5505520	19.4097660	20.0133960
Si	18.8423290	16.5034860	17.0671690
F	18.5734300	16.4188600	21.7831140
C	18.9999690	15.0917220	21.7648590
F	20.0195900	15.0059740	22.6463270
C	17.8544340	14.1717060	22.0687650
C	16.6766970	14.3197360	21.3262730
C	15.5091040	13.5927180	21.6086350
C	15.6183990	12.6311670	22.6298930
C	16.8016450	12.4519770	23.3545540
C	17.9340700	13.2313930	23.0948940
B	14.0825700	14.0357510	20.9208130
C	13.4783480	15.2884630	21.8043700
C	12.1439900	15.7046350	21.6209850
C	11.6084070	16.8047030	22.2976610
C	12.3872660	17.5531120	23.1858300
C	13.7055290	17.1483680	23.3926940
C	14.2330150	16.0329020	22.7233840
C	16.8699890	11.3916590	24.4243330
F	15.6531830	11.1358390	24.9794130
C	10.1795120	17.1959620	22.0186870
F	9.6925270	18.0946590	22.9163070
C	14.6130560	17.9031200	24.3218680
F	14.0175290	18.9467390	24.9382550
C	14.3887800	14.5658800	19.3979870
C	14.0600600	15.8549800	18.9489920
C	14.4156530	16.3178550	17.6731810
C	15.0786200	15.4885120	16.7697260
C	15.4039780	14.1949350	17.1892520
C	15.0839190	13.7530960	18.4775140
C	16.1215320	13.2484610	16.2595610
F	16.5230720	13.8456170	15.1042380
C	14.0944070	17.7449950	17.3293040
F	14.5652000	18.1330190	16.1214660

C	12.9901400	12.8159810	20.9587890
C	12.3655500	12.4837860	22.1774410
C	11.4460730	11.4354660	22.2831600
C	11.0921350	10.6814370	21.1628030
C	11.6827660	11.0076430	19.9406690
C	12.6135920	12.0505420	19.8434180
C	10.7915710	11.1750610	23.6132300
F	11.6767140	11.2770970	24.6490020
C	11.3588550	10.1939770	18.7166650
F	10.1489000	9.5722280	18.8023330
F	19.5188070	14.8991990	20.5182150
F	17.3324670	10.2006970	23.9302660
F	17.7079550	11.7376810	25.4441020
F	17.2370990	12.7146510	16.8408460
F	15.3296050	12.1913020	15.9068240
F	12.7620400	18.0102160	17.3568600
F	14.6660460	18.6066070	18.2638880
F	10.2273040	9.9381870	23.6939150
F	9.7930390	12.0784100	23.8730520
F	11.3382380	10.9523780	17.5824070
F	12.2880230	9.2079930	18.5014710
F	15.1539390	17.1081730	25.2841290
F	15.7009450	18.4267390	23.6234880
F	10.0460390	17.7647290	20.7792810
F	9.3454440	16.1172570	22.0378540
K	16.3307230	18.1753070	20.7552110
H	13.0372030	12.2778150	18.8634640
H	10.3697390	9.8692290	21.2382700
H	15.2601020	15.7296500	22.9444230
H	11.9730780	18.4131180	23.7100380
H	18.8434510	13.1174280	23.6839470
H	14.7527940	12.0183920	22.8863200
H	13.5061160	16.5269020	19.6096320
H	15.3486210	15.8404520	15.7754940
H	16.6622480	15.0414880	20.5040560
H	15.4053660	12.7544870	18.7848200
H	11.5037030	15.1473150	20.9327520
H	12.5947280	13.0670310	23.0725950
H	18.2818280	15.3556260	17.8574220
H	18.0194190	16.6975600	15.8292680
H	20.2618560	16.1848540	16.7064710
H	17.3056650	19.0947670	16.8502990
H	17.2490660	21.1687640	18.2029140
H	18.6910110	21.3864620	20.2293360
H	20.1864790	19.5009320	20.8962620
H	20.2484370	17.4265180	19.5534550

Ester

24

H	-1.1609130	-0.5382130	0.2997660
C	-0.6237730	0.1461910	0.9693260
H	0.4562440	-0.0117010	0.8527580
C	-1.0439450	-0.0873550	2.4093400
C	-2.3023300	-0.6318580	2.7071860
C	-2.6982650	-0.8210640	4.0348330
C	-1.8418770	-0.4631390	5.0816690
C	-0.5870040	0.0843490	4.7931270
C	-0.1917140	0.2720240	3.4652440
H	-2.9748100	-0.9116260	1.8925220
H	-3.6778990	-1.2522510	4.2515890
H	-2.1497570	-0.6142960	6.1181660
H	0.0888240	0.3634990	5.6042410
H	0.7892180	0.6996240	3.2436020
C	-0.9193900	1.5826640	0.5707120
O	-2.1756660	1.7029730	0.0821970
O	-0.1431760	2.5151120	0.7119990
C	-2.6216810	3.0510500	-0.2818440
C	-2.2246390	3.3945750	-1.7054430
H	-3.7115230	3.0062180	-0.1643960
H	-2.2056640	3.7666350	0.4403460
H	-2.6412360	4.3772570	-1.9722470
H	-1.1323640	3.4447640	-1.8114290
H	-2.6190040	2.6512810	-2.4127780

Catalyst_int_1

109

C	17.0853980	20.7422910	19.3242050
C	17.9849920	19.9159480	20.0263070
C	18.1555010	18.5883350	19.5843470
C	17.4553020	18.1034910	18.4744250
C	16.5760910	18.9435280	17.7782330
C	16.3851120	20.2620620	18.2091360
Si	18.9889970	20.5926940	21.4863660
O	15.8134210	18.1058050	23.1466030
C	15.9953120	19.2044760	23.6458930
O	15.6402910	20.2844080	22.8896240
C	15.6704720	21.6639600	23.3890300
C	14.3572470	22.0488550	24.0398720
C	16.5931680	19.4443850	25.0180990
C	17.0793510	18.1886550	25.6980750
C	18.4394530	17.8529090	25.6688200

C	18.9029590	16.7032670	26.3151860
C	18.0073980	15.8765380	26.9998310
C	16.6467330	16.2007210	27.0267040
C	16.1868750	17.3507870	26.3813470
K	14.5536890	18.6064820	20.6841040
F	12.8609110	17.4566720	25.4391280
C	12.1653200	18.0547840	24.4301710
F	11.0618800	18.6195890	24.9872330
C	11.8440490	17.0986280	23.3139530
C	12.8618060	16.2697780	22.8095260
C	12.6237900	15.3740160	21.7524210
C	11.3102870	15.3523060	21.2351880
C	10.2995410	16.1773180	21.7334570
C	10.5567050	17.0684710	22.7790760
B	13.7650350	14.3902860	21.0962920
C	14.1824800	14.9455180	19.6067340
C	15.2747390	14.3957220	18.8989590
C	15.5973810	14.7917340	17.5967350
C	14.8775930	15.8014200	16.9509660
C	13.8175410	16.3850480	17.6428900
C	13.4694290	15.9487970	18.9294410
C	8.9369340	16.1437630	21.0925660
F	8.9006620	16.9110620	19.9555420
C	16.7822600	14.1533860	16.9168120
F	17.9661850	14.6346700	17.4179310
C	13.0284330	17.5190330	17.0484880
F	11.7186150	17.2068020	16.8562010
C	13.1104010	12.8794230	20.9568500
C	12.2488920	12.3821090	21.9537940
C	11.7162190	11.0883300	21.9055940
C	12.0033940	10.2347340	20.8401910
C	12.8340600	10.7163270	19.8259940
C	13.3762380	12.0053070	19.8888850
C	10.7963780	10.6537130	23.0146020
F	10.4401650	9.3427380	22.9316510
C	13.1941880	9.8287020	18.6650060
F	13.2768750	10.5222930	17.4909620
C	15.0791670	14.3127630	22.0881430
C	16.2935880	14.9717820	21.8317960
C	17.3866780	14.8921710	22.7054700
C	17.2977000	14.1786740	23.8990040
C	16.0929170	13.5352100	24.1871290
C	15.0172780	13.5952270	23.2970470
C	18.6657740	15.5917580	22.3351600
F	19.0090610	15.3529010	21.0268630
C	15.9244270	12.7437370	25.4552940

F	15.5945780	11.4387210	25.2004220
F	17.0456840	12.7215460	26.2260510
F	14.9159680	13.2401200	26.2395900
F	18.5797730	16.9504150	22.4553590
F	19.7254110	15.2009980	23.0956250
F	8.5717000	14.8854940	20.7192330
F	7.9585240	16.6187600	21.9126480
F	12.9515450	19.0959030	23.9870400
F	9.6347790	11.3796300	23.0247840
F	11.3649150	10.8324540	24.2467780
F	14.4156330	9.2290640	18.8399960
F	12.2944950	8.8245810	18.4705220
F	16.8097710	12.8032440	17.0972900
F	16.8058020	14.3815960	15.5762360
F	13.0332760	18.6135010	17.9022360
F	13.5208400	17.9560010	15.8642940
H	14.0077330	12.3346850	19.0628820
H	11.5820830	9.2314500	20.7947010
H	13.8555350	16.3169390	23.2642990
H	9.7691940	17.7078630	23.1754400
H	18.1412550	14.1236500	24.5839510
H	14.1049170	13.0533420	23.5545470
H	12.5971930	16.4013890	19.4086950
H	15.1380350	16.1209250	15.9428180
H	16.4141280	15.5472790	20.9113180
H	15.8878350	13.6277920	19.3766710
H	11.0689430	14.6544700	20.4298500
H	11.9666780	13.0259750	22.7903600
H	20.4506370	20.6210530	21.1466110
H	16.9323500	21.7774270	19.6404230
H	18.8081180	19.7318880	22.7016430
H	18.5197270	21.9856210	21.7886420
H	18.8456470	17.9212770	20.1046780
H	17.6134710	17.0755800	18.1429890
H	16.0491190	18.5771240	16.8956900
H	15.7027520	20.9214330	17.6683980
H	14.3940890	23.1133450	24.3137830
H	14.1636950	21.4686270	24.9523610
H	13.5186110	21.8991190	23.3465930
H	17.4212430	20.1630530	24.9164070
H	15.8297920	19.9500900	25.6326080
H	19.1428870	18.4951780	25.1333100
H	19.9653560	16.4535560	26.2829610
H	18.3658170	14.9767360	27.5032490
H	15.9404100	15.5532950	27.5496290
H	15.1238720	17.5986560	26.4059950

H	16.5248490	21.7979620	24.0650170
H	15.8564010	22.2597940	22.4865280

Catalyst_ts_1

109

C	18.0725440	19.8492380	18.2087310
C	18.4427280	19.6527020	19.5449250
C	18.2043160	20.6492820	20.5122810
C	17.5926520	21.8504790	20.1036420
C	17.2066510	22.0421550	18.7732340
C	17.4420590	21.0395690	17.8248620
Si	18.6426970	20.3660430	22.3217830
O	16.8713540	19.1156010	22.6002880
C	16.3586420	20.1819460	23.1418690
O	15.3161410	20.6992560	22.3967820
C	14.6896010	21.9672540	22.7783190
C	13.3328710	21.7468640	23.4168530
C	16.2195490	20.2532300	24.6744120
C	17.5402810	20.2742800	25.3943430
C	18.0619800	21.4991390	25.8460390
C	19.3048240	21.5552630	26.4790510
C	20.0424210	20.3819090	26.6727180
C	19.5309080	19.1580670	26.2314210
C	18.2872970	19.1030600	25.5943860
K	15.2794420	18.8489320	20.2602330
F	12.5057270	18.9436780	21.2661580
C	11.9150220	18.1104930	22.2157620
F	11.0882780	17.2920560	21.5129850
C	12.9641370	17.3556350	22.9822970
C	13.2052030	17.6274000	24.3290860
C	14.2164850	16.9018500	24.9645840
C	14.9740960	15.9515690	24.2682590
C	14.7618170	15.6738730	22.9041590
C	13.7175880	16.3938760	22.2975650
B	15.5906730	14.4971580	22.0881890
C	16.0989430	15.0694230	20.6238120
C	17.4485590	15.2990810	20.2952760
C	17.8433990	15.7856660	19.0421670
C	16.9008980	16.1049140	18.0628030
C	15.5550700	15.8762510	18.3596970
C	15.1713680	15.3347690	19.5940880
C	14.4537570	17.1054440	26.4394670
F	13.6952070	16.2612000	27.2014910
C	19.3126280	15.9031670	18.7265160
F	19.8353280	14.7159310	18.3000350

C	14.4886290	16.3200350	17.3980220
F	13.9987120	17.5678640	17.7891670
C	16.8695160	13.9872950	22.9771070
C	17.0598250	12.6436210	23.3339460
C	18.1645420	12.2214630	24.0874180
C	19.1373200	13.1286560	24.4993600
C	18.9712480	14.4734480	24.1532120
C	17.8551340	14.8948090	23.4239110
C	19.9858270	15.4708190	24.6377730
F	19.9915310	16.6140980	23.8994770
C	18.2993590	10.7596610	24.4197620
F	19.2582310	10.5154380	25.3549390
C	14.5728830	13.2357950	21.8306880
C	13.5186610	12.9299210	22.7079270
C	12.7120020	11.7982860	22.5296650
C	12.9207550	10.9297540	21.4561570
C	13.9640540	11.2174890	20.5735930
C	14.7744180	12.3431300	20.7624960
C	11.5891340	11.5531250	23.5011580
F	10.5944050	12.4883490	23.3737530
C	14.2579480	10.3123060	19.4077520
F	15.4714660	9.6905240	19.5396840
F	12.0107320	11.6234720	24.8002070
F	11.0031690	10.3351740	23.3414830
F	13.3290930	9.3317540	19.2457910
F	14.3136490	11.0049940	18.2280550
F	19.7428140	15.8458180	25.9384330
F	21.2573440	14.9759820	24.6175100
F	17.1319680	10.2366280	24.9000870
F	18.6263580	10.0136330	23.3175720
F	14.1427600	18.3745050	26.8419220
F	15.7525400	16.8866220	26.7887940
F	11.1441060	18.9073210	22.9899540
F	19.5613880	16.8155820	17.7416020
F	20.0436790	16.2841590	19.8133580
F	14.9325650	16.4718610	16.1286640
F	13.4155460	15.4948830	17.3693340
H	15.5875570	12.5269340	20.0565200
H	12.2899670	10.0538890	21.3125480
H	15.7480060	15.4078920	24.8111460
H	12.6177680	18.3689460	24.8691990
H	20.0017980	12.8014100	25.0762340
H	16.3233680	11.8989520	23.0261360
H	14.1175820	15.0893190	19.7400350
H	17.2044970	16.4980890	17.0931610
H	17.7494490	15.9589940	23.1950640

H	18.2245280	15.0754020	21.0280490
H	13.4515980	16.1881010	21.2593480
H	13.3246780	13.5845770	23.5607460
H	19.5868100	21.4733350	22.7663090
H	17.4086880	22.6449310	20.8316400
H	19.3702650	19.0937580	22.6159300
H	17.3784620	21.1907090	23.0134600
H	18.9287550	18.7185140	19.8375020
H	18.2802530	19.0770410	17.4656070
H	17.1438030	21.1885400	16.7853390
H	16.7264900	22.9760870	18.4745450
H	12.8782960	22.7220480	23.6439360
H	13.4078870	21.1789300	24.3546440
H	12.6640380	21.2083790	22.7333550
H	15.6212910	21.1221100	24.9725570
H	15.6416910	19.3484920	24.9200000
H	17.4858620	22.4161380	25.6974390
H	19.6969860	22.5141770	26.8234120
H	21.0137160	20.4209550	27.1697490
H	20.0993110	18.2405680	26.3849060
H	17.8915330	18.1472300	25.2471370
H	15.3754720	22.5269640	23.4306900
H	14.5972830	22.5231440	21.8353870

Catalyst_Int_2

109			
C	16.3759180	23.8803470	21.9129520
C	15.7453890	22.7000310	21.4863520
C	14.5969790	22.2688350	22.1658550
C	14.0917700	22.9900860	23.2508580
C	14.7325240	24.1593550	23.6730020
C	15.8749900	24.6042840	22.9988990
C	16.3374870	21.8729190	20.3731160
C	17.5797740	21.1007370	20.8298480
O	17.9139390	20.1844110	19.8066860
C	19.2965090	19.7257670	19.8468540
C	20.2577900	20.7230020	19.2248570
O	17.3146190	20.3455610	22.0217390
Si	17.8376310	20.7830560	23.5949920
C	18.1134750	19.1443910	24.4717120
C	17.2365540	18.7180390	25.4865320
C	17.4103310	17.4789930	26.1110570
C	18.4733020	16.6524520	25.7356700
C	19.3593120	17.0629930	24.7330400
C	19.1781860	18.2964530	24.1031440

F	18.8220370	16.5330890	21.1460960
C	19.0359710	15.1725300	21.3632680
F	20.1753220	15.0781430	22.0827120
C	17.8430340	14.5456440	22.0271960
C	16.6133220	14.6209850	21.3552520
C	15.4239300	14.0975390	21.8842620
C	15.5491880	13.4644620	23.1396470
C	16.7707300	13.3761260	23.8114930
C	17.9401310	13.9209470	23.2660280
B	13.9579200	14.2761330	21.1350400
C	13.0574690	15.3818930	21.9455860
C	11.6820350	15.5074000	21.6647110
C	10.9145040	16.5598350	22.1716050
C	11.4920370	17.5497090	22.9720940
C	12.8465770	17.4314360	23.2800270
C	13.6044540	16.3526110	22.7975410
C	16.8658050	12.6370910	25.1229920
F	17.3964690	11.3863820	24.9574570
C	9.4558320	16.6330650	21.7966490
F	9.2911690	16.8008950	20.4482690
C	13.5433420	18.4813400	24.0976470
F	14.0475510	17.9926380	25.2624090
C	13.1570740	12.8435920	21.1143630
C	13.0270460	12.0196770	19.9830020
C	12.3769240	10.7811790	20.0363040
C	11.8311860	10.3048170	21.2304390
C	11.9245020	11.1183780	22.3595710
C	12.5559260	12.3656080	22.2942860
C	11.3230140	10.6862720	23.6696240
F	10.9167870	9.3877950	23.6659410
C	12.3232610	9.9180830	18.8047990
F	12.3145850	10.6507470	17.6553900
C	14.2460710	14.8904560	19.6363390
C	13.8610920	16.1884810	19.2598960
C	14.2823060	16.7791730	18.0588080
C	15.0645470	16.0727610	17.1456870
C	15.4212220	14.7625340	17.4762810
C	15.0415680	14.1976710	18.6982430
C	13.9334740	18.2230670	17.8302930
F	12.6006720	18.4670770	17.9139760
C	16.2957520	13.9486700	16.5570090
F	17.5476480	13.7744720	17.0845860
F	14.5197600	19.0143430	18.8226070
F	14.3707420	18.7087780	16.6493410
F	15.7870540	12.6986580	16.3526310
F	16.4582040	14.5204140	15.3348830

F	10.2300990	11.4410140	24.0044700
F	12.2094420	10.8228210	24.7034980
F	13.4097540	9.0832890	18.7221270
F	11.2206990	9.1162270	18.7753530
F	19.2795410	14.6464560	20.1321440
F	17.6747590	13.2801470	26.0185400
F	15.6575560	12.4751020	25.7231580
F	8.7892130	15.4871970	22.1248380
F	8.8045270	17.6600490	22.4053920
F	14.6314510	18.9917220	23.3965110
F	12.7619150	19.5415670	24.4061350
K	16.2622420	18.0315780	21.0791180
H	19.1001080	21.5733250	23.4058790
H	16.7923930	21.5808690	24.3093890
H	16.4042420	19.3566970	25.7910610
H	16.7161500	17.1600490	26.8911840
H	18.6115610	15.6863240	26.2238420
H	20.1926410	16.4205950	24.4426750
H	19.8810820	18.6017070	23.3227730
H	19.5751330	19.4923310	20.8891490
H	19.2974340	18.7840030	19.2808320
H	21.2750520	20.3040080	19.2321220
H	19.9762600	20.9340340	18.1837300
H	20.2834430	21.6706250	19.7818230
H	16.6371460	22.5032820	19.5224050
H	15.5991510	21.1489290	19.9939860
H	14.0953660	21.3521950	21.8455630
H	13.1993030	22.6345730	23.7701190
H	14.3413800	24.7236540	24.5218890
H	16.3773680	25.5195880	23.3187250
H	17.2674970	24.2374210	21.3902460
H	13.4188280	12.3507970	19.0210370
H	11.3347910	9.3362270	21.2753240
H	14.6539410	16.2687330	23.0993100
H	10.9026970	18.3867250	23.3435010
H	18.8917020	13.8544690	23.7918630
H	14.6702600	13.0234200	23.6100910
H	13.2265180	16.7755270	19.9283560
H	15.3913230	16.5271560	16.2115270
H	16.6045890	15.0741680	20.3608610
H	15.4139060	13.2004840	18.9438910
H	11.2051600	14.7704170	21.0132780
H	12.5618550	12.9887720	23.1916500
H	18.4184050	21.7937150	21.0279930

Catalyst_ts_2

124

C	0.8674800	-3.7194710	-2.2416680
C	0.5206650	-3.2639330	-0.9560900
C	0.3131150	-4.2615510	0.0138830
C	0.4840830	-5.6235220	-0.2627600
C	0.8437390	-6.0512230	-1.5386500
C	1.0228250	-5.0794400	-2.5279960
B	0.3606630	-1.6736550	-0.5400720
C	1.7340320	-1.1682900	0.2310820
C	2.3328870	-1.9242720	1.2636240
C	3.4341980	-1.4612840	1.9873540
C	4.0146330	-0.2187350	1.7043940
C	3.4586630	0.5353330	0.6747480
C	2.3372750	0.0729350	-0.0341860
C	3.9774700	-2.2605000	3.1462170
F	5.3380120	-2.2106700	3.2127050
C	4.0113300	1.8855020	0.3123930
F	3.0509310	2.8720160	0.5155200
C	0.2366660	-6.6129770	0.8435380
F	0.5576150	-7.8895060	0.5005070
C	1.4307980	-5.5311520	-3.9047820
F	1.2630810	-4.5678020	-4.8504990
C	-0.9145080	-1.6012650	0.4939240
C	-2.1972580	-1.9840430	0.0446110
C	-3.3224820	-1.9276940	0.8695660
C	-3.22228470	-1.4998060	2.1987010
C	-1.9598770	-1.1606890	2.6762620
C	-0.8337120	-1.2226650	1.8398810
C	-1.7593960	-0.6829510	4.0867420
F	-2.8865680	-0.6800490	4.8284780
C	-4.6497290	-2.3763350	0.3111230
F	-4.8612770	-1.8873640	-0.9462530
F	-1.2752970	0.6201480	4.0955680
F	-0.8248390	-1.4173900	4.7542570
C	0.1076230	-0.7159510	-1.8506430
C	-1.0623360	0.0286110	-2.0820340
C	-1.2298300	0.8234120	-3.2244930
C	-0.2161410	0.9371060	-4.1755580
C	0.9684780	0.2331720	-3.9536180
C	1.1225810	-0.5708920	-2.8199290
C	-2.5170920	1.5890530	-3.3874630
F	-3.6080150	0.8234110	-3.1193020
C	2.1230320	0.3469510	-4.9127680
F	3.2113970	0.9352820	-4.3240030
F	-4.7216070	-3.7386590	0.2132180

F	-5.7038920	-1.9798440	1.0749340
F	-2.5791440	2.6620530	-2.5304840
F	-2.6760160	2.0933540	-4.6438420
F	2.5450640	-0.8776580	-5.3519260
F	1.8252820	1.0832050	-6.0167050
F	5.0902900	2.2446190	1.0408710
F	4.3491970	1.9745490	-1.0023450
F	3.5126380	-1.7702540	4.3405730
F	3.6223650	-3.5695260	3.0955280
F	-1.0764760	-6.6253090	1.2315900
F	0.9606950	-6.3083620	1.9649880
F	2.7527590	-5.8959120	-3.9484190
F	0.7217690	-6.6241870	-4.3187680
K	0.4851690	1.7689790	1.9864730
O	-0.5614860	4.2650590	1.7767450
Si	-0.0526570	5.1345760	3.0966660
C	1.1818290	4.0350990	4.0443240
C	0.7245450	3.1077900	5.0046140
C	1.5727020	2.1204120	5.5210790
C	2.9013490	2.0423170	5.0860880
C	3.3845540	2.9709510	4.1560780
C	2.5319920	3.9560360	3.6429260
Si	-2.3745800	3.8404290	1.1161160
C	-4.0872660	3.3229470	0.3023840
C	-4.4666020	1.9721360	0.2174450
C	-5.6895370	1.5821570	-0.3412240
C	-6.5680820	2.5502260	-0.8400430
C	-6.2133100	3.9029130	-0.7725520
C	-4.9861090	4.2754760	-0.2099050
C	0.0917660	5.3258370	-0.9721490
O	0.9887320	5.9982870	-0.3726850
C	0.7709090	7.4713220	-0.1912020
C	1.4130530	8.2007060	-1.3442830
C	0.3759780	3.9560440	-1.4232050
C	0.7928820	4.1989350	-2.8783720
C	-0.1735020	4.4934520	-3.8539680
C	0.2163710	4.7008330	-5.1789000
C	1.5681140	4.6302400	-5.5298730
C	2.5336260	4.3593840	-4.5530070
C	2.1519360	4.1620320	-3.2255000
H	0.6736500	6.3964850	2.6948780
H	-1.1839390	5.4965980	4.0264710
H	-0.3146270	3.1434370	5.3443870
H	1.1943780	1.4058910	6.2551200
H	3.5595070	1.2627620	5.4751570
H	4.4237780	2.9222920	3.8237330

H	2.9225510	4.6624870	2.9048380
H	-0.3128860	7.6316720	-0.1168440
H	1.2493450	7.6763890	0.7714620
H	1.3013690	9.2804250	-1.1693350
H	2.4847420	7.9720260	-1.4133360
H	0.9239600	7.9555850	-2.2977330
H	1.1983990	3.5196070	-0.8473520
H	-0.5271060	3.3364290	-1.3643350
H	-1.2306130	4.5316690	-3.5859300
H	-0.5386440	4.9124900	-5.9378810
H	1.8713330	4.7843690	-6.5667630
H	3.5876240	4.2939000	-4.8271150
H	2.9056810	3.9473120	-2.4650420
H	1.0033990	-3.0048780	-3.0533250
H	0.9677000	-7.1108170	-1.7613160
H	0.1477740	-1.0189110	2.2790890
H	-4.1019730	-1.4432320	2.8389720
H	4.8805270	0.1391850	2.2609900
H	1.9312730	-2.9085170	1.5101850
H	-1.8813460	-0.0068870	-1.3610230
H	-0.3418190	1.5571950	-5.0612780
H	1.9389340	0.6988220	-0.8372500
H	2.0761820	-1.0866380	-2.6782570
H	-2.3151810	-2.3414040	-0.9811530
H	-0.0109660	-3.9772240	1.0179300
H	-0.8350730	5.8302380	-1.2745210
H	-1.7716560	2.4682030	0.8073120
H	-2.1811960	5.0281690	0.1718910
H	-2.9040870	4.1113560	2.5087390
H	-4.7203640	5.3387160	-0.1797170
H	-3.7817620	1.1975740	0.5832720
H	-6.8909860	4.6651730	-1.1666790
H	-5.9535120	0.5239270	-0.4038160
H	-7.5201580	2.2517710	-1.2850250

Pdt_1

29			
C	-0.4052270	-0.2171270	0.1628120
C	-0.5750450	-0.5457450	1.5207630
C	0.5297410	-0.4134240	2.3858130
C	1.7640930	0.0358990	1.9082890
C	1.9170140	0.3537490	0.5530650
C	0.8316160	0.2261510	-0.3197940
Si	-2.2372760	-1.1606340	2.1630350
H	-3.2382670	-1.1021190	1.0418050

H	-2.1233640	-2.5612930	2.6888520
H	0.4278870	-0.6581120	3.4467290
H	2.6098440	0.1359520	2.5919620
H	2.8821250	0.7020830	0.1789350
H	0.9468620	0.4759300	-1.3767770
H	-1.2474750	-0.3042820	-0.5291010
O	-2.7496140	-0.2109990	3.4550160
Si	-3.9307580	0.9560020	3.7398920
C	-5.3668850	0.2196140	4.7124600
H	-4.4487020	1.4779150	2.4279940
H	-3.2700650	2.0426360	4.5342180
C	-6.5812680	-0.1011060	4.0760850
C	-7.6393620	-0.6697730	4.7931820
C	-7.4970950	-0.9282720	6.1605710
C	-6.2973850	-0.6146020	6.8100240
C	-5.2435550	-0.0426780	6.0914430
H	-6.7069030	0.0964900	3.0077810
H	-8.5754920	-0.9106080	4.2848040
H	-8.3221560	-1.3719190	6.7219060
H	-6.1852470	-0.8123870	7.8782220
H	-4.3142350	0.2012750	6.6139910

Pdt_2

25

C	-0.1055580	-0.2850570	-1.9216580
C	-0.3792320	0.2750270	-0.6617410
C	0.7091600	0.7011780	0.1186690
C	2.0228160	0.6124810	-0.3651820
C	2.2726960	0.1001060	-1.6430590
C	1.1996050	-0.3644230	-2.4156730
C	-1.8232020	0.4269670	-0.2301070
C	-2.0792870	0.5094800	1.2735050
O	-3.4946370	0.6101380	1.4834840
C	-3.8750780	1.4142470	2.6124290
C	-5.2998090	1.0620120	3.0092180
H	-2.4160490	-0.4006250	-0.6531430
H	0.5455010	1.1106370	1.1170580
H	2.8572910	0.9208400	0.2717310
H	3.2946900	0.0402140	-2.0257440
H	1.3815500	-0.8252050	-3.3906430
H	-0.9374750	-0.6625450	-2.5224920
H	-3.1830760	1.2338850	3.4548570
H	-3.7999600	2.4863440	2.3446910
H	-5.6315490	1.7047530	3.8406820
H	-5.9947090	1.2109610	2.1674030

H	-5.3540360	0.0117950	3.3347130
H	-1.5633790	1.3796810	1.7137330
H	-2.2191870	1.3471790	-0.6932990
H	-1.7010680	-0.3954070	1.7852610

Without Catalyst Int_1

39

O	0.2894540	0.5731040	-0.5706740
Si	-0.0501800	-0.3218910	0.8371430
H	0.2369090	-1.7813770	0.6624630
H	0.9078860	0.2608790	1.8342160
C	-1.7966780	-0.0179530	1.5029380
C	-1.9693170	0.2021280	2.8832850
C	-3.2420340	0.4058840	3.4283510
C	-4.3669600	0.4039630	2.5967720
C	-4.2131730	0.1968440	1.2209970
C	-2.9404480	-0.0146880	0.6820150
H	-1.0993220	0.2224200	3.5460230
H	-3.3549390	0.5741790	4.5017060
H	-5.3607730	0.5682130	3.0188940
H	-5.0878230	0.1994360	0.5665690
H	-2.8300660	-0.1776880	-0.3914680
C	-0.0589730	0.1592660	-1.8708680
C	1.2078300	-0.1391420	-2.6997980
O	-0.9040480	-0.9814950	-1.7451020
H	-0.6233220	0.9813390	-2.3562880
C	-1.7642810	-1.2250830	-2.8716600
C	-2.5753890	-2.4723760	-2.5825490
H	-2.4193550	-0.3471370	-3.0320840
H	-1.1609150	-1.3632000	-3.7869950
H	-3.2490000	-2.6846620	-3.4249030
H	-1.9137360	-3.3381350	-2.4378460
H	-3.1833710	-2.3454070	-1.6755470
H	0.8875790	-0.3964940	-3.7216680
H	1.7755490	0.8008900	-2.7668060
C	2.0538170	-1.2378390	-2.1130810
C	3.0711090	-0.9452180	-1.1900090
C	3.8178890	-1.9682390	-0.5968670
C	3.5610980	-3.3041440	-0.9232630
C	2.5542180	-3.6080750	-1.8465700
C	1.8082350	-2.5826730	-2.4339040
H	3.2738060	0.0968250	-0.9314930
H	4.6043320	-1.7207810	0.1196600
H	4.1453480	-4.1044810	-0.4642920
H	2.3502850	-4.6481810	-2.1105000

H 1.0210150 -2.8275190 -3.1509360

Without Catalyst ts_1

39

C	18.4712360	20.7184000	18.1040660
C	18.5859740	20.1767090	19.3899230
C	18.3870820	20.9744220	20.5316490
C	18.0534900	22.3293980	20.3467070
C	17.9381390	22.8761810	19.0655460
C	18.1482080	22.0696240	17.9401960
Si	18.6092260	20.2491550	22.2688990
O	16.8850020	19.2764290	22.6104040
C	16.2918230	20.2808260	23.1695740
O	15.3384080	20.8389020	22.4224990
C	14.5727570	22.0089830	22.8736170
C	13.2827670	21.6062550	23.5590410
C	16.2319940	20.3982770	24.6892590
C	17.5386750	20.1081990	25.3810140
C	18.2926490	21.1624180	25.9194670
C	19.5226150	20.9165710	26.5339650
C	20.0119270	19.6088020	26.6222850
C	19.2635460	18.5506190	26.0963440
C	18.0327660	18.7980920	25.4810140
H	19.8222020	20.8954610	22.9481550
H	17.8798260	22.9663230	21.2189510
H	19.1599090	18.8431430	22.0838390
H	17.6420420	21.3449530	23.0036650
H	18.8355830	19.1182640	19.5047400
H	18.6312290	20.0846960	17.2287800
H	18.0565830	22.4938450	16.9378480
H	17.6829760	23.9314190	18.9427140
H	12.6917500	22.5111250	23.7631040
H	13.4611300	21.0944060	24.5142730
H	12.6889630	20.9476390	22.9105710
H	15.8544360	21.3826340	24.9903560
H	15.4682250	19.6527990	24.9787560
H	17.9160860	22.1855720	25.8450180
H	20.1012630	21.7472890	26.9428120
H	20.9740580	19.4149750	27.1007200
H	19.6376980	17.5272820	26.1663760
H	17.4537800	17.9710950	25.0658230
H	15.2156020	22.6388690	23.5039910
H	14.3730720	22.5502780	21.9406910

Without Catalyst ts_2

54

C	-1.4546900	2.9370130	-1.6651760
C	-1.3707200	3.3870330	-0.3382530
C	-1.1025750	4.7409340	-0.0790420
C	-0.9437740	5.6401150	-1.1359130
C	-1.0330130	5.1882700	-2.4571290
C	-1.2964330	3.8384990	-2.7198420
C	-1.4303870	2.3917310	0.8211690
C	0.0044230	2.2365670	1.1161330
O	0.5079110	2.8098520	2.1444370
C	1.9997120	2.7878020	2.2928720
C	2.3471880	3.5675820	3.5335270
O	0.5817680	-0.3445500	0.6803970
Si	1.7930970	-0.5445720	-0.4311070
C	1.3092890	-1.5987850	-1.9315630
C	0.6432050	-1.0322090	-3.0356630
C	0.2334510	-1.8214050	-4.1162100
C	0.4817780	-3.1987340	-4.1089300
C	1.1461170	-3.7802340	-3.0227660
C	1.5582680	-2.9847190	-1.9493080
Si	0.2240860	-0.9402710	2.5002270
C	-0.6521020	-2.5680200	1.9446930
C	-0.9528370	-2.8795870	0.6047520
C	-1.5728790	-4.0844200	0.2530330
C	-1.9157690	-5.0137800	1.2408270
C	-1.6407220	-4.7223240	2.5817380
C	-1.0206260	-3.5146480	2.9223110
H	-0.5818550	0.3528720	2.5793620
H	-0.0509540	-1.2338060	4.0287840
H	-1.8416880	1.4298360	0.4891590
H	-1.9878700	2.7683280	1.6875890
H	2.4092670	3.2325850	1.3766000
H	2.2807280	1.7263970	2.3551070
H	1.9497450	3.0848890	4.4362770
H	1.9692220	4.5973670	3.4776790
H	3.4423760	3.6116820	3.6205850
H	3.0460540	-1.1401150	0.1669730
H	0.4426600	0.0431230	-3.0593640
H	2.1304730	0.8370650	-0.9690900
H	2.0720830	-3.4547240	-1.1058440
H	1.3423840	-4.8550480	-3.0118020
H	0.1597280	-3.8179980	-4.9491160
H	-0.2756620	-1.3633040	-4.9666370
H	-1.6546920	1.8822550	-1.8683900
H	-1.3705330	3.4856980	-3.7500290

H	-0.8922630	5.8877970	-3.2832820
H	-0.7356700	6.6908710	-0.9267870
H	-1.0170770	5.0895470	0.9531920
H	-0.6887630	-2.1677980	-0.1764990
H	-1.7815620	-4.2993760	-0.7982880
H	-2.3956520	-5.9568980	0.9689280
H	-1.9108020	-5.4365470	3.3639850
H	-0.8189820	-3.2944040	3.9744510
H	1.7342050	-0.9253370	2.7150880
H	0.6673790	1.7943310	0.3688150